INFORMATION TO USERS

This material was produced from a microfilm copy of the original document. While the most advanced technological means to photograph and reproduce this document have been used, the quality is heavily dependent upon the quality of the original submitted.

The following explanation of techniques is provided to help you understand markings or patterns which may appear on this reproduction.

1. The sign or "target" for pages apparently lacking from the document photographed is "Missing Page(s)". If it was possible to obtain the missing page(s) or section, they are spliced into the film along with adjacent pages. This may have necessitated cutting thru an image and duplicating adjacent pages to insure you complete continuity.

2. When an image on the film is obliterated with a large round black mark, it is an indication that the photographer suspected that the copy may have moved during exposure and thus cause a blurred image. You will find a good image of the page in the adjacent frame.

3. When a map, drawing or chart, etc., was part of the material being photographed the photographer followed a definite method in "sectioning" the material. It is customary to begin photoing at the upper left hand corner of a large sheet and to continue photoing from left to right in equal sections with a small overlap. If necessary, sectioning is continued again — beginning below the first row and continuing on until complete.

4. The majority of users indicate that the textual content is of greatest value, however, a somewhat higher quality reproduction could be made from "photographs" if essential to the understanding of the dissertation. Silver prints of "photographs" may be ordered at additional charge by writing the Order Department, giving the catalog number, title, author and specific pages you wish reproduced.

5. PLEASE NOTE: Some pages may have indistinct print. Filmed as received.

University Microfilms International
300 North Zeeb Road
Ann Arbor, Michigan 48106 USA
St. John's Road, Tyler's Green
High Wycombe, Bucks, England HP10 8HR

BINDING AND TRANSPORT PROPERTIES OF NEUTRAL DIAMIDE AND CARBOXYLIC ACID IONOPHORES TOWARD Ca^{2+} , K^{+} , AND Na^{+}

by

TZE-CHEIN WUN

A dissertation submitted to the Graduate Faculty in Biochemistry in partial fulfillment of the requirements for the degree of Doctor of Philosophy, The City University of New York.

1978

This manuscript has been read and accepted for the Graduate Faculty in Biochemistry in satisfaction of the dissertation requirement for the degree of Doctor of Philosophy.

January 27, 1978
date

Robert Bittman
Chairman of Examining Committee
Dr. Robert Bittman

January 30, 1978
date

Executive Officer

Supervisory Committee

The City University of New York

ABSTRACT

BINDING AND TRANSPORT PROPERTIES OF NEUTRAL DIAMIDE AND CARBOXYLIC ACID IONOPHORES TOWARD Ca^{2+}, K^{+}, AND Na^{+}.

by

Tze-Chein Wun

Adviser : Professor Robert Bittman

The binding and transport properties of several naturally occurring antibiotic ionophores and synthetic ligands are studied. The naturally occurring ionophores studied are A23187, X537A, nigericin, and valinomycin. The synthetic ones include a series of neutral diamide ligands featuring N,N-di-n-propyl amides of 1,2-phenylenedioxydiacetic acid (P-PR), 2,3-naphthalenedioxydiacetic acid (N-PR), cis-and trans-1,2-cyclohexane-dioxydiacetic acids (c-C-PR and t-C-PR), and the N-methyl-N-carbethoxypentyl amide of cis-1,2-cyclohexanedioxydiacetic acid (c-C-5); in addition, macrocyclic polyether ligands (dicyclohexyl-18-crown-6 and dibenzo-18-crown-6) and the diazapolyoxamacrobicyclic ligand (2.2.1 cryptand) have been used.

The neutral diamide ionophores are shown to extract Group IIA cations and picrate anion from water into dichloromethane. The ratio of Ca^{2+} / picrate transferred was 1:2. The aromatic ligands, P-PR and N-PR, transfer Group IIA cations in the order: $Ba^{2+} \sim Sr^{2+} > Ca^{2+} > Mg^{2+}$. The cyclohexyl ligands, c-C-PR and t-C-PR, transfer with the selectivity order $Ca^{2+} > Ba^{2+}$, Sr^{2+}. The relative abilities of the diamide ligands to transfer Ca^{2+}-picrate is in the order of c-C-PR > c-C-5 > t-C-PR > P-PR, N-PR.

UV spectral titrations in methanol are used to construct Job and Scatchard plots, which establish the stoichiometries and binding constants

of diamide ligands with Group IIA cations. The aromatic ligands, P-PR and N-PR, show 1:1 binding stoichiometry with Group IIA cations at low ligand concentrations. Ligands of the cyclohexyl series (c-C-PR and t-C-PR) bind Ca^{2+} with varying stoichiometry (2:1, 3:2, and 4:3). The order of binding constants for the complexation of these ligands with Group IIA cations was $Ca^{2+} > Sr^{2+} > Ba^{2+} > Mg^{2+}$; for example, P-PR has binding constants of $7.33 \pm 0.25 \times 10^4$ M^{-1} for Ca^{2+}, $1.23 \pm 0.03 \times 10^4$ for Sr^{2+}, $4.24 \pm 0.09 \times 10^3$ for Ba^{2+}, and $4.04 \pm 0.24 \times 10^2$ for Mg^{2+}. The binding of Na^+ and K^+ with c-C-PR were weak, with binding constants of 56 M^{-1} and 11 M^{-1}, respectively.

The abilities of the diamide ligands, A23187, and X537A to enhance the rate of Ca^{2+} efflux from phospholipid vesicles are studied by a dialysis technique. The diamide ligands are less potent in enhancing membrane permeability to Ca^{2+} than A23187 and X537A. Lipid-soluble anions (tetraphenylborate, dipicrylamine, picrate, and 8-anilinonaphthalene-sulfonate (ANS^-)) markedly increase the rate and extent of Ca^{2+} transport mediated by the diamide ligands. The abilities of A23187, X537A, and the diamide ligands to transport Ca^{2+} across bilayer membranes are sensitive to the lipid composition of the vesicles.

At high cation concentration (1.5 M), the carboxylic acid ionophores, A23187, X537A, and nigericin induce a faster transport of K^+ and Na^+ across egg phosphatidylcholine (PC) vesicles than the neutral ionophores, valinomycin, c-C-PR, and dicyclohexyl-18-crown-6. At lower cation concentration (0.15-1.5 mM Ca^{2+} and 135 mM Na^+ or K^+), the transport of Ca^{2+} by A23187 is affected by the presence of Na^+ or K^+, indicating that

at close to physiological concentration of these cations, the selectivity of A23187 for Ca^{2+}, Na^{+}, and K^{+} is not complete. The rates of cation transport mediated by A23187 and c-C-PR are stimulated by the availability of an exchange mechanism among Ca^{2+}, Na^{+}, and K^{+}. The rates of c-C-PR- and A23187-induced Ca^{2+} transport are affected by a diffusion potential generated by valinomycin and K^{+}, indicating the electrogenic nature of c-C-PR- and A23187-mediated Ca^{2+} transport. In the absence of valinomycin and K^{+}, the initial rate of Ca^{2+} transport by A23187 has a second-order dependence on the A23187 concentration, indicating that a possibly neutral $(A23187)_2$-Ca^{2+} complex is the main species transported.

Complexation of Ca^{2+} bound to sarcoplasmic reticulum (SR) microsomes by the ionophores is studied using chlorotetracycline as a fluorescence probe. The abilities of the ionophores to decrease the fluorescence of chlorotetracycline (A23187 > X537A > N-PR > c-C-PR > c-C-5 > P-PR) parallel the abilities of the ionophores to induce net Ca^{2+} transport across vesicles made from SR lipids. Formation of diamide ionophore-Ca^{2+}-ANS^{-} complexes on dimyristoyl-PC vesicles is demonstrated.

Complexation of A23187 and X537A with Ca^{2+} in methanol, ethanol, and phospholipid vesicles are studied by UV and fluorescence spectroscopy. Evidence of the aggregation of A23187 was found. The aggregated state of A23187 binds Ca^{2+} with high affinity. The disaggregated state has low affinity for Ca^{2+}, possibly because of the solvation of the hydrophilic portion of A23187 by polar solvents.

ACKNOWLEDGMENTS

I wish to express my deepest gratitude to Professor Robert Bittman for helping me in every aspect of this thesis work. I am grateful to Dr. Irving J. Borowitz and Dr. W-O. Lin for supplying the neutral diamide ionophores. I wish to thank Dr. S. I. Chan of the California Institute of Technology, Dr. C-H. Huang of the University of Virginia School of Medicine, and Dr. E. Racker of Cornell University for discussions of some of the results I obtained.

The friendship and help of my colleagues (Dr. Lea Blau, Dr. Winston C-H. Chen, Mrs. Sanda Cleijan, Mr. Arun Dhundale, Mr. Yisrael Issacson, Mr. Zenowijz Majuk) and other members of the Chemistry Department of Queens College have made this study a wonderful experience. I also want to thank Mr. Robert Wurman's friendship and help in solving many electronic problems with instruments used in this research.

My family and friends, Ms. L. Sun, Mrs. S-M. Huang, Ms. L-H. Lin, Mr. Y-H. Shih, Mr. W. C-H. Chen have given me much moral support through the years of my graduate study. I also thank the Word Processing Center of Queens College and Ms. L-H. Lin for typing these manuscripts for publication.

Table of Contents

List of Figures

Part I: Two-Phase Extraction Properties of Neutral Diamide Ionophores for Group IIA Metal Cations

Part II : Binding Properties of Neutral Diamide Ligands for Alkaline-Earth Cations

List of Figures (Continued)

Part III : Ionophorous Properties of Neutral Diamide Ligands Toward Calcium

Part IV : Ionophorous Properties of Carboxylic Acid and Neutral Ionophores Toward Ca^{2+}, K^+, and Na^+ in Phosphatidylcholine Vesicles.

List of Figures (Continued) Page

List of Figures (Continued) Page

List of Tables

GENERAL INTRODUCTION

Ionophores are compounds of moderate molecular weight (about 200-2000) that form lipid-soluble complexes with cations, of which Ca^{2+}, Mg^{2+}, K^{+}, and Na^{+} are the most significant biologically. While the first-recognized ionophores were metabolites of microorganisms, several synthetic compounds were later found to have similar molecular properties (for reviews, see Pressman, 1976; Gómez and Gómez, 1977). In recent years, much interest in ionophore derives from the ability of the carboxylic acid ionophores, A23187 and X537A, to transport Ca^{2+} across biological membranes and hence modulate biological activities. More recently, a series of neutral diamides were developed by Simon's and Borowitz's groups (e.g., Ammann et al., 1973, 1975; Borowitz et al., 1977). These compounds were found to be specific for Group IIA cation in ion-selective electrodes. The purpose of this research is to investigate the binding and transport properties of these synthetic and naturally occurring ligands in order to provide insight into the molecular basis of ionophore action.

Some of the specific subjects delt with in this research are: (a) the selectivities of the ionophores and the molecular features desirable for binding and transporting cations (b) the behavior of ionophores in membranes as compared to that in organic solvent or aqueous-organic, two-phase systems (c) the effect of varying membrane composition on ionophore-mediated cation transport (d) the relationships among binding stoichiometries, charge on the ionophores, membrane potential, and ion-transport activity.

The thesis is devided into six parts. Part I deals with the selectivity of diamide ligands in extracting Ca^{2+} and picrate into an organic phase. Part II is a study of the binding stoichiometry and constants of the diamide ligands with Group IIA cations in methanol. In Part III, the effect of varying membrane composition on the ionophore-mediated Ca^{2+} transport is described. Part IV examines the transport selectivities of A23187, X537A, and cis-1,2-cyclohexanedioxydiacetic acid N,N,N',N'-tetra-n-propyl amide (c-C-PR) toward Ca^{2+}, K^{+}, and Na^{+}. Part V describes the complexation of the ionophores with Ca^{2+} bound to sarcoplasmic reticulum (SR) microsomes and the formation of ionophore-Ca^{2+}-8-anilinonaphthalenesulfonate (ANS^{-}) complexes on the dimyristoylphosphatidylcholine (DMPC) vesicles. Part VI is a study of the UV, and fluorescence spectra and binding properties of A23187 and X537A with Ca^{2+} in organic solvents and egg PC vesicles.

References:

Ammann, D., Bissig, R., Guggi, M., Pretsch, E., Simon, W., Borowitz, I. J., and Weiss, L. (1975), Helv. Chim. Acta 58, 1535-1548.

Ammann, D., Pretsch, E., and Simon, W. (1973), Helv. Chim. Acta 56, 1780-1787.

Borowitz, I. J., Lin, W-O., Wun, T-C., Bittman, R., Weiss, L., Diakiw, V., and Borowitz, G. B. (1977), Tetrahedron 33, 1697-1705.

Gomez-Puyou, and Gomez-Lojero (1977), Curr. Top. Bioenerg. 6, 221-257.

Pressman, B. C. (1976), Ann. Rev. Biochem. 45, 501-530.

Part I

Two-phase Extraction Properties of Neutral Diamide Ionophores For Group IIA Metal Cations.*

* This manuscript was published in Tetrahedron (1977), 33, 1697-1705. The preparations, UV spectra, preliminary proton and carbon-13 nmr studies of these ligands were described by Dr. I. J. Borowitz et al. in the same paper.

ABSTRACT: A series of neutral ligands featuring ether and N-methyl-N-carbethoxypentylamide groups as well as related ones bearing other diamide groups are shown to selectively chelate Group IIA cations by picrate extraction from water to methylene chloride. The observed selectivity sequences of cation extraction are briefly discussed.

Naturally occurring macrocyclic and acyclic ionophores are involved in the selective transport of essential metal cations across biological membranes (Chock and Titus, 1973; Prelog, 1971). Synthetic ionophores are of interest in that they provide model systems (Simon et al., 1973) which can be varied greatly in structure. They can solubilize metal cations in lipid-like solvents and are useful in applications such as cation analysis, catalysis, organic synthesis and the study of the mechanisms of ion transport across membranes.

Previously, an acyclic 1,2-ethylenedioxydiacetamide system was found to show selective Group IIA cation complexation (Simon et al., 1973). It was recently reported that aromatic and alicyclic analogues of this system display a wider range of selective binding properties in ion sensitive electrodes (Ammann et al., 1975). N-Methyl-N-carbethoxyundecylamides were originally used to enhance the lipophilic character of the potential ionophores and to give additional chelation sites. The Group IA and Group IIA cation selectivity of these ligands is somewhat less than

that exhibited by the corresponding N, N-dipropylamides (Ammann et al., 1975). The latter compounds are less soluble in the usual organic solvents than are the N-methyl-N-carbethoxyundecylamides and a compromise was sought via the use of the shorter and prepared from the acid chlorides. The ion selective behavior of the N-methyl-N-Carbethoxyundecylamides is about the same as that of the N, N-dipropylamides but their slight water solubility makes them less desirable for incorporation into liquid-membrane electrodes.

In this paper, the sectivities of various ligands was studied by picrate extraction. The extraction of metal cation picrates from water into an organic phase by a potential ligand provides a rapid screening of the selectivity of cation complexation of that ligand and a method for the comparison of the relative chelating abilities of different ligands.

EXPERIMENTAL SECTION:

Materials : The ligands were synthesized as described by Borowitz et al. (1977). The structures of these ionophores are shown in Figure 1. They are N, N-di-n-propyl amides of 1,2-phenylenedioxydiacetic acid (P-PR), 2,3-naphthalenedioxydiacetic acid (N-PR), and cis-and trans-1,2-cyclohexane-dioxydiacetic acids (c-C-PR and t-C-PR). The structures of the N-methyl N-carbethoxypentylamide of cis-1,2-cyclohexanedioxydiacetic acid (c-C-5), 1,2-phenylenedioxydiacetic acid N-methyl-N-octadecylamide (P-18), and cis-4-t-butyl-cis-1,2-cyclohexanedioxydiacetic acid N-methyl-N-5-carbethoxypentylamide (t-Bu-C-PR) are also shown.

Methods : Picrate extraction method was essentially that of Frendsdorff (1971). Aqueous solutions were made up from standardized stock solutions of picric acid by adding metal chlorides. The ionophores were dissolved in methylene chloride. Equal volumes of two solutions in stoppered centrifuge tubes were mixed and shaken in a vortex mixer for about 4 min. Phase separation was carried out in a table-top centrifuge.

Equilibrium picrate concentrations in both phases were determined with a Cary 14 spectrophotometer. Methods of determining picrate in the organic phase (the direct value and the value obtained by difference between total picrate and that in the aqueous phase) agreed well and the latter method was usually used. Picrate extinction coefficients in water (14,500 M^{-1} cm^{-1} at 354 nm) or methylene chloride (18,000 M^{-1} cm^{-1} at 370 nm) were determined in separate runs.

The data in Table 2 were obtained using test tubes containing an aqueous solution of 7.0×10^{-5} M picric acid and 1.4×10^{-4} M $CaCl_2$ with a trace amount of $^{45}CaCl_2$ (1.0 ml) to which was added methylene chloride (1.0 ml, with or without dissolved c-C-PR). The test tubes were capped, vortexed vigorously, rotated at 40 rpm for 15 min., and then centrifuged using a table-top centrifuge for about 5 min. Aliquots of the aqueous layer were taken for measurement of picrate absorbance at 356 nm with a Cary 14 spectrophotomer and for radioactivity counting with a Beckman LS 250 liquid scintillation counter. The net amount of Ca^{2+} transferred to the organic phase in the presence of picric acid was obtained by subtracting the amount of Ca^{2+} transferred in the absence of picric acid from the amount of Ca^{2+} transferred in its presence (see Table 2).

Results :

Extraction of metal cation picrates by the ligands. Table 1 summarizes the relative extractability of cations by various ligands. The cis ligands c-C-PR (Table 1) and c-C-5 (data not shown) behave similarly and extract cations in the order: $Ca^{2+} > Ba^{2+} \sim Mn^{2+} > Sr^{2+} > La^{3+} > Mg^{2+} > Na^{+}$. Thus the carbethoxypentyl group in c-C-5 did not enhance the ability of the ligand to extract cations. Both c-C-PR and c-C-5 show a high M^{2+}/M^{+} selectivity even in methylene chloride (dielectric constant= 9). Such selectivity should be enhanced in solvents of higher polarity (Morf and Simon, 1971). Incorporation of a tert-butyl group into c-C-PR produces a conformationally more rigid molecule; t-Bu-C-PR is somewhat less potent in its ability to extract Group II cations, but the selectivity sequence is retained. Thus some flexibility is apparently desirable in the cis-cyclohexanedioxy moiety. The trans isomer, t-C-PR, extracts less Group IIA cations than the cis - isomer c-C-PR. The 1,2-phenylenedioxy ligand P-PR and the naphthalenedioxy ligand N-PR extract cations to a lesser extent than t-C-PR and do so in the order: $Ba^{2+} \sim Sr^{2+} > Ca^{2+} > Mg^{2+} \sim Mn^{2+}$.

Ligands c-C-PR and c-C-5 extract Ca^{2+} much more effectively (76-85% of the total Ca^{2+} is extracted by 10-16 fold excess of ligand to picric acid at 10^{-2} M cation) than does dicyclohexyl-18-crown-6 ($\sim$ 10% of Ca^{2+} extracted by a 20-fold excess of ligand to picric acid at 10^{-2}M cation). Our ligands are generally selective for the complexation of the Group IIA cations while the crown ethers complex both Group IA and IIA cations (Pedersen and Frensdorff, 1972).

In picrate extraction measurements, the assumption is made that only picrate anions are transferred and not Cl^- which is used in the in situ preparation of the metal cation picrates. This was shown to be valid for the extraction of monovalent cation picrates with the actins by Eisenman et al., (1969). Data for divalent cation picrates have not been available. Since the estimate of the extent of cation transfer could be complicated by the transfer of picric acid, we measured the extent of picric acid transfer by each ligand. Although the transfer of picric acid is not insignificant, it is occasionally somewhat higher than the transfer of some picrates such as magnesium picrate (see Tables 1). This suggests that these ligands have affinity for protons as has been shown in ion-selective membrane measurements (Ammann, et al., 1975). The following data helped to validate the use of the picrate extraction method for divalent cations.

The transfer of $^{45}CaCl_2$ from water to methylene chloride without picric acid by c-C-PR was less than 5% of that obtained in the presence of picric acid (see Experimental Section and Table 1). In the presence of picric acid, such extractions gave picrate/$^{45}Ca^{2+}$ transfer ratios of 2.0. Furthermore, the percent of Ca^{2+} transferred by c-C-PR with calcium picrate alone or with calcium picrate-$CaCl_2$ containing varying amounts of excess Cl^- varied by only 3%. Much larger variation is expected if Cl^- were transferred. Thus the use of picrate transfer to estimate the amount of divalent cation transfer in our systems seems to be justified.

Discussion :

The extraction of cation picrates is mainly useful for the qualitative comparision of the relative ability of different ligands to transfer cations from water to an organic phase and for the relative ordering of cation transfer for a given ligand. The aromatic ring-containing ligands, P-PR and N-PR, transfer the Group IIA cations in the order: $Ba^{2+} \sim Sr^{2+} > Ca^{2+} > Mg^{2+}$, the same ordering found for their selectivity when incorporated in ion-selective liquid membrane electrodes by Ammann et al. (1975). A rationalization for this selectivity sequence is that it is related in an inverse manner to the free energies of hydration of the cations (Noyes, 1962;1964), i.e., the most strongly hydrated cation, Mg^{2+}, is the most difficult to transfer from water to an organic phase. Furthermore, this ordering is generally found for the binding of these cations to large anions (usually of strong acids); the larger cations can pack larger anions around themselves more easily (Williams, 1970). Perhaps such an argument can be extended to our chelated cations with the relatively large picrate counterions. The situation is more complicated, however, for the ligands c-C-PR and t-C-PR which transfer: $Ca^{2+} > Ba^{2+} > Sr^{2+}$ and $Ca^{2+} > Ba^{2+}, Sr^{2+}$, respectively, but show ion-selective electrode behavior (Chock and Titus, 1973) in the ordering: $Ca^{2+} > Sr^{2+} > Ba^{2+} \gg Mg^{2+}$ for both ligands. Among the reasons for the non-correspondence of the ordering obtained by these different methods which involve organic phase/water interfaces may be the differing polarities of the organic phase, the different stoichiometries of binding that probably pertain in these methods (Kirsch and Simon, 1976),

and the influence of ion-pairing especially in the picrate method (D. Haynes, private communication). The ligands P-PR and N-PR may be simpler in their behavior in that 1:1 stiochiometry of complexation is perhaps more readily obtained under a variety of conditions than with the other ligands. Assuming the yet unproven complexation of amide oxygen rather than nitrogen, the "cavity" formed by the ether oxygens and amide oxygens in a square-planar array is measured by Corey-Pauling-Koltun space-filling models to be 2.4 Å for P-PR and 2.0-2.2 Å for c-C-PR and t-C-PR. The flexible nature of the "cavity" observed does not allow firm conclusions, however.

It is of interest that the cis-ligand c-C-PR transfers more cation picrate than does the trans-ligand t-C-PR. Too rigid a structure causes a small decrease in the amount and selectivity of cation transfer (compare c-C-PR with its 4-tert-butyl derivative t-Bu-C-PR). As anticipated, the aromatic ring-containing ligands, P-PR and N-PR, which have less basic ether oxygens, transfer much less cation picrate. A similar situation occurs with dibenzo-18-crown-6 vs. dicyclohexyl-18-crown-6 (Frensdorff, 1971).

References

Ammann, D., Bissig, R., Güggi, M., Pretsch, E., Simon, W., Borowitz,I.J., and Weiss, L. (1975), Helv. Chim. Acta 58, 1535.

Borowitz, I.J., Lin, W-O., Wun, T-C., Bittman, R., Weiss, L., Diakiw, V., and Borowitz, G. B. (1977), Tetrahedron 33, 1697.

Chock, P.B., and Titus, E.O. in Lippard, S.J. "Progress in Inorg. Chem." Vol. 18, J. Wiley, New York, 1973, pp. 287-382.

Eisenman, G., Ciani, S., and Szabo, G. (1969), J. Memb. Biol. 1, 294.

Frensdorff, H. J. (1971), J. Amer. Chem.Soc., 93, 4684.

Kirsch, N.N.L., and Simon, W. (1976), Helv. Chim. Acta 59, 357.

Morf, W.E., and Simon, W. (1971), Helv. Chim. Acta 54, 2683.

Noyes, R. (1962), J. Amer. Chem. Soc., 84, 513.

Noyes, R. (1964), ibid., 86, 971.

Pedersen, C.J., and Frensdorff, H.K., (1972), Agnew. Chemie Int. Ed. Engl., 11, 16.

Prelog, V. (1971), Pure and Appl. Chem., 25, 197.

Simon, W., Morf, W.E., and Meier, P. Ch., "Structure and Bonding", Vol. 16, Springer Verlag, New York, 1973, pp. 113-160.

Williams, R.J.P. (1970), Quart. Rev. 24, 331.

TABLE 1 : Cation Picrate Extraction by Ligands[a]

	Fraction of Cation Extracted					
Ligand	Ca^{2+}	Sr^{2+}	Ba^{2+}	Mg^{2+}	Mn^{2+}	Picric Acid[b]
c-C-PR	0.84	0.43	0.50	0.15	0.50	0.14
t-C-PR	.37	.15	.19	.05	.50	.06
c-C-5	.64	.25	.30	.19	.29	.21
P-PR	.06	.11	.12	.04	.05	.05
N-PR	.06	.10	.12	.05	.05	.06
P-18	.10	.12	.13	.09	.09	.11
t-Bu-C-PR	.70	.28	.43	.07	.31	.07

---

[a] Experimental procedures as described except : done between equal volumes (1.5 ml) of water and CH_2Cl_2 at 26°. Ligand= 7.0×10^{-4} M, picric acid = 6.86×10^{-5} M, cation = 1.0×10^{-2}M using MCl_2. The error limit is estimated to be less than 0.01 for extractions performed in triplicate. [b] Fraction extracted = 0.04 without ligand. Done on a Cary 14 spectrophotometer.

TABLE 2 : Two-Phase Extraction of $^{45}Ca^{2+}$ by c-C-PR with and without Picric Acid

		Species Transferred[a]			
Conditions	Conc. c-C-PR	Total $^{45}Ca^{2+}$	Picrate	Net $^{45}Ca^{2+}$[b]	Mole Ratio $Pic^-/^{45}Ca^{2+}$
A. with Picric Acid	1.51×10^{-3}M	1.76×10^{-8}mol	3.44×10^{-8}mol	1.66×10^{-8}mol	2.07
	3.02×10^{-3}	2.60×10^{-8}	4.71×10^{-8}	2.52×10^{-8}	1.87
	6.04×10^{-3}	2.99×10^{-8}	5.65×10^{-8}	2.90×10^{-8}	1.95
B. without Picric Acid	1.51×10^{-3}M	0.098×10^{-8}mol			
	3.02×10^{-3}	0.080×10^{-8}			
	6.04×10^{-3}	0.087×10^{-8}			

[a] From water to methylene chloride. [b] Obtained by A - B.

FIG. 1

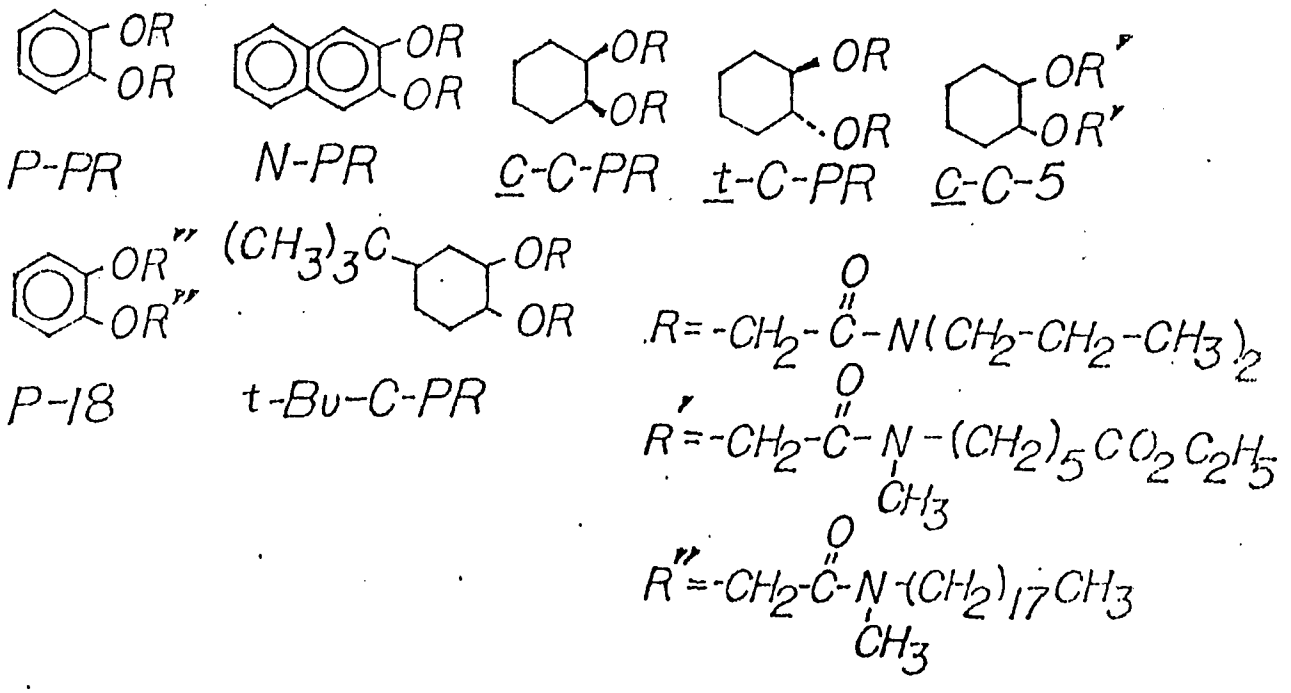

Part II

Binding Properties of Neutral Diamide Ligands for Alkaline-Earth Cations.*

* This manuscript was published in Biochemistry (1977), 16, 2074-2079.

ABSTRACT: The complexation of a series of aromatic and alicyclic N,N-di-n-propyl amides of 1,2 - ethylenedioxydiacetic acids with Group IIA metal ion bromides in anhydrous methanol was investigated by ultraviolet absorption spectroscopy. These synthetic ligands were previously found to show selectivity toward divalent over monovalent cations with respect to extraction of ions into bulk organic phase (Borowitz, I.J., Lin, W-O., Wun, T-C., Bittman, R., Weiss, L., Diakiw, V., and Borowitz, G.B. (1977), Tetrahedron,33 1697-1705). At low concentrations, ligands bearing benzene and naphthalene rings form 1:1 ligand to divalent cation complexes with each of the alkaline - earth metals, but ligands in the cyclohexyl series are stoichiometrically bound to cations in more than one type of complex. Binding isotherms obtained by Scatchard anaylsis and by the method of continuous variation revealed ligand to divalent ion mole ratios of 2:1, 3:2, and 4:3 for binding of cis - 1, 2- cyclohexanedioxydiacetic acid N,N- di-n-propyl amide with Ca^{2+}, Sr^{2+}, and Ba^{2+}, respectively. In contrast, Scatchard analysis of ultraviolet spectral changes showed that a 1:1 complex is formed between this ligand and Na^{+} with an apparent association constant of 56±2 M^{-1}; the constant for binding with K^{+} was smaller (11 M^{-1}). The order of apparent association equilibrium constants for complexation of Group IIA cations with this series of neutral ligands was $Ca^{2+}>Sr^{2+}>Ba^{2+}>Mg^{2+}$; for example, for 1,2- phenylenedioxydiacetic acid N,N- di-n-propyl amide the apparent binding constants at 25° were $7.33\pm0.25 \cdot 10^{4}$ M^{-1} for Ca^{2+}, $1.23\pm0.03 \cdot 10^{4}$ for Sr^{2+}, $4.42\pm0.09 \cdot 10^{3}$ for Ba^{2+}, and $4.04\pm0.24 \cdot 10^{2}$ for Mg^{2+}. The divalent cation binding properties of these synthetic diamide ligands are discussed in relation to those of other synthetic ligands and of two naturally occurring ligands.

For the design of synthetic multidentate compounds suitable for selective complexation with a large array of metal ions, some definitive information is available concerning the relationship between the structure of coordinating sites and selectivity toward different univalent cations (e.g., Pedersen, 1967,1270; Frensdorff, 1971; Pedersen and Frensdorff, 1972; Christensen et al., 1974; Vögtle and Weber, 1974; Koenig et al., 1976). Little information is available, however, regarding the structural features in ligands that govern selective complex formation with divalent metal ions (Morf and Simon, 1973; Lehn and Sauvage, 1975). We have recently accomplished the synthesis of a series of neutral 1,2-ethylene-dioxydiacetamide ligands, and investigated their relative selectivities toward various metal ions with respect to solubilization of group IA and group IIA cations in bulk organic phase (Borowitz et al., 1977). In this paper we describe quantitative measurements of the interaction of these ligands with alkaline-earth metal ions.

Experimental Section

Materials:

Anhydrous $CaBr_2$ $SrBr_2$, $BaBr_2$ (obtained from ROC/RIC), and $Ba(SCN)_2$ (obtained from Alfa Inorganics) were used as received and kept under nitrogen in a dessicator. Magnesium bromide · $6H_2O$ was supplied by Fisher Scientific Co. Anhydrous methanol (Matheson, Coleman & Bell) was spectral grade. The ligands were synthesized as described previously (Ammann et al., 1975; Borowitz et al., 1977). Figure 1 shows the structure of the N,N- di-n-propyl amides of 1,2- phenylenedioxydiacetic acid (P-PR), 2,3-naphthalenedioxydiacetic

acid (N-PR), and cis - and trans -1,2-cyclohexanedioxydiacetic acids (c-C-PR and t-C-PR). The structure of 1,2-phenylenedioxydiacetic N-methyl-N-octadecylamide (P-18) is also shown.

Methods:

Measurement of Metal Ion Binding to Ligands. Absorption spectra were measured using a Cary 14 spectrophotometer. Spectral titrations were carried out at room temperature (20°) using a 0-0.1 slidewire and a cell of 10-cm pathlength and 28-ml capacity, or a 1-cm cell of 6-ml capacity and a 0-0.1 or 0-1 slidewire. Concentrated solutions of ligands and metal bromides were prepared in methanol. Aliquots of these solutions were added by microsyringe to methanolic solutions of ligands. The total volume of added cation solution was less than 0.2 ml. The absorbance changes were corrected for the absorption of the metal bromide in the absence of ligands. Titration of N-PR was carried out at 324nm. Titrations of P-PR and P-18 were conducted at 280nm for $CaBr_2$ and $SrBr_2$ and 283nm for $BaBr_2$. Titrations of c-C-PR and t-C-PR were done at 230nm.

The stoichiometry of the binding of metal ions to the ligands was determined by the method of continuous variation (Job, 1928). The Job plots were obtained by plotting the absorbance change vs. the mole fraction of metal ion relative to the sum of the cation and ligand concentrations; during the titration the sum of the cation and ligand concentrations was maintained constant. The sum of the concentrations and the range of ratios over which the relative concentrations were varied are indicated in the figure captions.

The mole fraction at which the maximum absorbance change occurs and the ratio of the slopes of the linear portions of the two lines give the stoichiometry of the binding.

Apparent association constants, K_{app}, for metal ion binding to ligands were determined from Scatchard plots (1949). The concentration of ligands was maintained constant in the titration. Binding isotherms were constructed from data obtained by two methods. In method A, the stoichiometry of binding is known to be 1:1 from the Job plot. The Scatchard equation, $r/C=K_{app}(n-r)$, is used to obtain K_{app}, by plotting r/C vs. r, where r is the molar ratio of cation bound to the total ligand, C is the molar concentration of free cation, and n is the number of moles of cation bound per mole of ionophore (1.0). The value of r is calculated from $r=\Delta A/\Delta A_m$, where ΔA is the absorbance change and ΔA_m is the maximum absorbance change. The latter is determined at saturating concentrations of metal ions. The value of C is calculated from $C=C_T-(\Delta A/\Delta A_m)\cdot[L]$, where C_T is the total cation concentration added, and L is the ligand concentration. The value of K_{app} is calculated from the binding isotherm by an iterative procedure. An initial value of ΔA_m is obtained from experiments where cation is in large excess. This value is used to calculate C by the above equation. A slightly different value of ΔA_m is obtained from the intercept of a double-reciprocal plot of ΔA vs. C. This ΔA_m is then used to recalculate r and C. The procedure is repeated until the best fit is obtained for the extrapolated line of the Scatchard plot to a value of unity.

(The x-intercept of the extrapolated straight line of the Scatchard plot gives the stoichiometry of binding,which was determined from Job plot data to be one mole of cation bound per mole of ligand.) The negative of the slope gives K_{app}. The values of K_{app} and n are determined by a least-squares analysis. Note that the beginning part of the titration gives data points at low r values. Method B was used when the stoichiometry of binding was found to be other than 1:1 in the Job plot; the Scatchard equation, $R/L = K_{app}(N-R)$, is used to obtain K_{app} by plotting R/L vs R. Here R is the molar ratio of ligand to the cation added, L is the molar concentration of free ligand, and N is the number of moles of ligand bound per mole of cation. The value of R is calculated from $R=L_T \cdot (\Delta A/\Delta A_m)/C_T$, where L_T is the total ligand concentration. C_T is the total concentration of cation. The value of L is calculated from $L = L_T - L_T \cdot (\Delta A/\Delta A_m)$. Note that the beginning part of the titration corresponds to data points at large R values in this plot.

Results

UV Spectra. The absorption spectra of P-PR, P-18, and N-PR are shown in Figure 2 A,B, and C (solid curves). Upon addition of $CaBr_2$ or $Ba(SCN)_2$, the spectra changed with distinctive isosbestic point(s). Addition of other divalent salts ($SrBr_2$,$BaBr_2$,$MgBr_2$) caused similar changes (spectra not shown). Addition of divalent cations to c-C-PR (Figure 2E) and t-C-PR (spectrum not shown) caused decreases in extinction coefficients at shorter wavelengths.

Stoichiometry and Binding Constants of P-PR-M^{2+} and N-PR-M^{2+} Complexation.

Job and Scatchard plots of the titrations of metal ion binding to P-PR and N-PR showed that a single class of binding sites is present over the concentration ranges of the ligands and the metal ions used (Figure 3). The Scatchard plots shown in Figure 3B for the interaction of $CaBr_2$ with P-PR and N-PR in methanol are similar to those obtained for the binding of $SrBr_2$ and $BaBr_2$ to these ligands. The number of binding sites is 1.0 mole of M^{2+} per mole of ligand. The binding of $MgBr_2$ to N-PR shows other than 1:1 complexation at the beginning of titration, but the molar ratio in the latter part of titration (approaching saturation) appears to be 1.0 (Figure 3C).

When higher ligand concentrations are used, deviation from 1:1 stoichiometry is observed. A Scatchard plot of Ca^{2+} binding to P-PR at a ligand concentration of 6.6×10^{-4}M shows that at the beginning of the titration species higher than 1:1 complexes are present in the solution (Figure 4); however, the stoichiometry approaches a molar ration of 1.0 at the end of the titration. For N-PR, deviation from Beer's law was found in the concentration range of 10^{-4}-10^{-3}M, suggesting possible aggregation of ligand. The Job plot is asymmetrical and the Scatchard plot shows deviation from 1:1 complexation (data not shown) at this concentration.

Complexation of c-C-PR and t-C-PR with M^{2+} and c-C-PR with Na^+ and K^+ in Methanol. The Job plot of the binding of $CaBr_2$ to c-C-PR shows a 2:1 ligand to ion ratio (Figure 5A). The Scatchard plot (Figure 5B) confirms this stoichiometry and gives a binding constant of $8.70 \pm 0.24 \cdot 10^4 M^{-1}$, which is the highest for this series of ligands.

The Scatchard plot of Na^+ - c-C-PR binding (insert, Figure 5B) shows that a 1:1 complex is formed and gives an apparent association constant of $56\pm2M^{-1}$. Scatchard analysis of the titration data for the interaction of c-C-PR with K^+ gives a binding constant of approximately 11 M^{-1}. (Because of the limited solubility of KBr in methanol, only the beginning part of the titration could be performed.) Thus the association of c-C-PR with Na^+ is stronger than that with K^+, but with each of these cations the magnitude of the binding constant is low.

Figure 6A shows the Job plot of the binding of $SrBr_2$ to c-C-PR. The maximum absorption change occurs at a Sr^{2+} mole ratio of 0.4 and the slope ratio is 1.5. Hence the ligand to ion ratio of c-C-PR-Sr^{2+} binding is 1.5:1. Figure 6B shows the Job plot of the interaction of $BaBr_2$ with c-C-PR, giving a slope ratio of 1.3:1. The Scatchard plot (Figure 6C) confirms these stoichiometries and gives binding constants of $2.26\pm0.10\cdot10^4M^{-1}$ for $SrBr_2$ and $1.07\pm0.09\cdot10^4$ M^{-1} for $BaBr_2$.

Figure 7A shows the Job plot of t-C-PR-Ca^{2+} binding. The maximum absorption change occurs at a Ca^{2+} mole ratio of 0.5, but the curve is asymmetrical with a slope ratio of 1.5. The Scatchard plot (Figure 7B) confirms these parameters, showing that the ligand to ion ratio is 1.5:1 at the beginning part of the titration and 1:1 at saturation.

Complexation of P-18 with Ca^{2+}. Figure 8 shows the Scatchard plot of the binding of $CaBr_2$ to P-18. The ligand to cation mole ratio is 0.38:1. It is possible that self-association of P-18 may account for this behavior even though P-18 may have the same binding sites as the other ligands.

A summary of the binding constants of these ligands with divalent cations in methanol shows that for P-Pr, N-Pr, and c-C-PR, the order of binding with divalent cations is $Ca^{2+} > Sr^{2+} > Ba^{2+} > (Mg^{2+})$ (Table 1). For each divalent cation (except Mg^{2+}), the order of affinity toward ligand has the general trend of c-C-PR>P-PR≈N-PR.

Discussion

The combined use of the methods of continuous variation and of Scatchard plots provide data concerning the stoichiometry and binding constant of complexation in solution.

At low concentrations, the aromatic ligands, P-PR and N-PR, form 1:1 ligand:divalent cation complexes with all of the alkaline-earth metals in methanol, whereas with ligands in the cyclohexyl series a 2:1 ligand to ion complex is formed with Ca^{2+} by c-C-PR, and both 3:2 and 1:1 complexes are formed with Ca^{2+} by t-C-PR. In addition, the stoichiometry of the complex formed by c-C-PR depends on the divalent cation (Table I). Variations in ion-binding stoichiometries have been reported for other ionophores. Cyclic polyethers, which form 1:1 complexes with many cations (Pedersen, 1967), also form complexes having polyether to metal mole ratios of 2:1 and 3:2, depending on the sizes of the cavity and cations (Pedersen, 1970; Frensdorff, 1971). The carboxylic ionophorous antibiotic A23187 forms 2:1 ligand to cation complexes with alkaline-earth metals in ethanol (Pfeiffer et al., 1974; Deber and Pfeiffer, 1976) and in the crystalline state (Smith and Duax, 1976) but 1:1 as well as nonintegral mole ratios have been reported with these cations under other conditions (Alpha and Brady, 1973; Case et al., 1974). The polyether, carboxylic ionophorous antibiotic X537A also forms 2:1 and 1:1 ionophore to divalent cation complexes (Degani and Friedman, 1974; Caswell and Pressman, 1972; Johnson et al., 1970). The depsipeptide monovalent ionophore valinomycin forms both 1:1 and 2:1 ionophore to K^+ complexes in ethanol, depending on the cyclopeptide concentration (Ivanov, 1975). Both 1:1 and 2:1 complexation of ligand with $CaCl_2$

was reported with an acyclic ligand (a derivative of dioxaoctanediacetamide) at high ligand concentration (Büchi and Pretsch, 1975). This variation in mole ratios in complexes formed by the synthetic ligands and well-known ionophores suggests that ion-binding properties are sensitive to changes in ligand-ligand interactions, ligand conformation, and cation size and charge. Studies on the possible participation of the aromatic ring in the interaction of cation with our ligands are in progress. These studies may clarify the origin of the differences found in stoichiometry for aromatic and nonaromatic ligands.

The relatively small difference in the apparent binding constants of P-PR and C-PR for Ca^{2+} may arise because opposing factors in P-PR partially offset each other. Relative to C-PR, P-PR has a higher dipole moment because of colinearity of the side chains. This effect is expected to increase the association contants (Simon et al., 1973). Opposed to this is the lower basicity of the coordinating sites in the aromatic ligand. This tends to weaken the interaction with cations, as shown for dibenzo-18-crown-6 relative to the dicyclohexyl analog (Pedersen and Frensdorff, 1972).

The fact that c-C-PR forms a 2:1 complex with Ca^{2+} (Figure 5) suggests a possible correlation between ion-binding stoichiometry of neutral carrier molecules and their ion-transporting activity. We have found that c-C-PR transports Ca^{2+} across artificial membranes faster than N-PR and P-PR, which form 1:1 complexes with

Ca^{2+} (Wun and Bittman, 1977). The ion in a 2:1 ligand to cation complex may be better shielded from the hydrophobic membrane interior than cation in a 1:1 complex, resulting in more facile transmembrane ion transport.

Complex formation in solution may involve various species. In an equilibrium of the type $nL+M \rightleftharpoons L_nM$, where L and M are interacting components, species such as LM, $L_2M....L_{n-1}$ and L_nM may coexist in solution. At high ligand concentration and high ligand to cation ratio, complexes having ligand to cation mole ratios higher than 1:1 may exist in solution, causing deviations from 1:1 stoichiometry at the beginning of some of the titrations (Figures 4 and 7). However, a simple 1:1 stoichiometric relationship is found when titrations are performed at lower ligand concentrations (Figure 3). The $MgBr_2$ used has 6 molecules of hydration. The low association constant of ligand $-Mg^2$ binding (Table I) and the deviation from 1:1 stoichiometry for N-PR-Mg^{2+} interaction (Figure 3C) are not likely to arise from the small amount of H_2O ($\sim$ 0.07% at the end of titration) present; further addition of H_2O to a final concentration of 0.14% in the titrated solution did not cause appreciable dissociation of the complex, as judged from the absorbance of the solution.

The order of apparent binding strengths for complexation with divalent cations ($Ca^{2+} > Sr^{2+} > Ba^{2+} > Mg^{2+}$) found for each ligand (Table I) may indicate that a field-strength effect is operative,

i.e., stronger binding by the smaller and more intensely charged ions. This suggests that in complex formation ion-dipole interaction between the cation and the negative dipoles of the ligand is important. Magnesium ion may deviate because its small radius does not allow efficient "packing" of all of the necessary chelating sites (the "radius-ratio" effect as described by Williams, 1970).

The order of binding affinity obtained for the synthetic ligands toward alkaline-earth cations ($Ca^{2+} > Sr^{2+} > Ba^{2+} > Mg^{2+}$) differs from the ion complexation order found for X537A in methanol and in two-phase extraction studies ($Ba^{2+} > Sr^{2+} > Ca^{2+} > Mg^{2+}$) (Degani et al., 1973; Degani and Friedman, 1974; Pressman, 1973), A23187 in aqueous media ($Ca^{2+} > Mg^{2+} \gg Sr^{2+} \gg Ba^{2+}$) (Pfeiffer et al., 1974), and polyanionic acyclic ligands in aqueous media (generally $Ca^{2+} > Mg^{2+} > Sr^{2+} > Ba^{2+}$) (Sillen and Martell, 1964, 1971). It also differs from the selectivity sequences displayed by two types of electrically neutral polycyclic ligands that form inclusion complexes with cations, the diazapolyoxamacrobicyclic ligands ("cryptands") and the cyclic polyethers. Cryptands having large cavity size display the sequence $Ba^{2+} > Sr^{2+} > Ca^{2+} > Mg^{2+}$ (Lehn and Sauvage, 1975). Dicyclohexyl-18-crown-6 in aqueous solution has the selectivity sequence $Ba^{2+} > Sr^{2+} \gg Ca^{2+}, Mg^{2+}$ (Izatt et al., 1971). The order we found is the same as the selectivity sequence obtained in liquid membrane electrodes for a dioxaoctane diacetamide ligand (Kirsch and Simon, 1976); however, the order of binding affinity found for the interaction in ethanol of the alkaline-earth ions with the

latter ligand differs from this sequence. The ordering $Ca^{2+} > Sr^{2+} > Ba^{2+} \gg Mg^{2+}$ is also found in aqueous solution for proteins such as troponin and some extracellular enzymes (Williams, 1970) and for ligands such as 3-oxadiacetic acid and 1,2-bis-(carboxymethoxy) ethane (Miyazaki et al., 1974) and 1,2-phenylenedioxydiacetic acid (Suzuki et al., 1968). The ligands we describe here appear to be novel in that they display a moderate degree of selectivity for Ca^{2+} over the other alkaline-earth metal ions while retaining a marked selectivity for divalent vs. monovalent cations.

Since the existence of selective complexation does not necessitate high stability, it is also of interest to compare the stability constants of the complexes formed by our ligands with those of natural and other synthetic ligands. The apparent binding constants for association of the synthetic ligands with Ca^{2+} in methanol (Table 1) are comparable, and even slightly higher, than that found for X537A-Ca^{2+} complexation in methanol (Degani et al., 1973), in 80% ethanol and 50% methanol (Caswell and Pressman, 1972), and in absolute ethanol (Cornelius et al., 1974). Our ligands form stronger complexes with alkaline-earth cations in methanol than do the dioxaoctanediacetamide ligands bearing N-phenyl or N-(W-carbethoxyundecyl) groups in ethanol (Kirsch and Simon, 1976). However, the macrobicyclic cryptands form much tighter complexes with these ions in 95% methanol (Lehn and Sauvage, 1975).

References

Alpha, S.R., and Brady, A.H. (1973), J. Amer. Chem. Soc. 95, 7043-7049.

Ammann, D., Bissig, R., Güggi, M., Pretsch, E., Simon, W., Borowitz, I.J., and Weiss, L. (1975), Helv. Chim. Acta 58, 1535-1548.

Borowitz, I.J., Lin, W-O., Wun, T-C., Bittman, R., Weiss, L., Diakiw, V., and Borowitz, G. B. (1977), Tetrahedron, in press.

Büchi, R., and Pretsch, E. (1975), Helv. Chim. Acta 58, 1573-1583.

Case, G. D., Vanderkooi, J.M., and Scarpa, A. (1974), Arch. Biochem. Biophys. 162, 174-185.

Caswell, A. H., and Pressman, B.C. (1972), Biochem. Biophys. Res. Commun. 49, 292-298.

Christensen, J.J., Eatought, D.J., and Izatt, R.M. (1974), Chem. Rev. 74, 351-384.

Cornelius, G., Gärtner, W., and Haynes, D.H. (1974), Biochemistry 13, 3052-3057.

Deber, C.M., and Pfeiffer, D.R. (1976), Biochemistry 15, 132-140.

Degani, H., Friedman, H.L., Navon, G., and Kosower, E.M. (1973), J. Chem. Soc. Chem. Commum., 431-432.

Frensdorff, H. K. (1971), J. Amer. Chem. Soc. 93, 600-606.

Ivanov, V.T. (1975), Ann. N. Y. Acad. Sci. 264, 221-243.

Izatt, R.M., Nelson, D.P., Rytting, J.H., Haymore, B.L., and Christensen, J.J. (1971), J. Amer. Chem. Soc. 93, 1619-1623.

Job, P. (1928), Ann. Chim. 9, 113-203.

Johnson, S.M., Herrin, J., Liu, S.J., and Paul, I.C. (1970), J. Amer. Chem. Soc., 92, 4428-4435.

Kirsch, N.N.L., and Simon, W. (1976), Helv. Chim. Acta 59, 357-363.

Koenig, K.E., Helgeson, R.C., and Cram, D.J. (1976), J. Amer. Chem. Soc. 98, 4018-4020.

Lehn, J.M., and Sauvage, J.P. (1975), J. Amer. Chem. Soc. 97, 6700-6707.

Miyazaki, M., Shimoishi, Y., Miyata, H., and Toei, K. (1974), J. Inorg. Nucl. Chem. 36, 2033-2038.

Morf, W. E., and Simon, W. (1973), Helv. Chim. Acta 54, 2683-2704.

Pedersen, C. J. (1967), J. Amer. Chem. Soc. 89, 7017-7036.

Pedersen, C. J. (1970), J. Amer. Chem. Soc. 92, 386-391.

Pedersen, C. J., and Frensdorff, H. (1972), Angew. Chem. Int. Ed. Engl. 11, 16-25.

Pfeiffer, D. R., Reed, P. W., and Lardy, H.A. (1974), Biochemistry 13, 4007-4014.

Pressman, B.C. (1973), Fed. Proc. 32, 1698-1703.

Scatchard, G. (1949), Ann. N.Y. Acad. Sci. 51, 660-672.

Sillen, L. G., and Martell, A.E. (1964), Chem. Soc. Spec. Publ. No.17.

Sillen, L. G., and Martell, A. E. (1971), Chem. Soc. Spec. Publ. No. 25.

Simon, W., Morf, W.E., and Meier, P.Ch. (1973), Struct. Bonding (Berlin) 16, 113-160.

Smith, G.D., and Duaz, W.L. (1976), J. Amer. Chem. Soc., 98, 1578-1580.

Suzuki, K., Hattori, T., and Yamasaki, K. (1968), J. Inorg. Nucl. Chem. 30, 161-166.

Vögtle, F., and Weber, E. (1974), Angew. Chem.Int. Ed. Engl. 13, 149-150.

Williams, R.J.P. (1970), Quart, Rev., Chem. Soc. 23, 331-365.

Wun, T-C., and Bittman, R. (1977), Biochemistry 16, 2080-2086.

Table I: Stoichiometry and Binding Constants for Interaction of Ligands and Divalent Cations in Methanol.

Ligand	Ligand Concentration (M)	Salt	Molar Ratio of Ligand : M^{2+}	K_{app} [a]
P-PR	1.13×10^{-5}	$CaBr_2$	1:1	$7.33\pm0.25\cdot10^4$
	6.60×10^{-4}	$CaBr_2$	1.35:1 and 1:1	-
	1.13×10^{-5}	$SrBr_2$	1:1	$1.23\pm0.03\cdot10^4$
	1.13×10^{-5}	$BaBr_2$	1:1	$4.42\pm0.09\cdot10^3$
	1.13×10^{-5}	$MgBr_2$	1:1	$4.04\pm0.24\cdot10^2$
N-PR	5.53×10^{-6}	$CaBr_2$	1:1	$4.81\pm0.21\cdot10^4$
	5.53×10^{-6}	$SrBr_2$	1:1	$1.09\pm0.03\cdot10^4$
	5.53×10^{-6}	$BaBr_2$	1:1	$3.98\pm0.08\cdot10^3$
	5.25×10^{-6}	$MgBr_2$	1:1	$4.70\pm0.28\cdot10^2$
c-C-PR	9.63×10^{-5}	$CaBr_2$	2.08:1	$8.70\pm0.24\cdot10^4$
	9.63×10^{-5}	$SrBr_2$	1.54:1	$2.26\pm0.10\cdot10^4$
	9.63×10^{-5}	$BaBr_2$	1.31:1	$1.07\pm0.09\cdot10^4$
t-C-PR	9.63×10^{-5}	$CaBr_2$	1.5:1 and 1:1	$7.72\pm0.34\cdot10^4$ [b]
P-18	1.02×10^{-5}	$CaBr_2$	0.38:1	$1.60\pm0.08\cdot10^5$

[a] The units of K_{app} are M^{-1} for complexation with P-PR and N-PR, M^{-2} for Ca^{2+} c-C-PR, and noninteger values for the other complexes. The error limits represent 90 % confidence levels. [b] The binding constant is for the 1:1 complex.

FIGURE CAPTIONS

Figure 1: Structures of P-PR, N-PR, c-C-PR, t-C-PR, and P-18.

Figure 2: Uv spectra of P-PR, P-18, N-PR, and c-C-PR in methanol and the effect of addition of divalent cations.

(A) ____, spectrum of 3.37×10^{-4} M P-PR; __.__, spectrum after addition of 8.73×10^{-5} M $CaBr_2$; __..__, addition of 1.75×10^{-4} M $CaBr_2$; - - -, addition of 8.73×10^{-4} M $CaBr_2$. (B) ____, spectrum of 2.80×10^{-5} M P-18; __.__, spectrum after addition of 1.33×10^{-5} M $CaBr_2$; __..__, addition of 5.32×10^{-5} M $CaBr_2$; - - - -, addition of 2.39×10^{-4} M $CaBr_2$. (C) ____, spectrum of 2.06×10^{-4} M N-PR; __.__, spectrum after addition of 3.23×10^{-4} M $Ba(SCN)_2$; __..__, addition of 6.46×10^{-4} M $Ba(SCN)_2$; addition of 2.91×10^{-3} M $Ba(SCN)_2$. (D) The difference spectra of N-PR and its complexes with $Ba(SCN)_2$. The sample cuvette contained 3.23×10^{-4} M (__.__), 6.46×10^{-4} M (__..__), or 2.91×10^{-3} M (- - - -) $Ba(SCN)_2$ plus 2.06×10^{-4} M N-PR. The reference cuvette lacked $Ba(SCN)_2$. (E) ____, spectrum of 3.44×10^{-5} M c-C-PR; __.__, spectrum after addition of 6.46×10^{-6} M $CaBr_2$; __..__, addition of 1.29×10^{-5} M $CaBr_2$; ——, addition of 2.91×10^{-5} M $CaBr_2$.

Figure 3: Interaction of $CaBr_2$ and $MgBr_2$ with P-PR and N-PR. (A) Job plot for the interaction of P-PR with $CaBr_2$ in methanol. The sum of the concentrations of $CaBr_2$ and P-Pr was kept constant at 2.45×10^{-4} M. The change in absorbance was measured at 280 nm. (B) Scatchard plot of the binding of $CaBr_2$ to (O) P-PR and (●) N-PR in methanol. In the titration with P-PR (1.13×10^{-5}M), the concentration of $CaBr_2$ was varied from 5.0×10^{-6} M to 2.87×10^{-4} M;

for N-PR (5.53×10^{-6}M), the concentration of $CaBr_2$ was varied from 4.95×10^{-6}M to 2.85×10^{-4}M. The values of r, C, and K_{app} were calculated as described in the Methods section. (C) Scatchard plot of the binding of $MgBr_2$ to (○) P-PR and (●) N-PR in methanol, In the titration with P-PR (1.13×10^{-5}M), the concentration of $MgBr_2$ was varied from 5.31×10^{-4}M to 5.36×10^{-3}M; for N-PR (5.53×10^{-6}M), the concentration of $MgBr_2$ was varied from 8.39×10^{-4}M to 4.89×10^{-3}M.

Figure 4: Scatchard plot of the binding of $CaBr_2$ to P-PR in methanol. The concentration of P-PR was 6.60×10^{-4}M. The concentration of $CaBr_2$ was varied from 6.25×10^{-5}M to 1.53×10^{-3}M.

Figure 5: Interaction of $CaBr_2$ and NaBr with c-C-PR. (A) Job plot for the interaction of c-C-PR with $CaBr_2$ in methanol. The sum of the concentration of $CaBr_2$ and c-C-PR was kept constant at 2.30×10^{-4}M. The change in absorbance was measured at 230nm. (B) Scatchard plot of the binding of $CaBr_2$ to c-C-PR in methanol. The concentration of c-C-PR was 9.63×10^{-5}M. The concentration of $CaBr_2$ was varied from 4.06×10^{-6}M to 3.94×10^{-4}M. Insert: Scatchard plot of the binding of NaBr to c-C-PR in methanol. The concentration of c-C-PR was 9.63×10^{-5}M. The concentration of NaBr was varied from 1.18×10^{-3}M to 3.46×10^{-2}M.

Figure 6: Interaction of $SrBr_2$ and $BaBr_2$ with c-C-PR. (A) Job plot for the interaction of c-C-PR with $SrBr_2$ in methanol. The sum of the concentrations of $SrBr_2$ and c-C-PR was kept constant at 2.33×10^{-4} M. The change in absorbance was measured at 230nm. (B) Job plot for the interaction of c-C-PR with $BaBr_2$ in methanol. The sum of the concentrations of $BaBr_2$ and c-C-PR was kept constant at 3.19×10^{-4} M. The change in absorbance was measured at 230nm. (C) Scatchard plot of the binding of (O) $SrBr_2$ and (●) $BaBr_2$ to c-C-PR in methanol. The concentration of c-C-PR was 9.63×10^{-5} M. The concentration of $SrBr_2$ was varied from 1.70×10^{-5} M to 6.62×10^{-4} M. The concentration of $BaBr_2$ was varied from 1.62×10^{-5} to 9.31×10^{-5} M.

Figure 7: Interaction of $CaBr_2$ with t-C-PR. (A) Job plot for the interaction of t-C-PR with $CaBr_2$ in methanol. The sum of the concentrations of $CaBr_2$ and t-C-PR was kept constant at 2.95×10^{-4}M. The change in absorbance was measured at 230nm. (B) Scatchard plot of the binding of $CaBr_2$ to t-C-PR in methanol. The concentration of t-C-PR was 9.63×10^{-5} M. The concentration of $CaBr_2$ was varied from 7.08×10^{-6} M to 2.41×10^{-4} M.

Figure 8: Scatchard plot of the binding of $CaBr_2$ to P-18 in methanol. The concentration of P-18 was 1.02×10^{-5} M. The concentration of $CaBr_2$ was varied from 1.31×10^{-6} M to 2.01×10^{-4} M.

FIG. 1

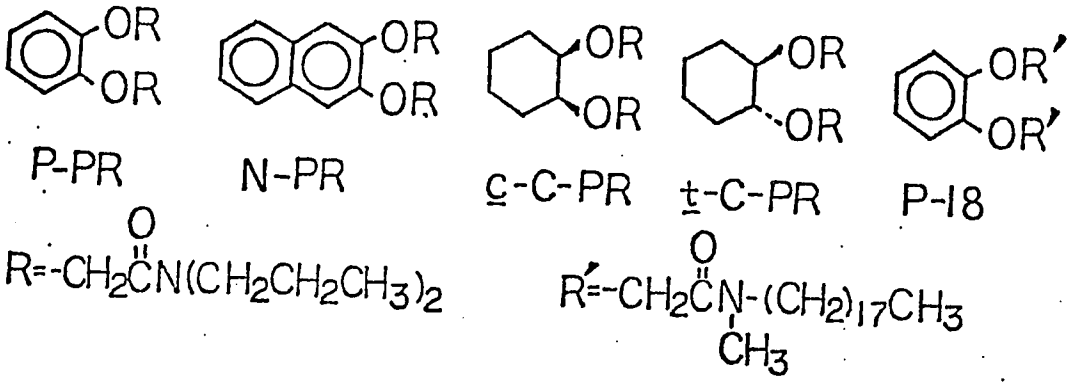
OR
OR
OR
OR
OR
OR
OR
OR
OR'
OR'
P-PR
N-PR
c-C-PR
t-C-PR
P-18
R=-CH2CN(CH2CH2CH3)2
R'=-CH2CN-(CH2)17CH3
CH3

FIG. 2

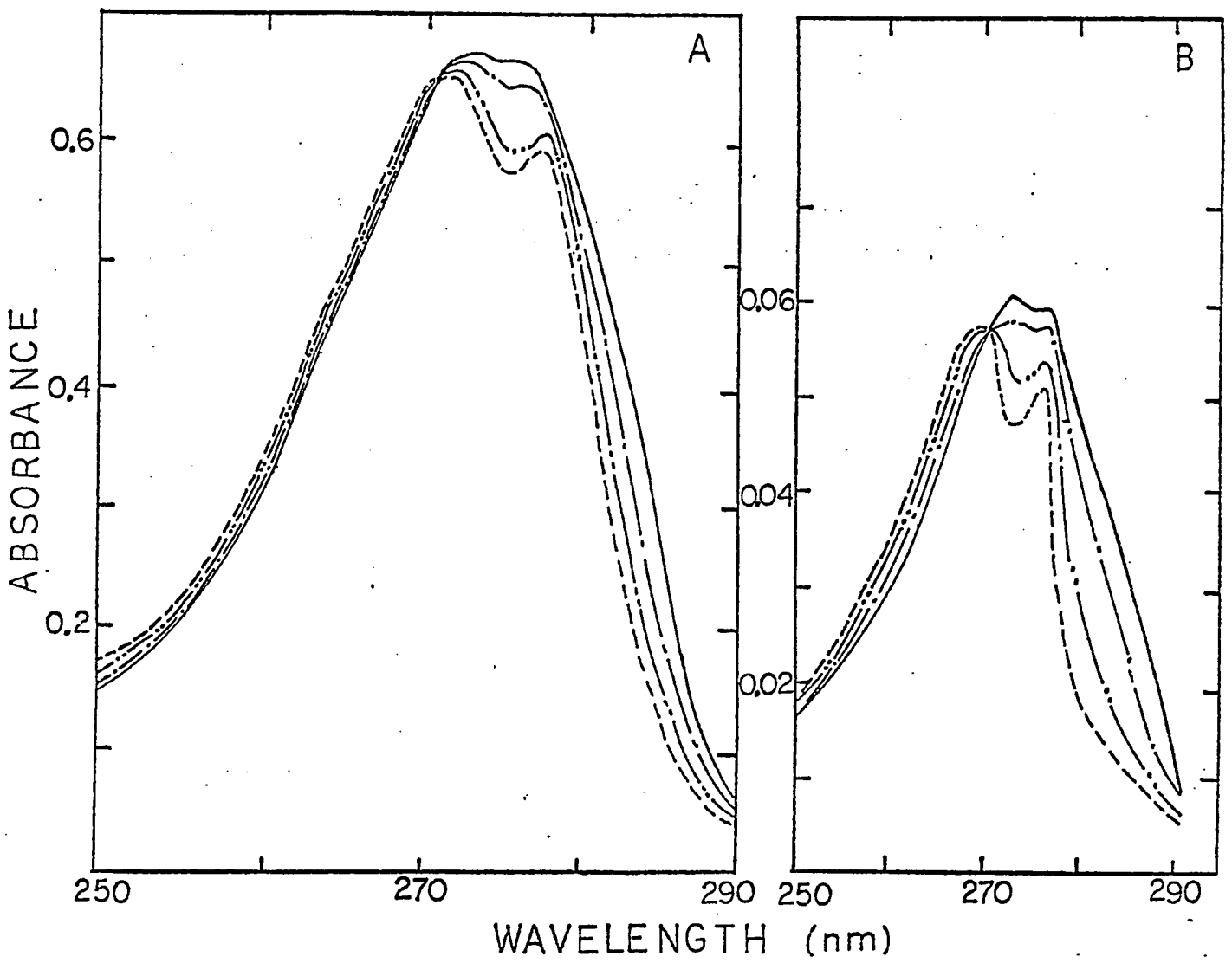
A
B
ABSORBANCE
0.6
0.4
0.2
0.06
0.04
0.02
250
270
290
250
270
290
WAVELENGTH (nm)

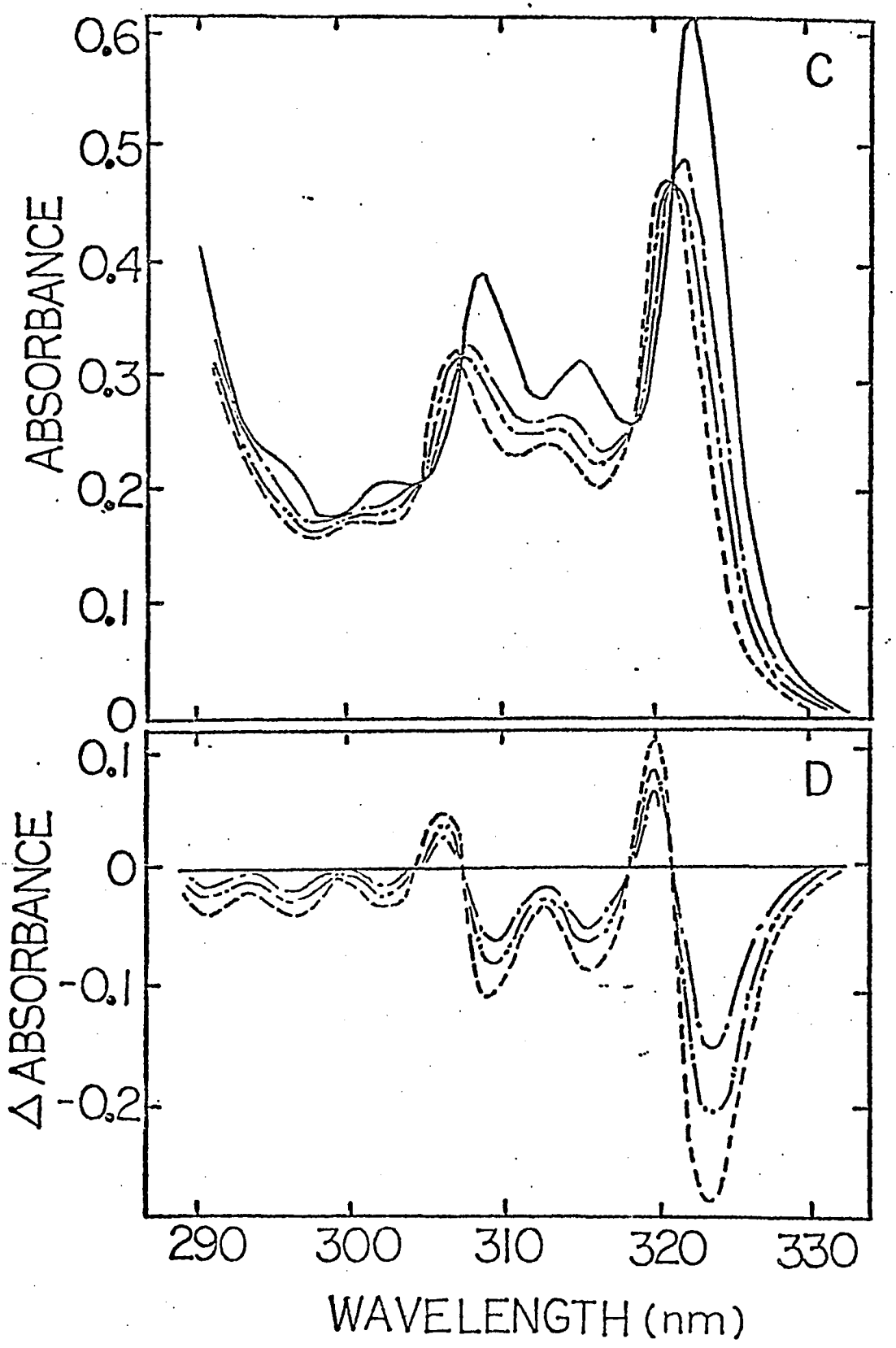
C
D
ABSORBANCE
Δ ABSORBANCE
0.6
0.5
0.4
0.3
0.2
0.1
0
-0.1
-0.2
290
300
310
320
330
WAVELENGTH (nm)

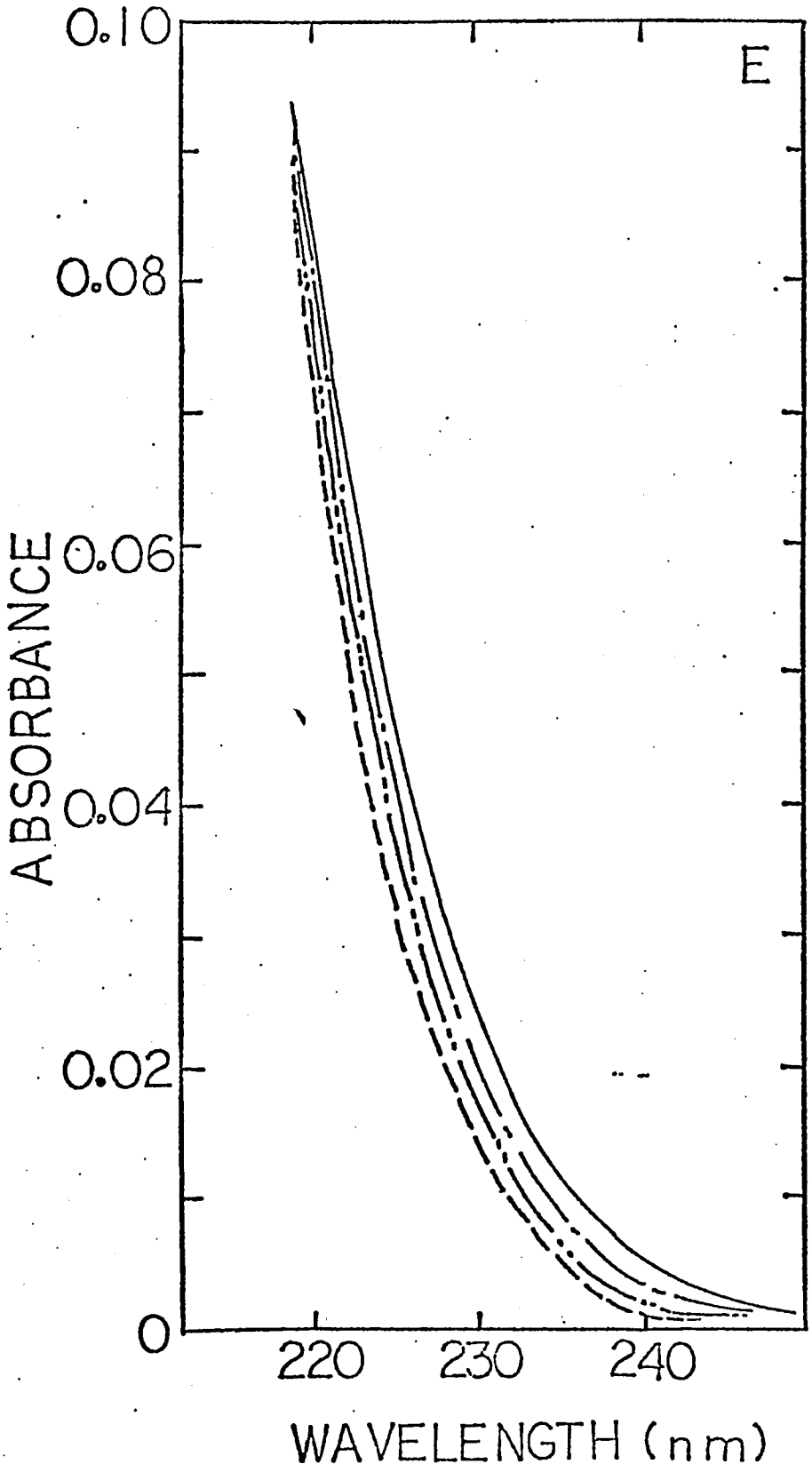
0.10
0.08
0.06
0.04
0.02
0
E
ABSORBANCE
220
230
240
WAVELENGTH (nm)

FIG.3

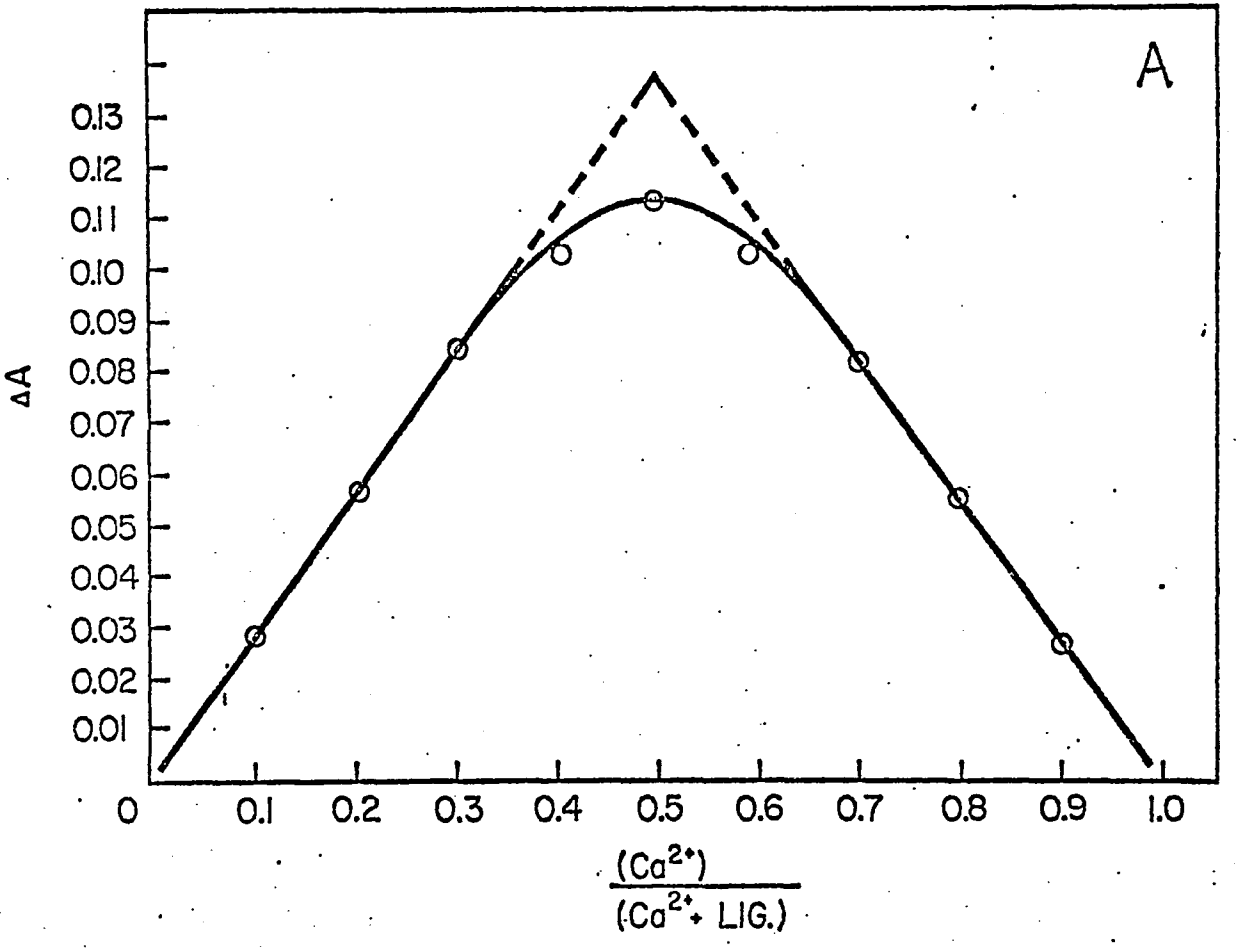
A
0.13
0.12
0.11
0.10
0.09
0.08
0.07
0.06
0.05
0.04
0.03
0.02
0.01
ΔA
0
0.1
0.2
0.3
0.4
0.5
0.6
0.7
0.8
0.9
1.0
(Ca2+)
(Ca2+ + LIG.)

FIG. 3

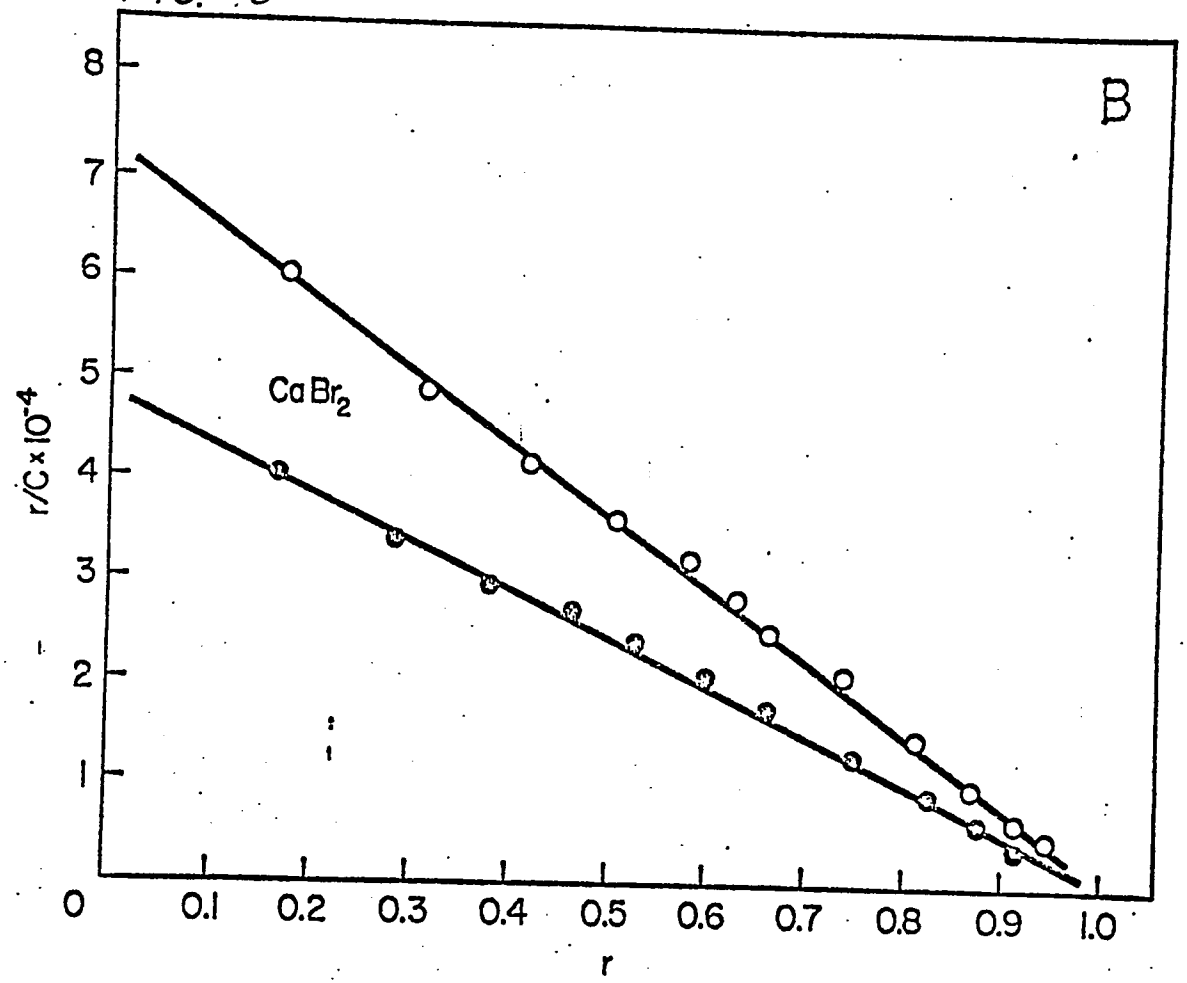

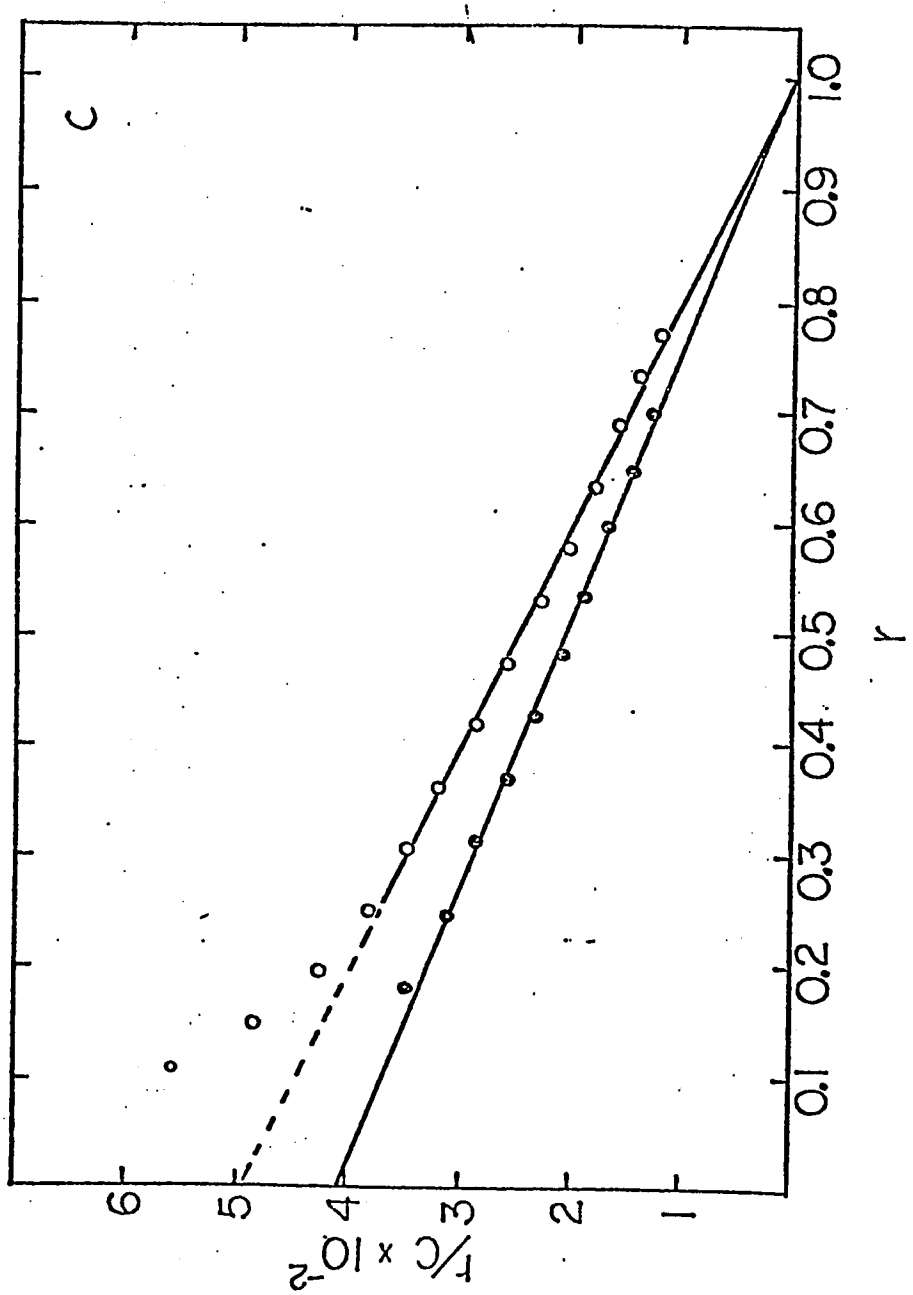
C
r
1/C x 10^-2
0.1
0.2
0.3
0.4
0.5
0.6
0.7
0.8
0.9
1.0
1
2
3
4
5
6

FIG. 4

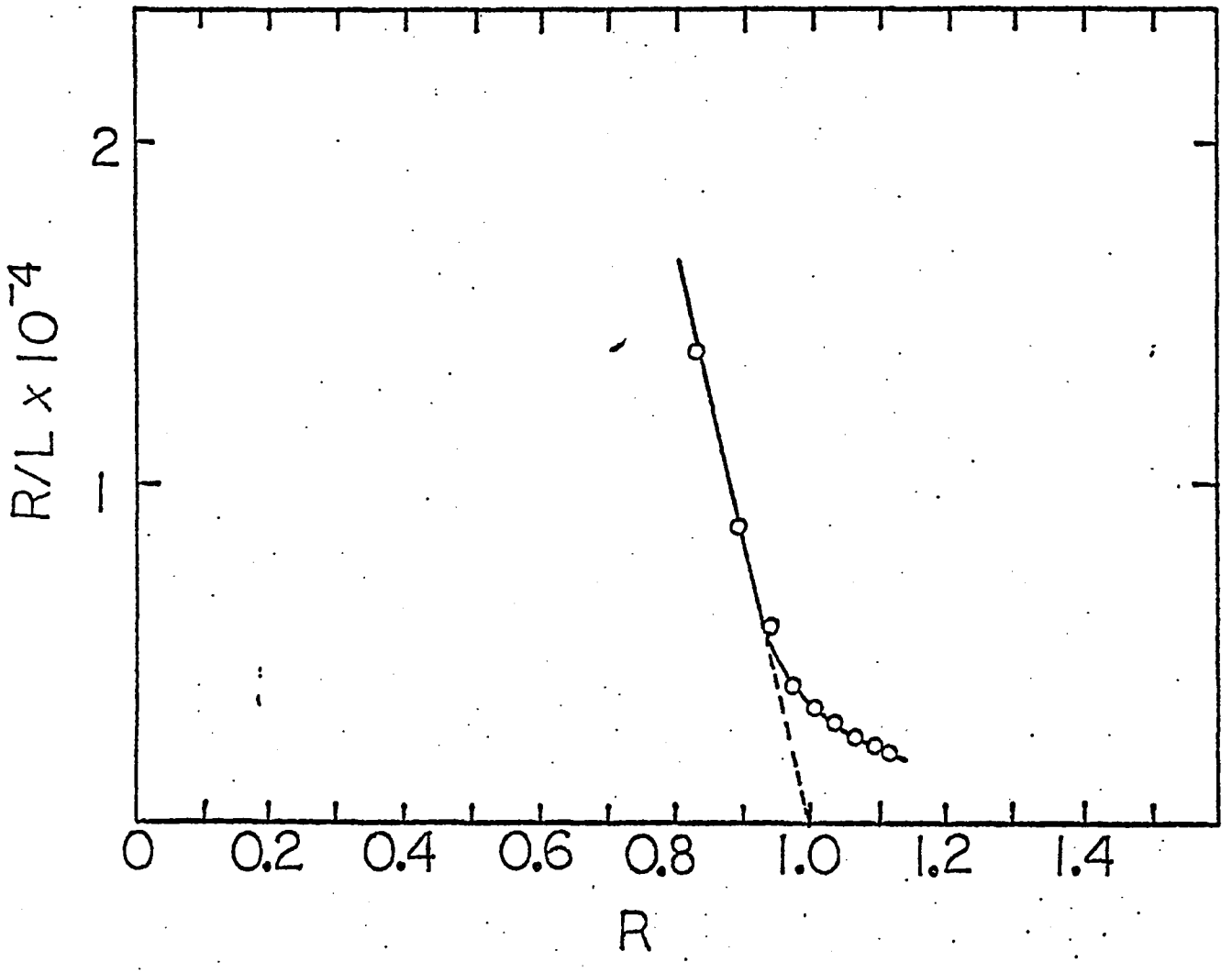

FIG. 5

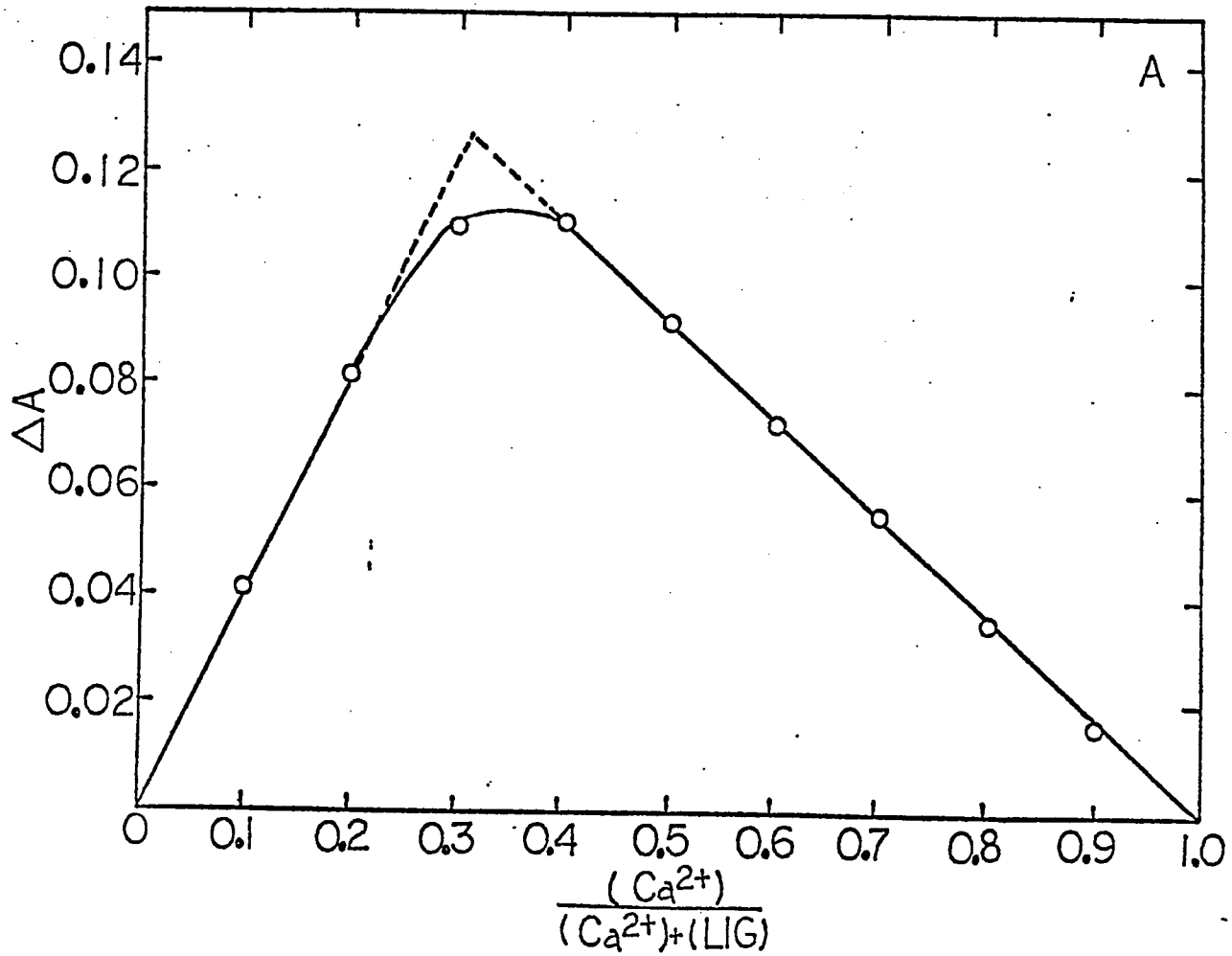
0.14
0.12
0.10
0.08
0.06
0.04
0.02
ΔA
A
0
0.1
0.2
0.3
0.4
0.5
0.6
0.7
0.8
0.9
1.0
(Ca2+)
(Ca2+)+(LIG)

R/L x 10⁻⁵
1
2
0
0.2
0.4
0.6
0.8
1.0
1.2
1.4
1.6
1.8
2.0
R
10
20
30
40
50
60
0.2
0.4
0.6
0.8
1.0
B

FIG. 6

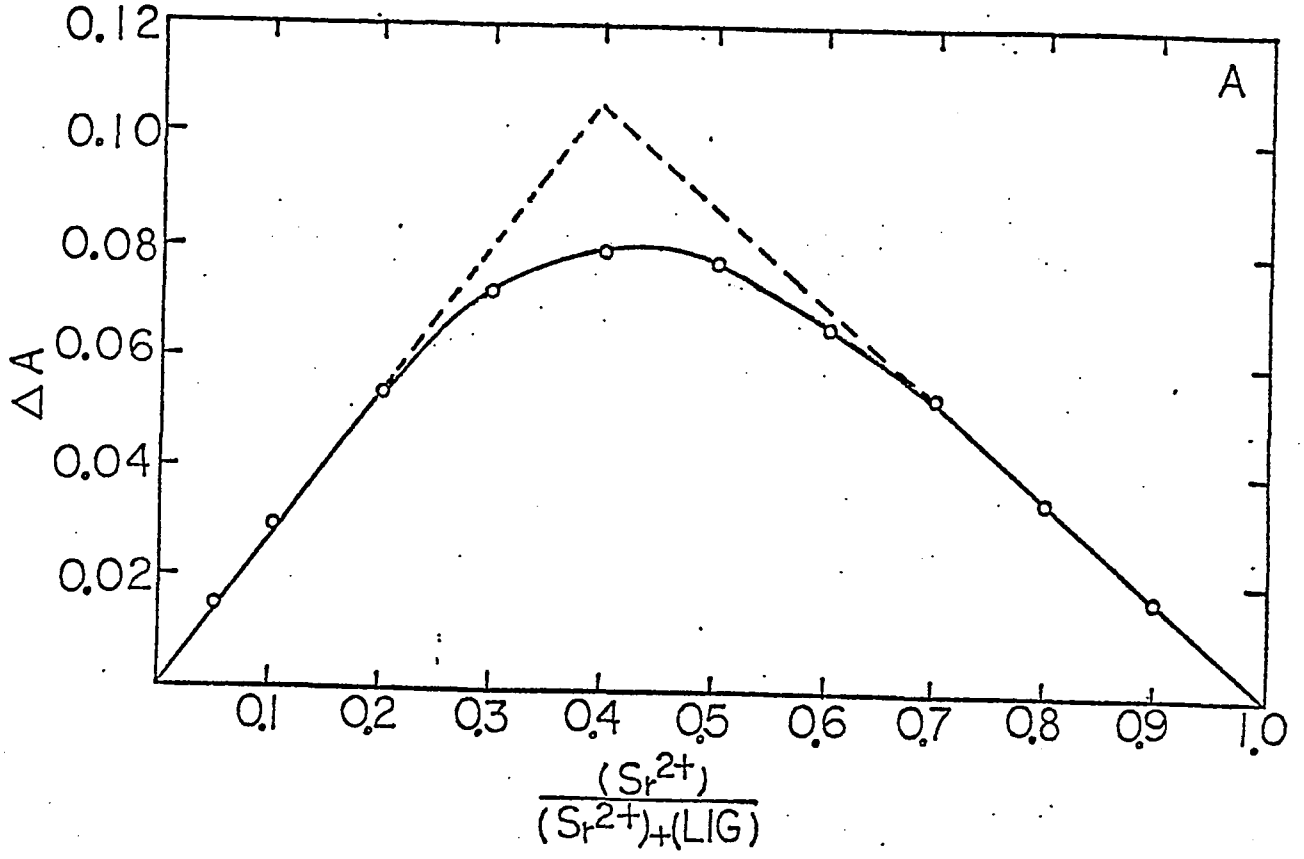
0.12
0.10
0.08
0.06
0.04
0.02
ΔA
A
0.1
0.2
0.3
0.4
0.5
0.6
0.7
0.8
0.9
1.0
(Sr2+)
(Sr2+)+(LIG)

FIG. 6

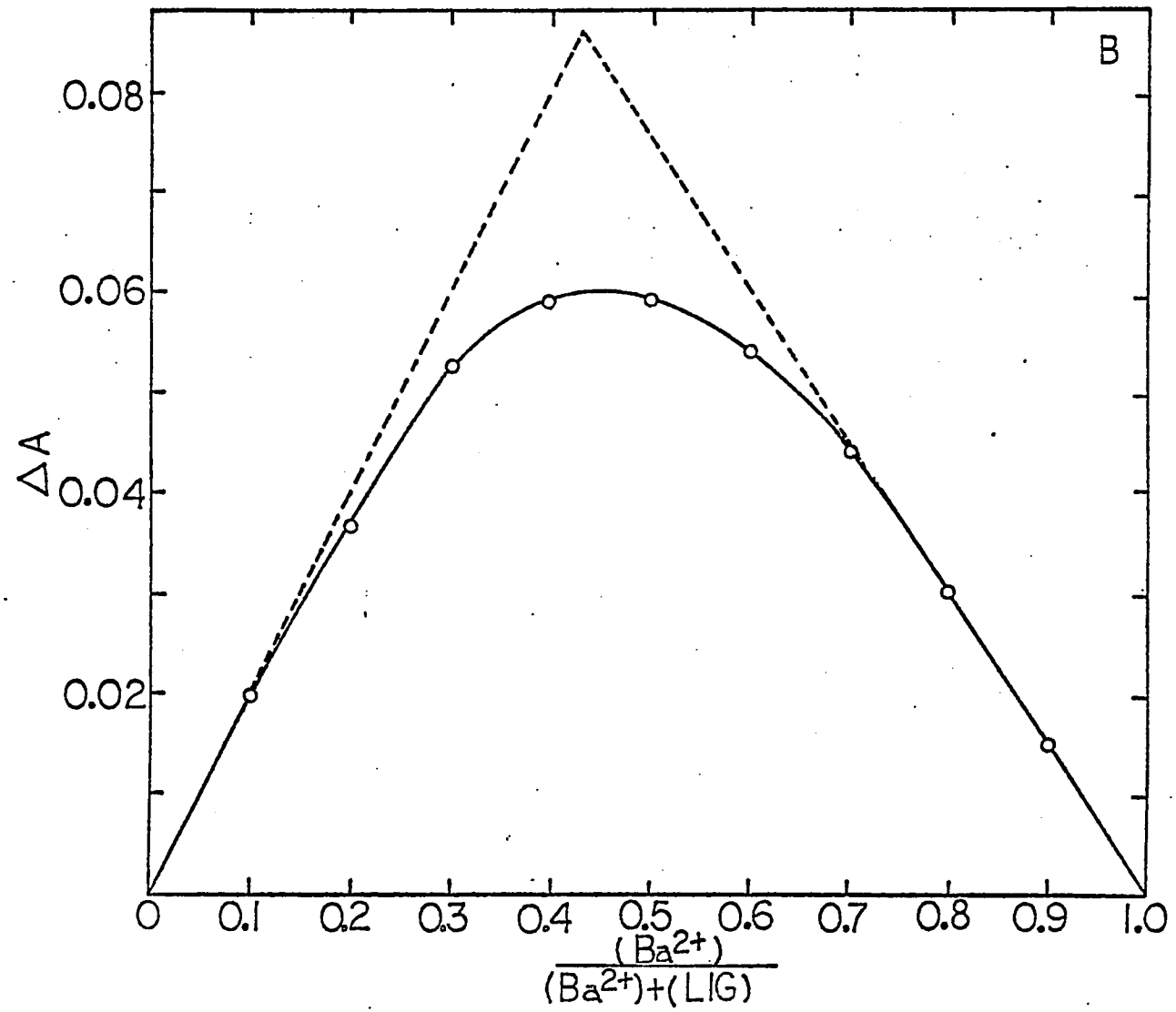

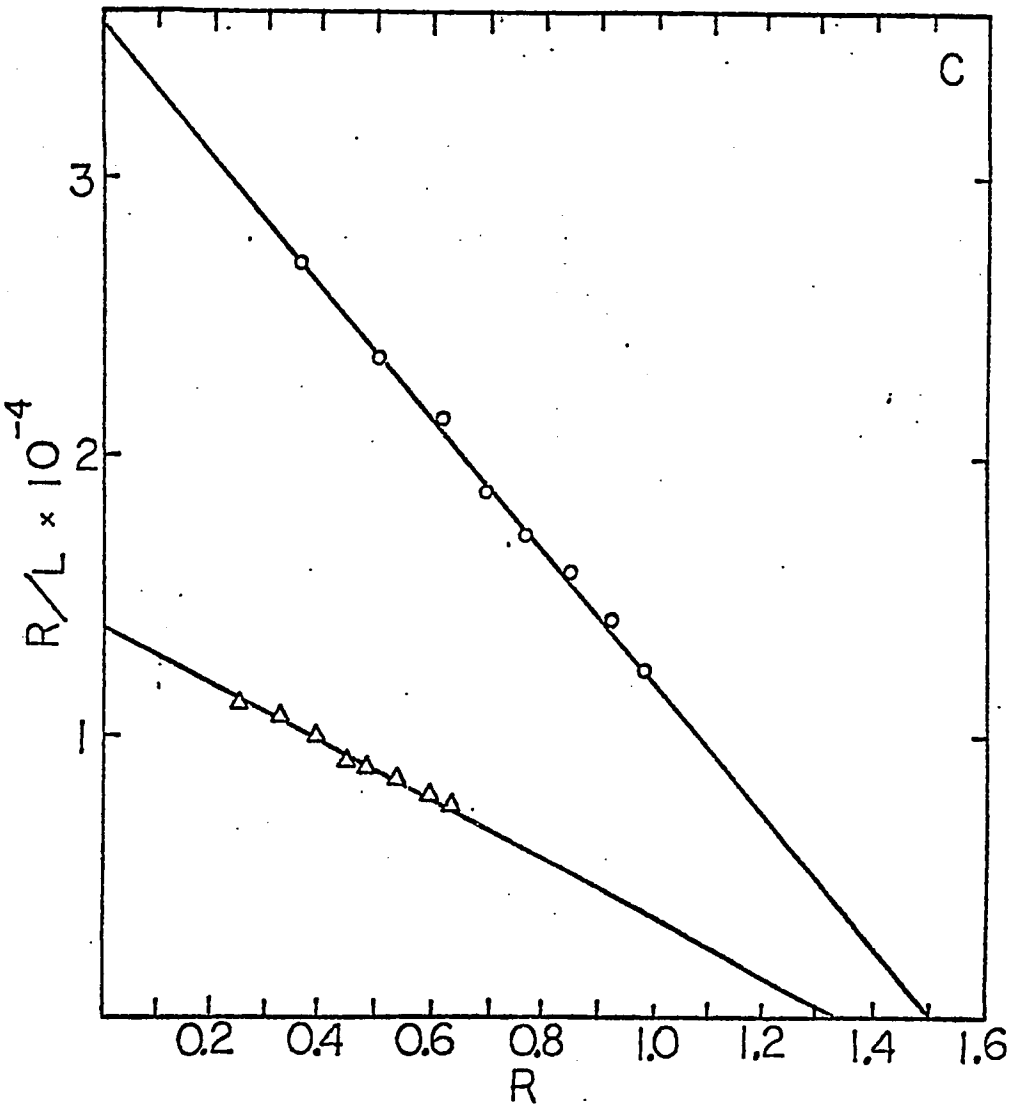
C
3
2
1
R/L × 10^-4
0.2
0.4
0.6
0.8
1.0
1.2
1.4
1.6
R

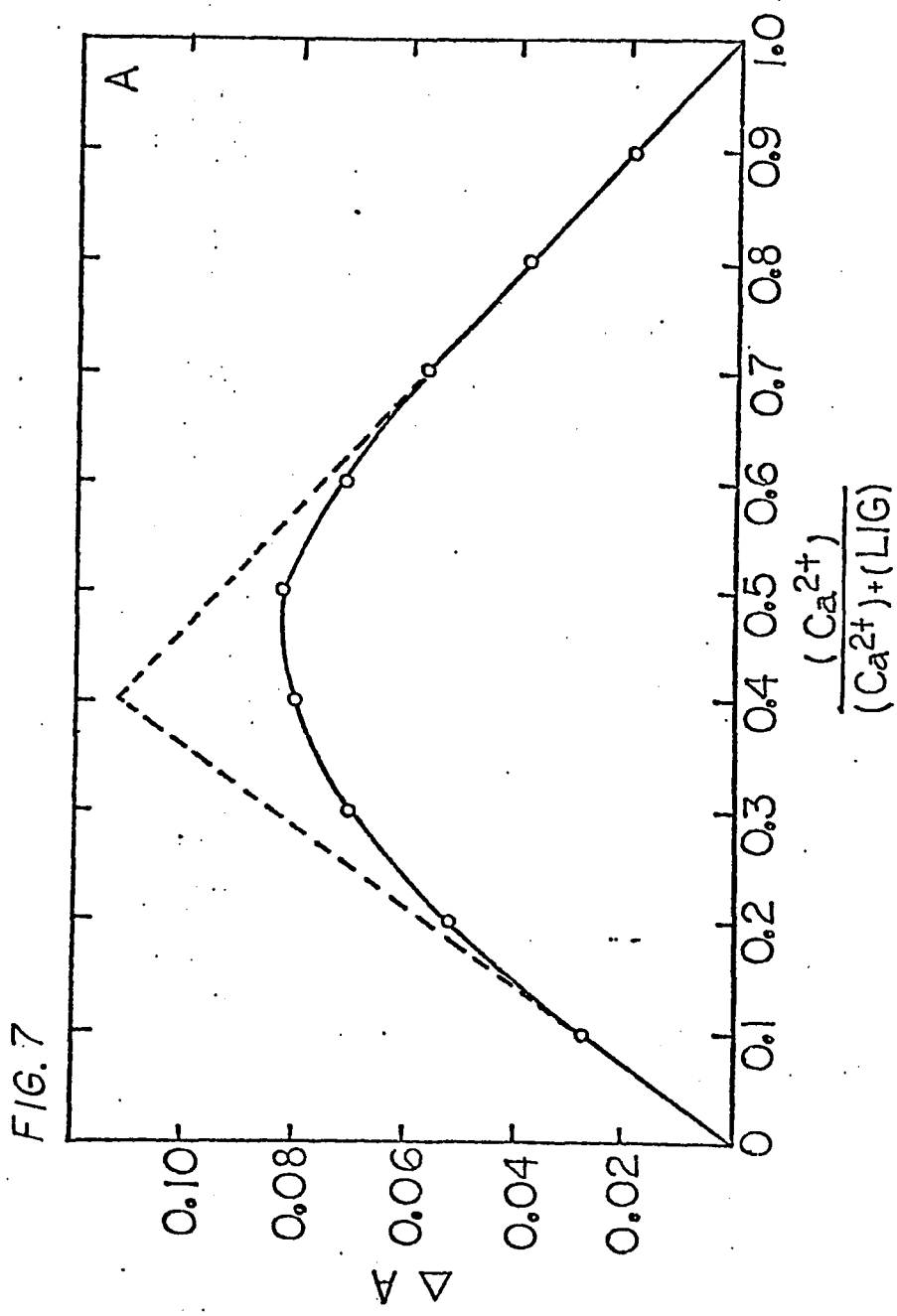
A
0.10
0.08
0.06
0.04
0.02
Δ A
0
0.1
0.2
0.3
0.4
0.5
0.6
0.7
0.8
0.9
1.0
$\frac{(Ca^{2+})}{(Ca^{2+})+(LIG)}$

FIG. 7

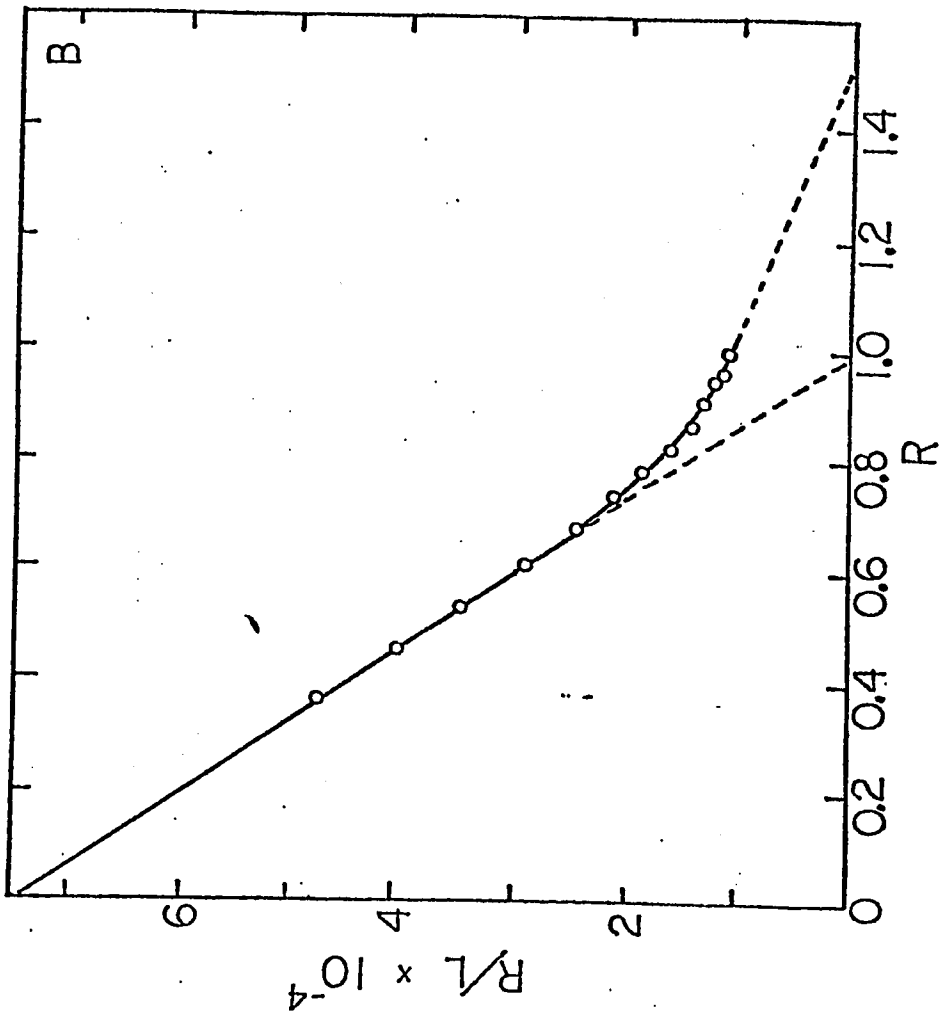
B
R
0
0.2
0.4
0.6
0.8
1.0
1.2
1.4
2
4
6
R/L x 10^-4

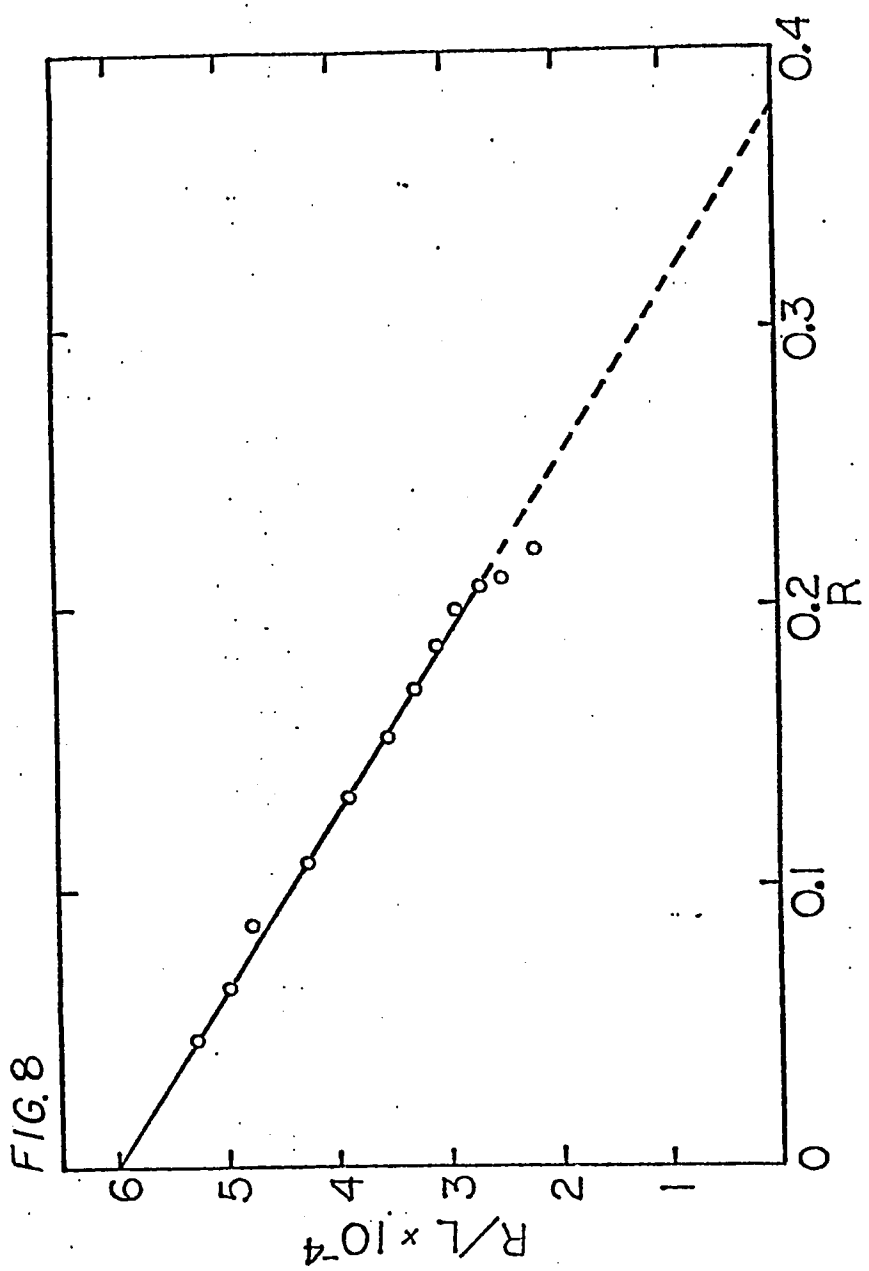

FIG. 8

Part III

Ionophorous Properties of Neutral Diamide Ligands toward Calcium.*

* This manuscript was published in Biochemistry (1977), 16, 2080-2086.

ABSTRACT: The ability of a series of aromatic and alicyclic analogs of 1,2-ethylenedioxydiacetic acids bearing N,N-di-n-propyl amide or N-methyl-N-carbethoxypentyl amide linkages to enhance the rate of $^{45}Ca^{2+}$ efflux from vesicles was studied. The ligands were less potent in enhancing membrane permeability to Ca^{2+} than A23187 and X537A. Lipid-soluble anions markedly increased the rate and extent of Ca^{2+} transport mediated by these neutral ligands. The abilities of these synthetic diamide ligands and naturally occurring ionophores to transport Ca^{2+} across bilayer membranes were sensitive to the lipid composition of the vesicle. The mechanism of Ca^{2+} transport mediated by this series of synthetic ligands is discussed.

[1] The abbreviations used are: SR, sarcoplasmic reticulum; PC, phosphatidylcholine; PS, phosphatidylserine; OA, octadecylamine; DC, dicyclohexyl-18-crown-6; ANS^-, 8-anilino-1-naphthalenesulfonate; DPA^-, dipicrylamine; Pic^-, picrate; Ph_4B^-, tetraphenylborate.

The synthesis and metal ion binding properties of a series of neutral 1,2-ethylenedioxydiacetamide ligands have been discussed in earlier communications (Borowitz et al., 1977; Wun et al., 1977). The abilities of these ligands to solubilize cations in bulk organic phase in a selective fashion (Borowitz et al., 1977) and to form complexes with alkaline-earth metal ions in a binding order largely controlled by the field-strength effect of the cation (except Mg^{2+}) (Wun et al., 1977) led us to determine whether these ligands have ionophorous activity. We describe here the properties of these ligands as carriers of Ca^{2+} across phospholipid bilayer membranes and some aspects of the mechanisms by which they increase Ca^{2+} transport.

The abilities of these neutral ligands to promote Ca^{2+} efflux from vesicles are compared with the activities of two naturally occurring carboxylic ionophorous agents, X537A and A23187. These lipophilic antibiotics form complexes with cations, functioning as mobile carriers of cations in many biological membranes; their biological activity apparently is derived from their ability to effect the equilibration of certain cations across membranes by transporting them in response to concentration gradients (Henderson et al., 1969; Pressman, 1970; Scarpa and Inesi, 1972; Reed and Lardy, 1972; Pressman, 1973). These ionophores have recently become widely used as tools for investigating the influence of Ca^{2+} flux across natural membranes on the regulation of various biological phenomena. The major transported species in X537A-and A23187-mediated Ca^{2+} permeation appears to be uncharged (Reed and Lardy, 1972; Wong et al., 1973; Pfeiffer et al., 1974;

Case et al., 1974; Pfeiffer et al., 1976) whereas the synthetic diamide ligands must form positively charged complexes with metal ions. Despite the difference in the charge of the complexes formed between cations and the synthetic and natural ligands, comparison of the ionophorous activity of the synthetic ligands with that of naturally occurring Ca^{2+} ionophores may allow us to predict what molecular features should be built into future synthetic analogs to approach the effects of the ionophorous antibiotics.

Experimental Section

Materials.

Egg phosphatidylcholine (PC)[1] was isolated and purified from hen egg yolk and its purity ascertained as described previously (Bittman and Blau, 1972). Bovine-brain phosphatidylserine (PS) was obtained from General Biochemicals, octadecylamine (OA) from K & K Laboratories, and cholesterol from Sigma Chemical Co. Cholesterol was recrystallized twice from methanol. Chlorotetracycline was purchased from Nutrional Biochemical Corp., 8-anilino-1-naphthalenesulfonate (ANS^-) was from Sigma Chemical Co., and sodium tetraphenylborate (Ph_4B^-) and dipicrylamine (DPA^-) were from Aldrich Chemical Co. Calcium -45 was purchased from New England Nuclear Corp. A23187 was donated by Eli Lilly and Co. X537A was donated by Hoffmann-LaRoche. Dicyclohexyl-18-crown-6 (DC) was a gift of Dr. H. Frensdorff of Du Pont Central Research. The ligands were synthesized as described previously (Ammann et al., 1975). The structures of these ionophores are shown in Figure 1. They are the N,N-di-n-propyl amides of 1,2-phenylenedioxydiacetic acid (P-PR), 2,3-naphthalenedioxydiacetic acid (N-PR), and cis-and trans-1,2-cyclohexanedioxydiacetic acids

(c-C-PR and t-C-PR). The structure of the N-methyl N-carbethoxypentylamide of cis-1,2-cyclohexanedioxydiacetic acid (c-C-5) is also shown.

Methods

Preparation of Phospholipid Vesicles. Vesicles were prepared from rabbit sarcoplasmic reticulum (SR) microsomal phospholipids, egg PC, 80 mol % PC-20 mol % PS, 95 mol % PC-5 mol % OA, and 50 mol % PC-50 mol % cholesterol. SR was prepared by a modification of the procedure of Martonosi et al. (1968). SR microsomal phospholipids were obtained by extracting SR microsomes with chloroform/methanol (2/1, v/v) as described by Folch et al. (1957). The desired amount of lipid was transferred to a vial and organic solvent was removed by a stream of nitrogen to form a thin lipid film. The residue was dispersed in a medium containing 10 mM imidazole buffer, pH 7.0, 0.15 mM $CaCl_2$ (with $^{45}Ca^{2+}$), and 135 mM NaCl by agitation on a Vortex mixer at room temperature with 2 glass beads for 3 min. The dispersion was sonicated for 450 sec under nitrogen with circulating cold water using a Branson S110 sonifier at power level 3. The sonicated dispersion was stored at 4° for about 2 hours prior to molecular sieve chromatography.

Characterization of Egg PC Vesicles. The volume trapped in the vesicles in the presence of 0.5 M $K_3Fe(CN)_6$, 10 mM imidazole (pH 7.0), 135 mM NaCl, and 0.15 mM $CaCl_2$ was measured by the method of Newman and Huang (1975), except that chromatography of vesicles was done on a Sephadex G-50 column. The trapped volume was found to be 0.320 ± 0.004 l/mole of phospholipid. The addition of 1.41×10^{-4} M c-C-PR or N-PR to the vesicles (4.7 mM egg PC) followed by a 4-hour dialysis against a medium containing 10 mM imidazole buffer, pH 7.0, and 135 mM NaCl did not lead to appreciable leakage of the trapped $K_3Fe(CN)_6$. This indicates that the vesicle is not ruptured by the addition of the ionophores at this concentration.

Removal of Untrapped $^{45}Ca^{2+}$. Radioactive ions that were not trapped in the vesicle were removed by gel filtration. The suspension was passed through a column (1.5 x 30 cm) of Sephadex G-50 and eluted with 10 mM imidazole buffer, pH 7.0, containing 135 mM NaCl. The diluted suspension of vesicles thus obtained, free of untrapped $^{45}Ca^{2+}$, was used in leakage experiments.

Assay of $^{45}Ca^{2+}$ Release. Stock solutions of the diamide ionophores and DC were prepared in DMF, and A23187 and X537A were dissolved in ethanol. A 10-µl aliquot of ionophore solution (or DMF or ethanol) was added to one-ml portions of ^{45}Ca-loaded vesicles (approximately 2.5-4.5 µmoles lipid phosphorus). Vesicles were placed in 1-cm diameter Visking tubing. The bags were knotted with air bubbles trapped, and placed in test tubes containing 4 ml of 10 mM imidazole buffer, pH 7.0, and 135 mM NaCl. The sealed test tubes were rotated at 2 rev. per min. Aliquots (0.1 ml) of the dialysates were taken for radioactive counting at various time intervals. Fluxes are expressed as the percentage of the initial trapped radioactivity lost as a function of time. Experiments with the same preparation of vesicles showed that the Ca^{2+} concentration of the dialysate at a given time did not vary by more than 5%. The initial rate of Ca^{2+} efflux did not vary by more than 5% when different preparations of egg-PC vesicles were made in medium containing 0.15 or 1.5 mM $CaCl_2$.

Complexation of Vesicle-Bound Ca^{2+} by Ionophores Using Chlorotetracycline as Fluorescence Probe. The method is essentially the same as described by Jilka and Martonosi (1975). Details of the experiment are described in the caption to Figure 8.

Determination of Phospholipid Concentration. Phospholipid determinations were done by digesting 0.1 to 0.3 ml aliquots of vesicle suspensions with 0.1 ml of concentrated H_2SO_4 at 250-260° for 15 min. After a few drops of 30% H_2O_2 were added, the sample was redigested for 5 min. The solution was then diluted to give a H_2SO_4 concentration of approximately 1 N. The concentration of inorganic phosphate was determined by the method of Taussky and Shorr (1953).

Measurement of Ionophore Distribution between n-Butanol and Water. To 5 ml of distilled water saturated with n-butanol was added 1.5 ml of n-butanol containing $1\text{-}2\times10^{-4}$ M N-PR, or c-C-PR. The mixture was shaken on a Vortex mixer at room temperature for at least 1 min and then centrifuged to separate the organic and aqueous phases. The n-butanol layer was withdrawn, 10 µl of n-butanol was added to this layer to reduce the turbidity, and the concentrations of ionophores were calculated from the absorbance using the following extinction coefficients in n-butanol: N-PR, 3185 $M^{-1}cm^{-1}$ at 323 nm; P-PR, 1593 $M^{-1}cm^{-1}$ at 280 nm; and c-C-PR, 2065 $M^{-1}cm^{-1}$ at 230 nm. Partition coefficients were obtained by dividing the concentration of ionophore in the n-butanol layer by the concentration of ionophore in the aqueous layer. The concentration of ionophore in the aqueous layer was obtained by subtracing the ionophore concentration in the organic layer from the total concentration added.

Measurement of Ionophore Distribution between Egg-PC Vesicles and Water. Ionophores were added to 1ml of vesicles (3.56 mM egg PC in 1 mM imidazole, pH 7.0) contained in dialysis bags and the suspensions were dialyzed against 5 ml of 1 mM imidazole, pH 7.0, for 4-5 hours with rotation at 2 rev. per min.

After dialysis, 0.8 ml of vesicles was withdrawn and 1.2 ml of diethyl ether was added to disrupt the vesicles and extract the ionophore. The ether phase was withdrawn after separation by centrifugation, 10 μl of ether was added to the ether layer to reduce the turbidity, and the absorbance was measured. The extinction coefficients of the ionophores in ether were N-PR, 3475 $M^{-1}cm^{-1}$ at 323 nm; P-PR, 2020 $M^{-1}cm^{-1}$ at 280 nm; c-C-PR, 1516 $M^{-1}cm^{-1}$ at 230 nm. Under the extraction conditions used, nearly all the c-C-PR and P-PR was extracted into the ether layer, while N-PR was only partially extracted. The N-PR has a partition coefficient of ether to water-vesicle layer of about 1.80 ± 0.05. This value was used to calculate the amount of N-PR remaining with the vesicles.

Results

Ionophore-Enhanced Ca^{2+} Permeability of Bilayer Vesicles. Figure 2 illustrates the stimulation of Ca^{2+} release produced by addition of various ionophores to vesicles prepared from SR lipids. Of the total lipids of SR microsomes, 89% are phospholipids, in which PC is predominant (71%), followed by phosphatidylethanolamine and sphingomyelin (6%) (Waku et al., 1971). The relative abilities of the ionophores to induce Ca^{2+} release from vesicles prepared from SR lipids (Figure 2) follow the same order as their abilities to decrease chlorotetracycline fluorescence in intact SR microsomes loaded with Ca^{2+}, with the exception of DC (T-C. Wun and R. Bittman, unpublished results). Notably, N-PR is markedly more effective than the other synthetic ionophores in causing Ca^{2+} efflux from SR lipid vesicles.

The abilities of the naturally occurring and synthetic ionophores to transport Ca^{2+} across vesicles prepared from other phospholipids were examined. The kinetics of ionophore-induced transport of Ca^{2+} from vesicles prepared from egg PC are strikingly different from those observed in vesicles derived from SR lipids (Figure 3). Relative to their ability to enhance the rate of passive Ca^{2+} diffusion through SR phospholipid bilayer membranes, X537A and N-PR have markedly depressed potencies in egg PC vesicles. The peculiar leveling off after dialysis of a few hours is not completely understood at present. With vesicles prepared from 20 mol % PS-80 mol % egg PC, c-C-PR was found to be highly effective in promoting Ca^{2+} release relative to the other synthetic ionophores (Figure 4). In these negatively charged bilayers the net efflux of Ca^{2+} induced by A23187 and X537A is somewhat depressed compared with that in egg-PC bilayers (Figure 3). In contrast, this lipid environment enhances the abilities of the neutral diamide ionophores (which form positively charged complexes) to catalyze transmembrane efflux of trapped Ca^{2+}. To further examine the influence of bilayer charge on the ability of the ionophores to induce Ca^{2+} transport vesicles were prepared from 5 mol % OA-95 mol % egg PC. The results obtained for Ca^{2+} release from these positively charged bilayers are shown in Figure 5. The rates and extents of Ca^{2+} release induced by all of the ionophores except A23187 are depressed in these vesicles relative to the values obtained in uncharged bilayer membranes. Figure 6 shows the ionophore-induced

Ca^{2+} leakage from vesicles prepared from 50 mol % egg PC-50 mol % cholesterol. The $^{45}Ca^{2+}$ efflux rate in the presence of X537A is enhanced compared to the rates observed in the other bilayers derived from egg lecithin. All of the other ionophores have depressed activities relative to their abilities to stimulate Ca^{2+} transport across cholesterol-lacking bilayers.

Examination of the effect of lipid composition on the abilities of ionophores to stimulate Ca^{2+} release reveals several striking features (Table I). First, when the rates of Ca^{2+}efflux from SR vesicles induced by various ionophores are normalized to the rate observed in the presence of 4.78×10^{-7}M A23187, the relative potencies of A23187: X537A: N-PR: c-C-PR: c-C-5: P-PR :DC are 100: 5.38: 0.34: 0.043: 0.007: 0.007: 0.019. Very similar values of relative potencies are observed for the abilities of the ionophores to decrease chlorotetracycline fluorescence by 50 % in intact SR microsomes loaded with Ca^{2+} (T-C, Wun and R. Bittman, unpublished data). Second, the relative potencies of the ionophores vary when the composition of the lipids in the membrane is altered; for example, N-PR has much higher potency in vesicles prepared from SR lipids than in the vesicles prepared from egg PC alone or from mixtures of egg PC and other lipids. The activity of X537A is depressed in bilayers prepared from egg PC, PS-egg PC, and OA-egg PC relative to the activity in vesicles prepared from SR lipids; however, higher X537A activity was observed in vesicles prepared from an equimolar mixture of egg PC and cholesterol than from egg PC alone. Third, the amount of Ca^{2+} captured by the vesicles depends on the lipid composition. Vesicles containing negatively charged phospholipids (those prepared from SR lipids

and PS-egg PC) captured more Ca^{2+}. Egg PC, which is a neutral phospholipid, captured less Ca^{2+}. Egg PC-OA bilayers, which are positively charged, captured the least amount of Ca^{2+}. Fourth, the synthetic ionophores do not increase the permeability of bilayers to Ca^{2+} in proportion to the amount of Ca^{2+} trapped in the vesicle. For example, the presence of 20 mol % PS in egg PC vesicles increased the amount of captured Ca^{2+} to about 3 times the amount trapped in egg PC vesicles; however, with the exception of A23187 and X537A, the ionophores enhanced the rate of transport by a factor greater than 3. The presence of 5 mol % of positively charged OA decreased Ca^{2+} captured by vesicles by about 3.8 times, but with the exception of A23187 and N-PR the rates of transport did not decrease proportionately. Since A23187 and X537A are negatively charged and the synthetic ionophores are neutral molecules, their complexes with Ca^{2+} differ in charge. The presence of membrane charges may regulate transport of charged complexes to a greater extent than those complexes that are not charged. Fifth, incorporation of cholesterol into the vesicle depressed the potencies of A23187, N-PR, c-C-PR, P-PR, t-C-PR, c-C-5, and DC relative to their activities in pure egg-PC bilayers. Since incorporation of cholesterol into egg-PC bilayers increases the extension of the fatty acid chains and reduces the amplitude of motion of their long axes (Schreier-Muccillo et al., 1973), transport of these ionophore-Ca^{2+} complexes may be limited by the increased rigidity of the cholesterol-containing bilayers. However, the rate of movement of Ca^{2+}-X537A complex(es) across the membrane is not limited by cholesterol incorporation.

Effect of Lipophilic Anions on Ionophore-Mediated Ca^{2+} Transport. The stoichiometry of ionophore-Ca^{2+} interaction is 1 : 1 for P-PR and N-PR at low concentration, 2 : 1 (ligand to metal ion) for c-C-PR, and biphasic (1.5:1 and 1:1, depending on the extent of saturation) for t-C-PR (Wun et al., 1977). These ionophores are far less potent carriers of Ca^{2+} than the two carboxylic ionophores, X537A and A23187, suggesting that the charge is not fully enveloped in the permeant species. The possibility that lipophilic anions would enhance the movement of Ca^{2+}-ionophore complexes across the bilayer was investigated. Figure 7 shows that the lipid-soluble anions ANS^-, Ph_4B^-, DPA^-, and Pic^- do not appreciably transport Ca^{2+} themselves. However, in the presence of c-C-PR, they greatly enhance the rate and extent of Ca^{2+} transport. The order in which these lipophilic anions enhance c-C-PR-mediated Ca^{2+} transport is $Ph_4B^- > DPA^- > Pic^- > ANS^-$. (The difference in the ability of Ph_4B^- and DPA^- to enhance c-C-PR-mediated Ca^{2+} efflux is clearly observed when lower concentrations of Ph_4B^- and DPA^- are used.) The transport of Ca^{2+} by X537A A23187 (which are negatively charged at pH 7.0) is not enhanced by Ph_4B^- at the concentration tested (Figure 7B, dashed curves). Hence, neutralization of the charge in the synthetic ionophore-Ca^{2+} complex or formation of lipophilic ion pairs may greatly enhance the transport of Ca^{2+} across the membrane.

Distribution of N-PR, c-C-PR, and P-PR in n-Butanol-Water and Egg-Lecithin Vesicle-Water Systems. Lipophilic ionophorous antibiotics form complexes with cations, increasing cation solubility in the hydrocarbon-like membrane interior and increasing the cation permeability of membranes

(Harris, 1972). To characterize the lipophilicity of the synthetic ionophores, their partitioning in 1-octanol-water (Hansch, 1969) was determined. N-PR, c-C-PR, and P-PR are nearly completely partitioned into the octanol phase (data not shown). The partition coefficients of these ionophores in a n-butanol-water system are identical within experimental error (Table II). However, measurement of the partitioning of these ionophores in an egg-PC vesicle-water system shows that P-PR has a markedly lower partition coefficient in egg-PC vesicles than N-PR and c-C-PR (Table III).

Studies of the Complexation of Vesicle-Bound Ca^{2+} with Ionophores. In order to determine whether complexation on the vesicle surface plays an important role in determining the ability of the synthetic ionophores to transport Ca^{2+}, complexation of vesicle-bound Ca^{2+} with c-C-PR and N-PR was studied using chlorotetracycline. Vesicles were prepared from egg PC or from a mixture of egg PC and PS in a medium containing Ca^{2+}. On addition of EDTA (1mM), Ca^{2+} outside the vesicle was chelated (as measured by reduction of chlorotetracycline fluorescence) but Ca^{2+} inside the vesicle was not released. On addition of ionophore, Ca^{2+} inside the vesicle binds to the ionophore and the fluorescence of chlorotetracycline is decreased. Figure 8A shows that the rate of decrease of chlorotetracycline fluorescence induced by addition of c-C-PR is slow. Figure 8B shows a log-log plot of the decrease in chlorotetracycline vs. ionophore concentration. N-PR forms complexes with vesicle-bound Ca^{2+} at lower concentrations than c-C-PR in both

egg PC vesicles and 20 mol % PS-80 mol % egg PC vesicles. The ratio of the slopes of the lines for N-PR to c-C-PR is approximately 2 in each vesicle preparation. This indicates that the stoichiometries of ionophore-Ca^{2+} complexes on these vesicle surfaces are different for N-PR and c-C-PR. It is interesting that uv titration of N-PR and c-C-PR with $CaBr_2$ in methanol at low concentration gives a stoichiometry of 1:1 for N-PR:Ca^{2+} and 2:1 for c-C-PR:Ca^{2+} (Wun et al., 1977).

Discussion

The kinetics of ionophore-mediated Ca^{2+} transport can be roughly divided into two domains: interfacial reactions and transport of complexes across the membrane interior. The overall transport activity depends not only on the ability of ionophores to form lipophilic complexes with Ca^{2+}, but also on the ability of such complexes to traverse the membrane interior and to dissociate at the other side of the membrane. It is apparent from the results reported here that the potencies of several synthetic and two naturally occurring ionophores to transport Ca^{2+} across different bilayers vary with the lipid composition. The major factors involved in the complicated interplay between the membrane, ionophores, and cation can, in some cases, be elucidated by studying the transport through various types of membranes.

The importance of the phospholipid hydrocarbon chain in determining the rates of ion diffusion across the membrane has been established. Valinomycin-induced leakage of $^{86}Rb^{+}$ across bilayers was found to depend on the length and degree of unsaturation of the fatty acyl chains (de Gier et al., 1970). The dependence of valinomycin-induced and of nonactin-induced K^{+} permeability on temperature was demonstrated (Johnson and Bangham, 1969; Krasne et al., 1971). It has been concluded that membrane fluidity may control the permeation of ionophore-cation complexes. Transport activity may also depend on the concentration of the permeant complexes in the membrane which, in turn, depends on the dielectric constant of the membrane interior, the charge or dipole

of the membrane surface, and the polar and nonpolar interactions between ionophore and Ca^{2+} and between lipid and ionophore. Our experiments with this series of neutral ionophores provide some insight into the relationships between stoichiometry of complexation with cation, surface complexation, lipid composition, and Ca^{2+} transport activity. The greater efficiency of the alicyclic ligand c-C-PR than the aromatic ligands N-PR and P-PR in enhancing the rate of Ca^{2+} permeation in most vesicles (Figures 3, 4, and 5) except those derived from SR (Figure 2) may be related to the ability of c-C-PR to form a 2:1 ionophore-Ca^{2+} complex, which may shield Ca^{2+} from the bilayer interior better than is possible in a 1:1 complex. The difference in the potencies of c-C-PR and N-PR in egg-PC vesicles is apparently not related to their abilities to form complexes with Ca^{2+} on the vesicle surface, since Figure 8 shows that their surface complexation properties are not markedly different. The greater efficiency of N-PR than c-C-PR in SR vesicles (Figure 2) can be partially attributed to the more extensive degree of complexation of N-PR with Ca^{2+} on the SR membrane (T-C. Wun and R. Bittman, unpublished data -). However, the origin of the variation in potencies of these two ionophores in bilayers of varying lipid composition is not fully understood. The lower potency of P-PR observed in all of the vesicles tested is consistent with its lower extent of partitioning into the bilayer (Table III) compared with c-C-PR and N-PR. Comparison of c-C-5 and c-C-PR indicates that the presence of a short apolar side chain terminating in a carbethoxyl

group does not result in enhanced Ca^{2+}-transporting activity. In fact, the N, N-dipropyl amide has a higher potency than the N-methyl-N-carbethoxypentyl analog of cis-1,2-cyclohexanedioxydiacetic acid in each vesicle system we examined.

Incorporation of cholesterol into the bilayer reduces the valinomycin-facilitated exchange of Rb^{+} (de Gier et al., 1970) and decreases the ionophore-induced Ca^{2+} permeability across egg PC bilayers for all of the ionophores examined except X537A (Figure 6). This is consistent with the well-known importance of membrane fluidity in regulating permeability. The permeability of ionophore-Ca^{2+} complexes within the lipid phase may be decreased as a result of the decrease in membrane fluidity caused by cholesterol incorporation. Cholesterol may also modulate membrane permeability to ions by altering the strength and orientation of dipolar groups at the membrane surface, which would make the interior more positive to the bulk aqueous phase than in cholesterol-free phospholipid bilayers (Szabo et al., 1972; Szabo, 1974). It is not yet clear why the activity of X537A is enhanced in cholesterol-containing vesicles (Figure 6).

Several possibilities may be considered for the gradual leveling off of the rate of Ca^{2+} efflux noted in the presence of ionophores. (a) The trapped volume in the vesicle is about 6.4×10^{-7} l (1 ml of 4mM egg-PC vesicle) and is negligible compared with the volume of bathing medium (5 ml). It is unlikely that enough Ca^{2+} can leak out from the vesicle to permit return of Ca^{2+} to reduce the net efflux at low percentage of leakage. (b) The transport of Ca^{2+} by the synthetic ionophores may give rise to an electrochemical potential that may compensate for the concentration gradient. Addition of EDTA to the

bathing medium or a change to a new dialysis medium did not eliminate the leveling off of Ca^{2+} efflux. This indicates that the electrical potential gradient generated during the ionophore-mediated Ca^{2+} efflux is not the major factor which gives rise to leveling off. Leveling off was also observed in an isotope flux experiment in which egg-PC vesicles containing trapped $^{45}Ca^{2+}$ were dialyzed vs. an equal concentration of unlabeled Ca^{2+}. (c) It is not likely that a minimum intravesicular Ca^{2+} concentration was reached that prevented further release, because a 10-fold increase in captured Ca^{2+} does not prevent leveling off (data not shown). (d) The vesicles do not show appreciable aggregation after 4 hours of dialysis, as judged from absorbance and light-scattering measurements at 400 nm. Among the remaining possible explanations are a slow aggregation of the ionophores in the vesicle and a time-dependent change in the localization of the ionophores within the vesicle bilayer.

The ligands we used bind selectively to Ca^{2+}, favoring complexation with this ion over the other ions that play a fundamental role in a variety of biological processes (Na^{+}, K^{+}, and Mg^{2+})(Wun et al., 1977). The approaches developed here may be applied to a study of the effects of other more potent synthetic analogs of this type to probe Ca^{2+}-mediated events.

References

Ammann, D., Bissig, R., Güggi, M., Pretsch, E., Simon W., Borowitz, I.J., and Weiss, L. (1975), Helv. Chim. Acta 58, 1535-1548.

Bittman, R., and Blau, L. (1972), Biochemistry 11, 4831-4839.

Borowitz, I.J., Lin, W-O., Wun, T-C., Bittman, R., Weiss, L. Diakiw, V., and Borowitz, G.B. (1977), Tetrahedron, in press.

Case, G.D., Vanderkooi, J.M., and Scarpa, A. (1974), Arch. Biochem. Biophys. 162, 174-185.

de Gier, J., Haest, C.W.M., Mandersloot, J.G., and van Deenen, L.L.M. (1970), Biochim. Biophys. Acta 211, 373-375.

Folch, J., Lees, M., and Sloane-Stanley, G.A. (1957), J. Biol. Chem. 226, 497-509.

Hansch, C. (1969), Acc. Chem. Res. 2, 232-239.

Henderson, P.J.F., McGivan, J.D., and Chappell, J.B. (1969), Biochem. J. 111, 521-535.

Jilka, R.L., and Martonosi, A.N. (1975), J. Biol. Chem. 250, 7511-7524.

Johnson, S.M., and Bangham, A.D. (1969), Biochim. Biophys. Acta 193, (1)82-91.

Krasne, S., Eisenman, G., and Szabo, G. (1971) Science 174, 412-415.

Martonosi, A., Donley, J., and Halpin, R.A. (1968), J. Biol Chem. 243, 61-70.

Newman, G.C. and Huang, C. (1975), Biochemistry 14, 3363-3370.

Pfeiffer, D.R., Reed, P.W., and Lardy, H.A. (1974), Biochemistry 13, 4007-4014.

Harris, E.J. (1972), in Transport and Accumulation in Biological Systems, 3rd edition, University Park Press, Baltimore.

Pressman, B.C. (1970), Antimicrob. Chemother. 1969, 28.

Pressman, B.C. (1973), Fed. Proc. 32, 1698-1703.

Reed, P.W., and Lardy, H.A. (1972), J. Biol. Chem. 247, 6970-6977.

Scarpa, A., and Inesi, G. (1972), FEBS Letters 22, 273-276.

Schreier-Muccillo, S., Marsh, D., Dugas, H., Schneider, H., and Smith, I.C.P. (1973), Chem Phys. Lipids 10, 11-27.

Szabo, G. (1974), Nature 252, 47-79.

Szabo, G., Eisenman, G., McLaughlin, S.G.A., and Krasne, S. (1972), Ann. N.Y. Acad. Sci. 195, 273-290.

Taussky, H.H. and Shorr, E. (1953), J. Biol. Chem. 202, 675-685.

Waku, K., Uda, Y., and Nakazawa, Y. (1971), J. Biochem. 69, 483-491.

Wong, D.T., Wilkinson, J.R., Hamill, R.L., and Horng, J-S. (1973), Arch. Biochem. Biophys. 156, 578-585.

Wun, T-C., Bittman, R., and Borowitz, I.J. (1977), Biochemistry 16, 2074-2079.

Table 1: Influence of Lipid Composition on Ionophore-Induced Efflux of Ca^{2+} from Vesicles.[a]

Lipid Composition of vesicle	Temperature (°C)	Phospholipid Concentration (mM)	mmol Ca^{2+} bound per mol phospholipid	Rate of Ca^{2+} Efflux (pmol Ca^{2+}/μmol ionophore/hr:)							
				A23187	X537A	N-PR	c-C-PR	t-C-PR	c-C-5	P-PR	DC
SR	4	2.5	2.2	2920	157	9.9	1.25	0.55	0.20	0.20	0.55
egg PC	26	3.6	0.61	2670	23.4	0.47	2.18	-	1.25	-0	-
20 mol % PS -80 mol % egg PC	26	3.6	2.5	3201	69.1	2.55	15.6	1.28	5.43	0.64	0.32
5 mol % OA -95 mol % egg PC	20	3.0	0.16	711	2.44	0.12	0.26	-0	0.09	-0	-0
50 mol % Cholesterol -50mol % egg PC	26	2.4	0.35	474	43.6	0.12	-0	-0	-0	-0	-0

[a] The rate of $^{45}Ca^{2+}$ efflux during the first hour of dialysis following addition of ionophore was measured and corrected for the spontaneous leak of Ca^{2+} during the first hour in the presence of DMF.

Table II: Partition Coefficients of Ionophores between n-Butanol and Water.

Ionophore	Partition Coefficient
N-PR	13.4 ± 1.1
P-PR	14.3 ± 1.0
c-C-PR	13.6 ± 1.2

Table III: Partitioning of Ionophore between Egg-PC Vesicles and Water.

Ionophore	Total Amount of Ionophore Added to the Vesicle	Amount of Ionophore remaining in the dialysis bag after dialysis	% of Ionophore Remaining with the Vesicle
NPR	2.64×10^{-7} mole	2.69×10^{-7} mole	~100
P-PR	2.64×10^{-7} mole	1.04×10^{-7} mole	27
c-C-PR	2.64×10^{-7} mole	2.67×10^{-7} mole	~100

FIGURE CAPTIONS

Figure 1: Structures of P-RR, N-PR, c-C-PR, t-C-PR, and c-C-5.

Figure 2: Effect of ionophores on the rate of Ca^{2+} efflux from vesicles prepared from SR lipids. The conditions are described in the experimental section. The SR phospholipid concentration was 2.5 μmol P/ml. The amount of Ca^{2+} captured in the vesicles was 2.2 nmol Ca^{2+}/μmol phospholipid. The temperature was 4°. The ionophore concentrations were 1.41×10^{-4} M for N-PR, c-C-PR, c-C-5, t-C-PR, P-PR, and DC; 8.47×10^{-6} M for X537A; and 4.78×10^{-7} M for A23187. The experiment was performed at 4° because the leakage of Ca^{2+} in SR vesicles in the absence of ionophores at room temperature amounts to 53 % of the trapped Ca^{2+}.

Figure 3: Rate of Ca^{2+} efflux from egg-PC vesicles in the presence of ionophores. The concentration of phospholipid was 3.6 μmol P/ml. The amount of Ca^{2+} captured in the vesicle was 0.61 nmol Ca^{2+} /μmol phospholipid. The temperature was 26°. The ionophore concentrations were the same as in Figure 2.

Figure 4: Rate of Ca^{2+} efflux from 20 mol % PS-80 mol % egg-PC vesicles in the presence of ionophores. The total concentration of phospholipid was 4.5 μmol P/ml. The amount of Ca^{2+} captured in the vesicles was 1.9 nmol Ca^{2+} /μmol phospholipid. The temperature was 26°. The ionophore concentrations were the same as in Figure 2.

Figure 5: Rate of Ca^{2+} efflux from 5 mol % octadecylamine-95 mol % egg PC vesicles in the presence of ionophores. The phospholipid concentration was 3.0 μmol p/ml. The amount of Ca^{2+} captured in the vesicle was 0.16 nmol Ca^{2+} /μmol phospholipid. The temperature was 20°. The ionophore concentrations were the same as in Figure 2.

Figure 6: Rate of Ca^{2+} efflux from 50 mol % cholesterol-50 mol % egg PC vesicles in the presence of ionophores. The phospholipid concentration was 2.4 μmol P/ml. The amount of Ca^{2+} captured in the vesicle was 0.35 nmol Ca^{2+} /μmol phospholipid. The temperature was 26°. The ionophore concentrations were the same as in Figure 2.

Figure 7: Effect of lipophilic anions on ionophore-mediated Ca^{2+} transport across egg-PC vesicles. (A). Vesicles were prepared in the medium described in the Experimental Section. The phospholipid concentration and the amount of Ca^{2+} captured were 3.5 μmol P/ml and 0.35 nmol Ca^{2+} /μmol phospholipid, respectively. A separate vesicle preparation was used which had a phospholipid concentration of 2. μmol P/ml, and captured 0.3 nmol Ca^{2+} /μmol phospholipid. The concentrations of c-C-PR, ANS^-, Ph_4B^-, DPA^-, and Pic^- were 2.82×10^{-5} M. At the point indicated by the arrow, more picric acid was added to the dialysis medium to make the amount of picric acid 5 times that of c-C-PR. The temperature was 25°. Addition of (a) c-C-PR+Ph_4B^-; (b) c-C-PR+DPA^-; (c) c-C-PR+Pic^-; (d) c-C-PR+ANS^-; (e) c-C-PR; (f) DMF; (g) Ph_4B^-; (h) DPA^-; (i) Pic^-; (j) ANS^-. (B) Addition of (k) c-C-PR (1.41×10^{-4} M) and ANS^- (1.41×10^{-4} M); (l) c-C-PR (1.41×10^{-4} M); (m) ANS^- (1.41×10^{-4} M). In (k) and (m) the dialysis medium also contained 1.41×10^{-4} M ANS^-. Dashed curves: The

experimental conditions were the same as described above except that vesicles were prepared in a medium containing 10 mM imidazole, pH 7.0, 135 mM NaCl, and 1.5 mM $CaCl_2$. The phospholipid concentration was 2.6 μmol P/ml. The amount of Ca^{2+} captured was 3.32 nmol/μmol phospholipid. Addition of (∝) O, X537A (8.47×10^{-6} M) and Ph_4B^- (1.41×10^{-4} M); (∝') ●, X537A (8.47×10^{-6} M); (y)□,A23187 (9.56×10^{-8} M) and Ph_4B^- (1.41×10^{-4} M); (y')■,A23187 (9.56×10^{-8} M); (z) Ph_4B^-(1.41×10^{-4} M); (z') ethanol.

Figure 8: Complexation of vesicle-bound $Ca^{2+}$by ionophores using chlorotetracycline as fluorescence probe.
(A) Changes in chlorotetracycline fluorescence upon complexation of vesicle-bound Ca^{2+} by c-C-PR. Vesicles (1 mM phospholipid) were prepared by dispersing and sonicating 20 mol % PS and 80 mol % egg PC in a medium containing 10 mM imidazole buffer, pH 7.0, 135 mM NaCl, and 0.2 mM $CaCl_2$. Chlorotetracycline was added to make a final concentration of 1.0×10^{-5} M. Addition of EDTA (final concentration of 1 mM) caused a decrease in fluorescence intensity of chlorotetracycline. After the fluorescence reached a relatively steady level (~2 min), the reaction was started by addition of a concentrated ionophore solution in DMF. The DMF concentration was 1.25% (v/v). The ionophore concentrations are indicated in the figure. The fluorescence intensity was monitored using excitation and emission wavelengths of 390 and 530 nm, respectively. The net fluorescence decrease was obtained from the difference between the fluorescence intensity in the presence of ionophore and DMF and the fluorescence intensity in the presence of DMF alone. The temperature was 27°.

(B) Log-log plot of the fluorescence decrease vs. ionophore concentration. The complexation of Ca^{2+} bound to PS-egg-PC vesicles with N-PR (Δ) and c-C-PR (O) was measured as described in (A) after the reaction mixture had been incubated for 25 min. The complexation of Ca^{2+} bound to egg-PC vesicles with N-PR (▲) and c-C-PR (●) was measured as described in (A), except that the chlorotetracycline concentration was 2.24×10^{-5} M and the reaction mixture was incubated for 25 min before fluorescence measurements were made. Vesicles were prepared from egg PC (1 mM) in a medium containing 10 mM imidazole buffer, pH 7.0, 135 mM NaCl, and 0.6 mM $CaCl_2$.

FIG. 1

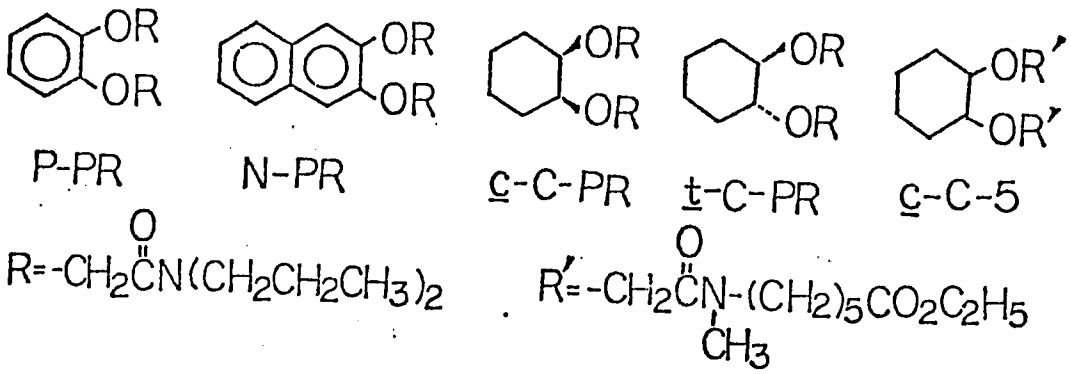
OR
OR
OR
OR
OR
OR
OR
OR
OR'
OR'
P-PR
N-PR
c-C-PR
t-C-PR
c-C-5
R=-CH2CN(CH2CH2CH3)2
R'=-CH2CN-(CH2)5CO2C2H5
CH3

FIG. 2

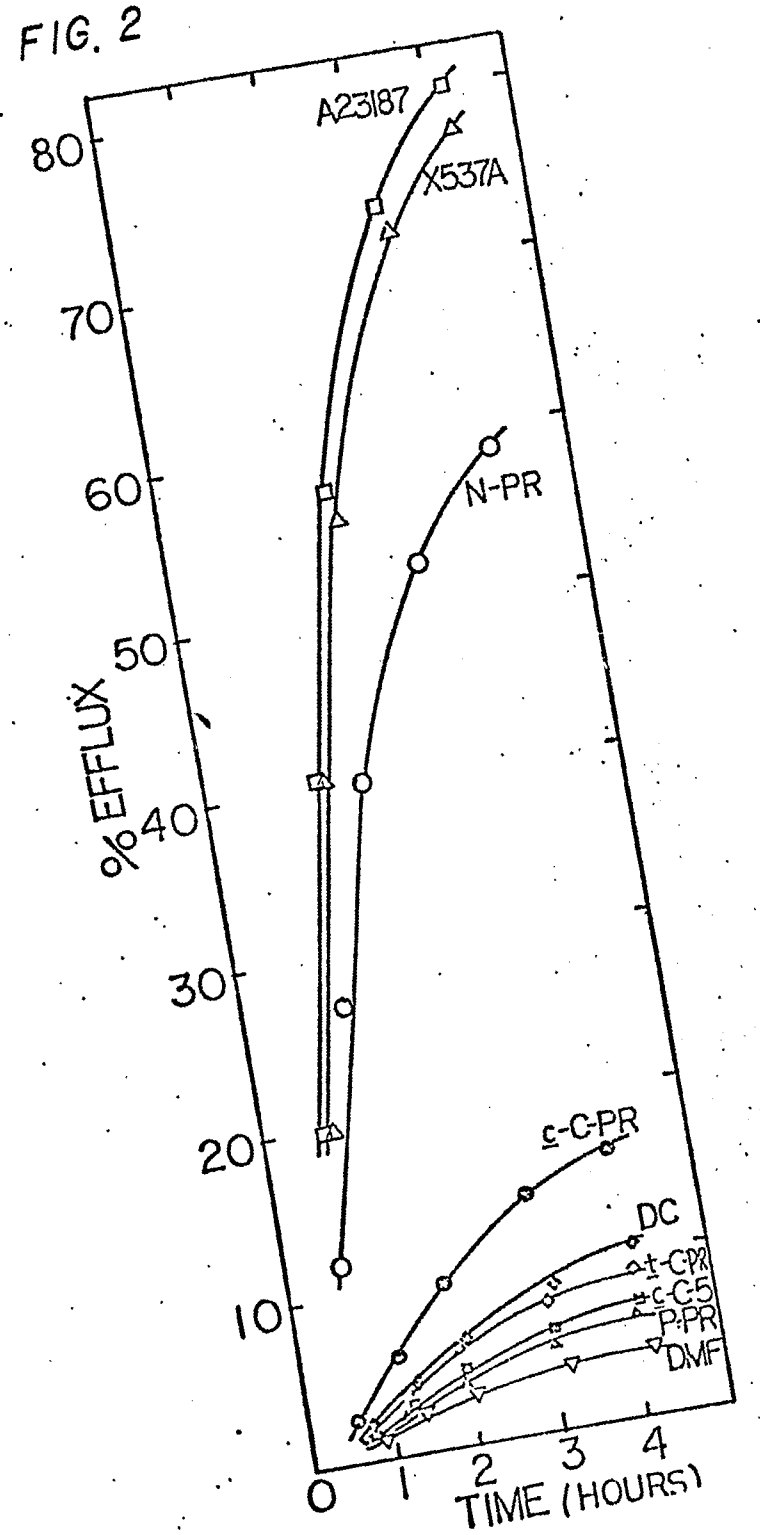
A23187
X537A
N-PR
c-C-PR
DC
t-C-PR
c-C-5
P-PR
DMF
% EFFLUX
80
70
60
50
40
30
20
10
0
1
2
3
4
TIME (HOURS)

FIG. 3

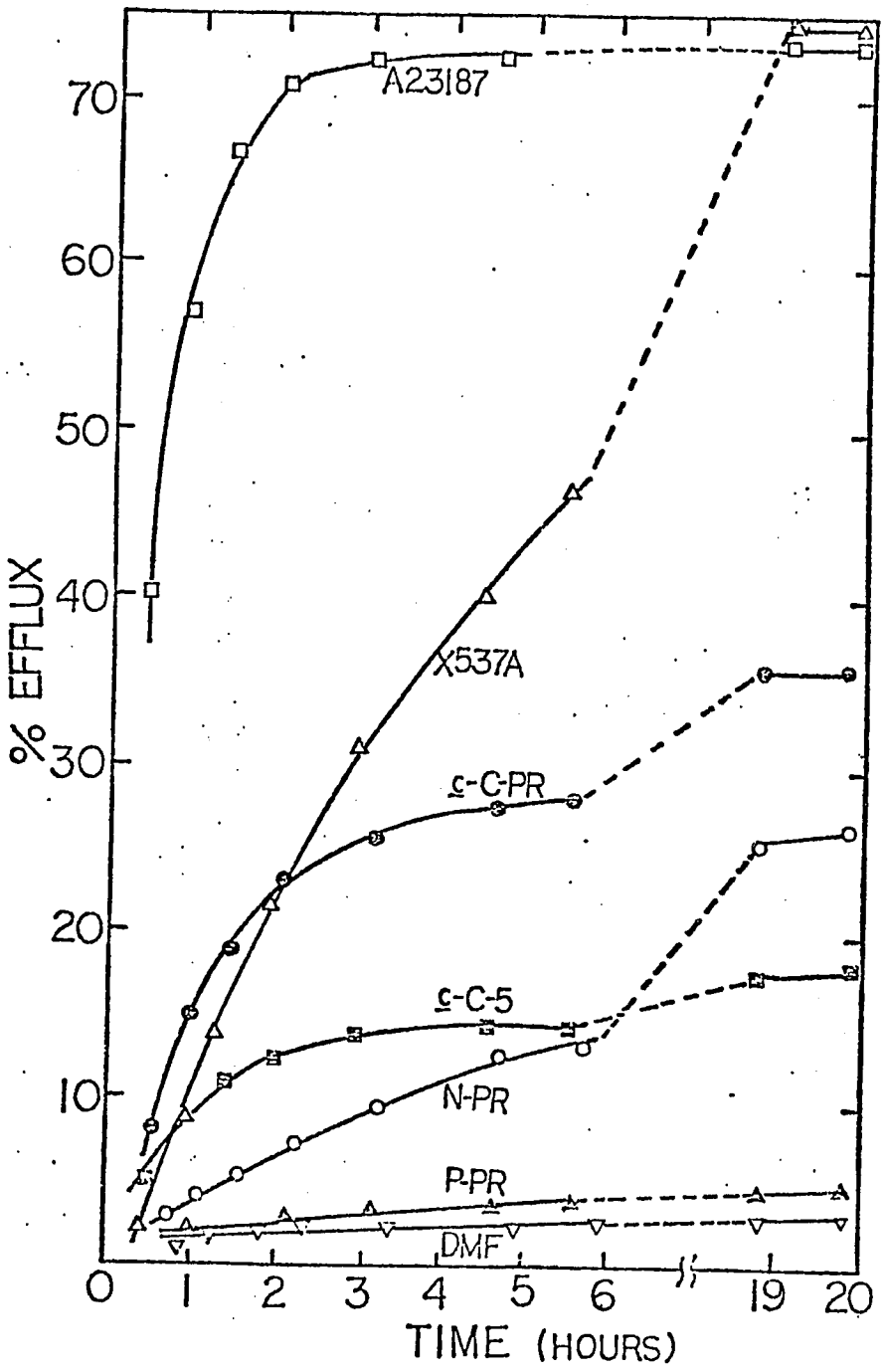
A23187
X537A
c-C-PR
c-C-5
N-PR
P-PR
DMF
% EFFLUX
TIME (HOURS)
0
1
2
3
4
5
6
19
20
10
20
30
40
50
60
70

FIG. 4

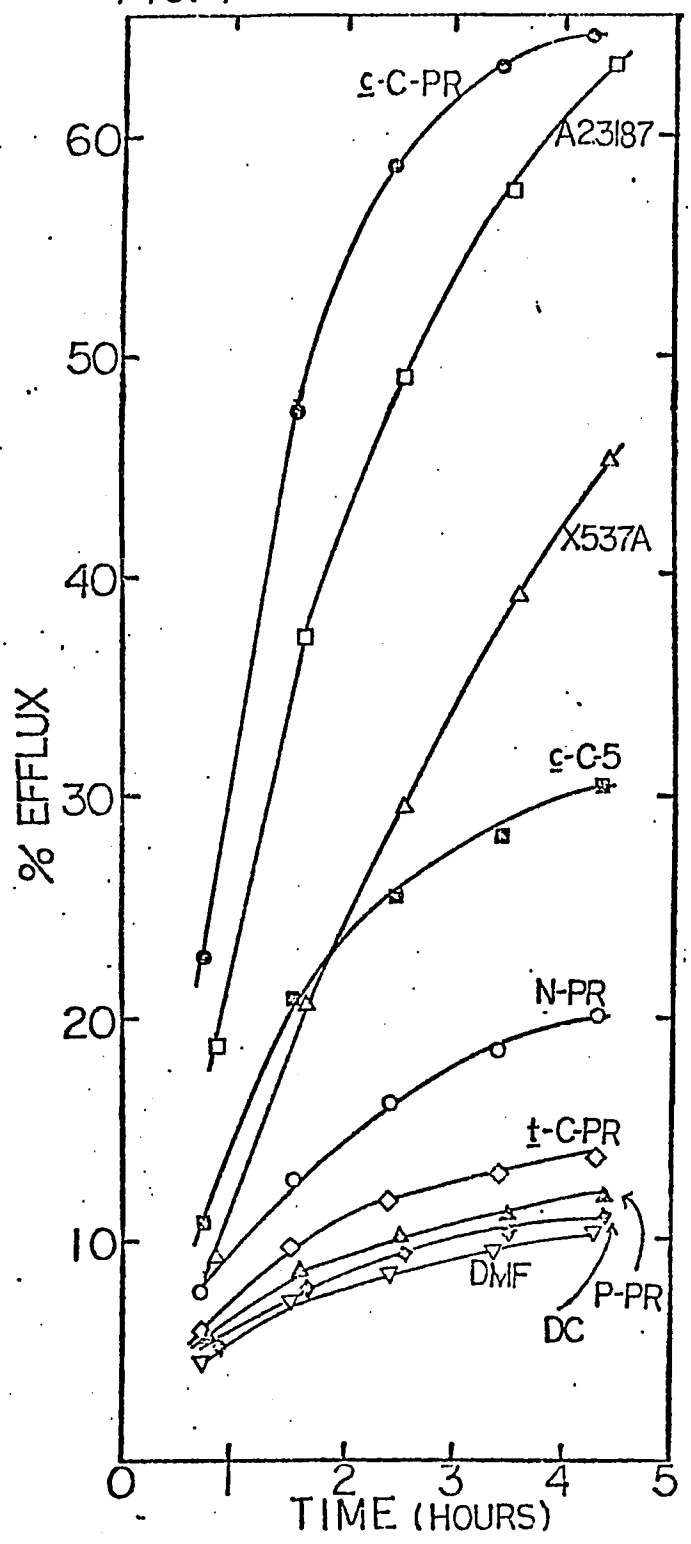
c-C-PR
A23187
X537A
c-C-5
N-PR
t-C-PR
DMF
P-PR
DC
% EFFLUX
TIME (HOURS)
0
1
2
3
4
5
10
20
30
40
50
60

FIG. 5

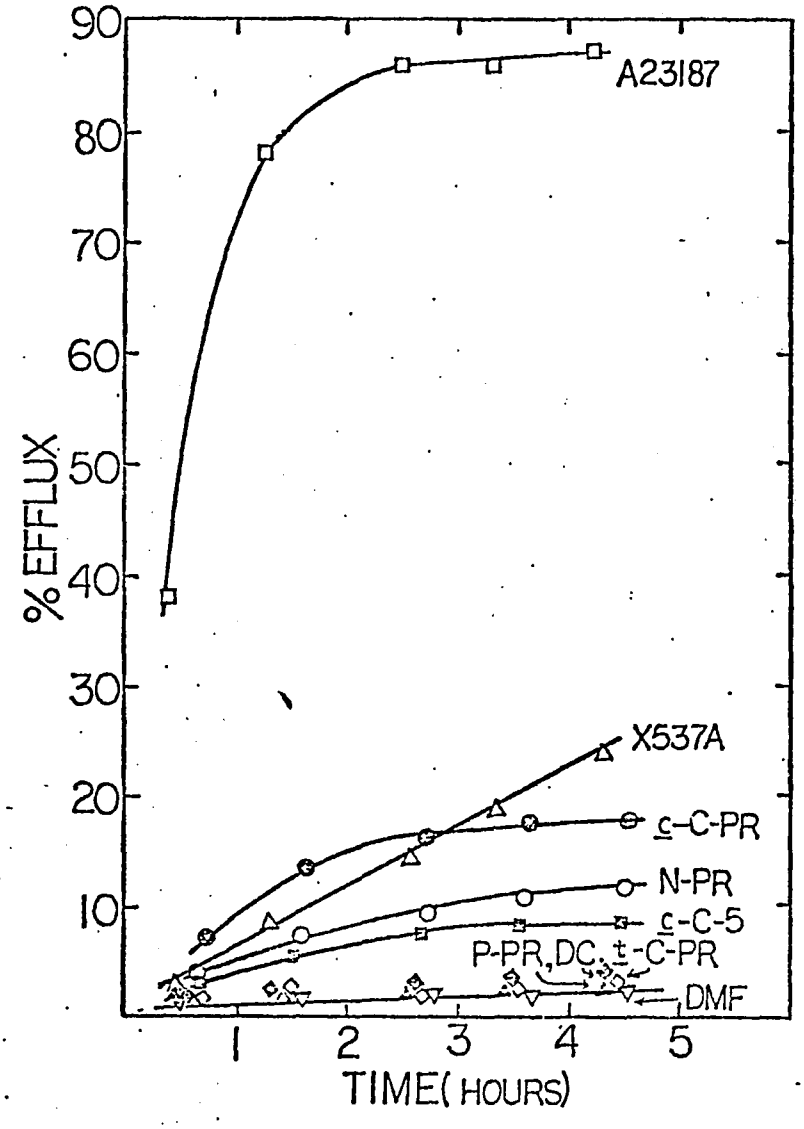
90
80
70
60
50
40
30
20
10
% EFFLUX
A23187
X537A
c-C-PR
N-PR
c-C-5
P-PR, DC, t-C-PR
DMF
1
2
3
4
5
TIME(HOURS)

FIG. 6

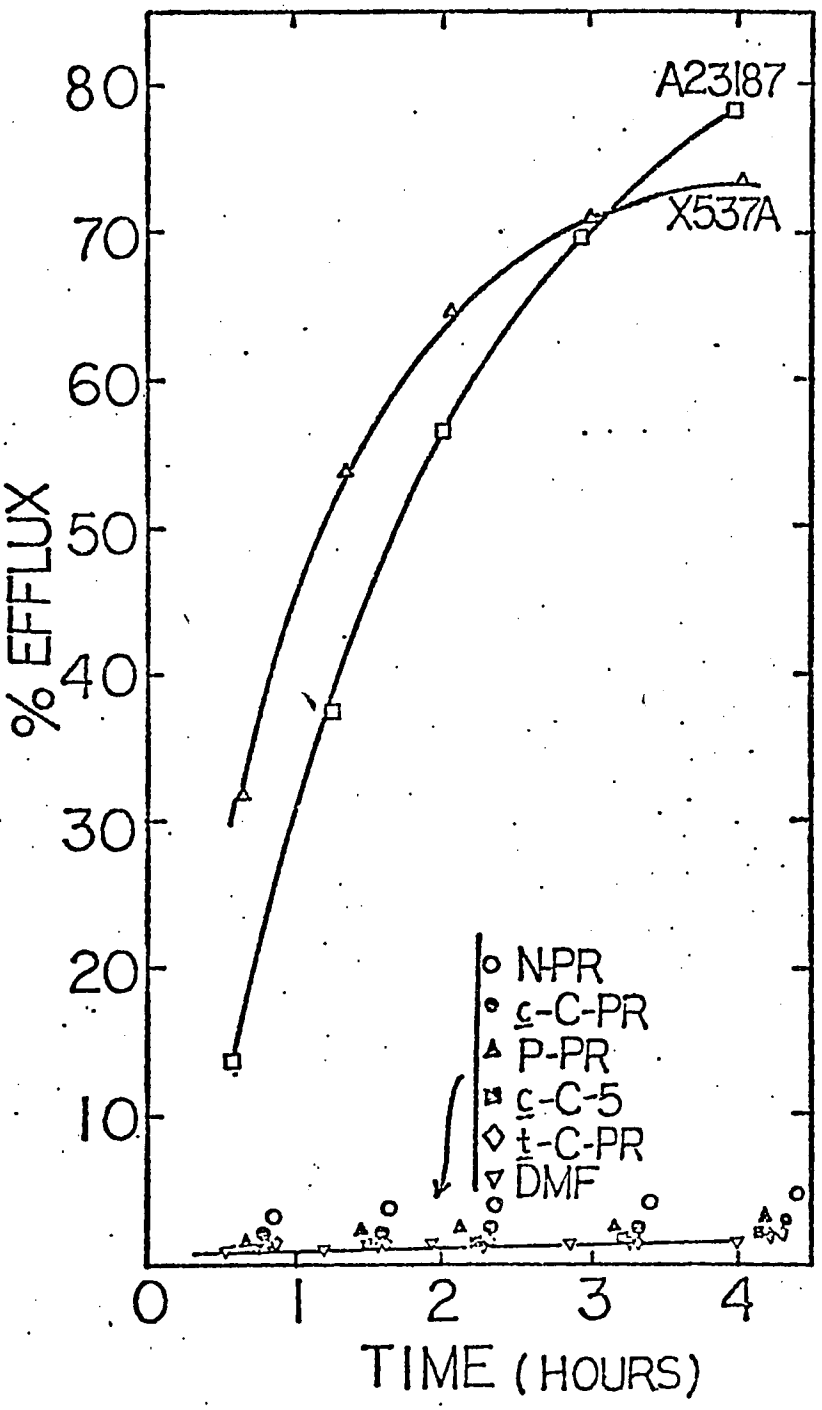
A23187
X537A
% EFFLUX
80
70
60
50
40
30
20
10
0
1
2
3
4
TIME (HOURS)
N-PR
c-C-PR
P-PR
c-C-5
t-C-PR
DMF

FIG. 7

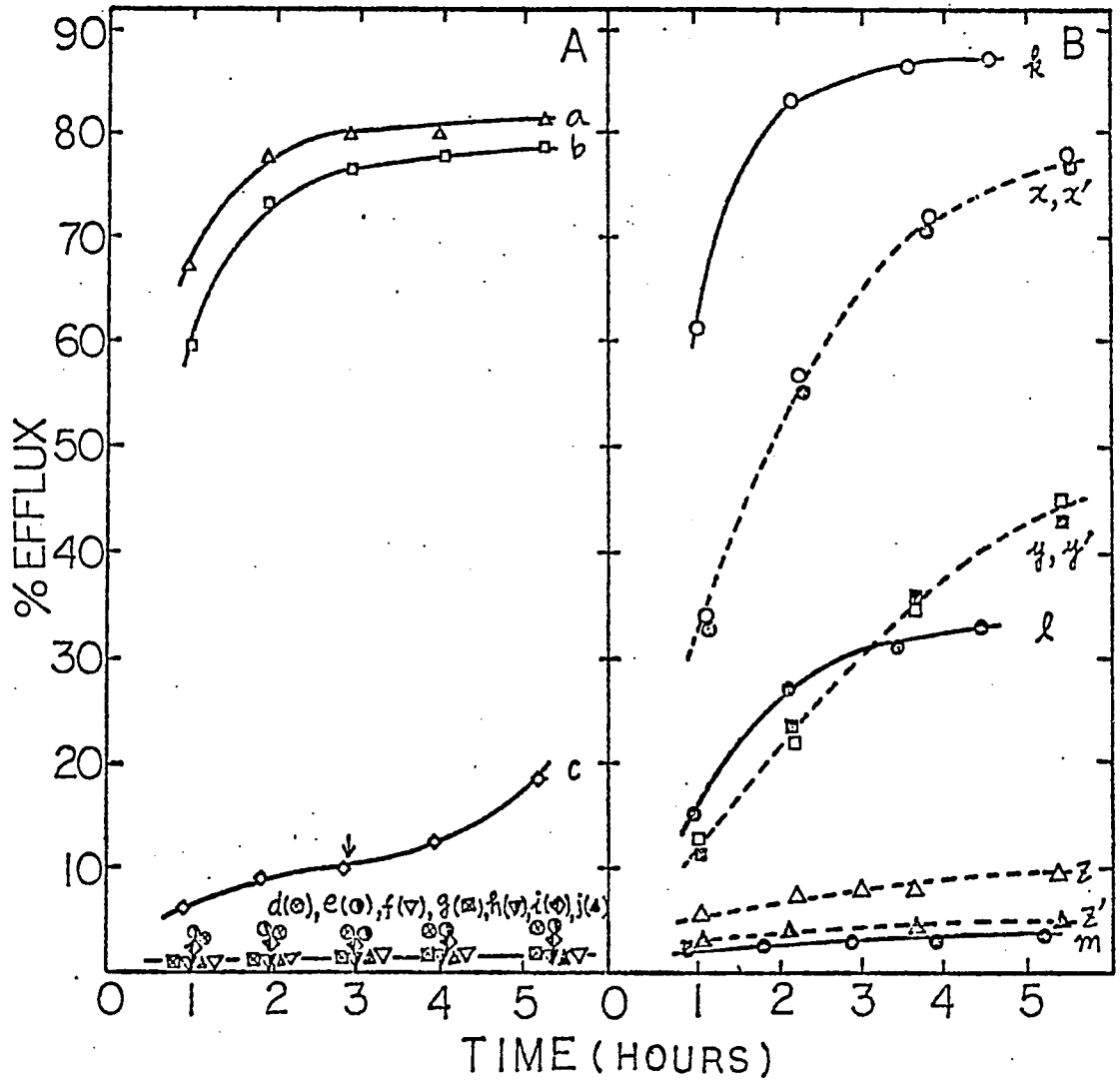
A
B
a
b
c
d(⊙), e(⊙), f(▽), g(⊠), h(▽), i(Φ), j(▲)
k
x, x'
y, y'
l
z
z'
m
% EFFLUX
TIME (HOURS)
90
80
70
60
50
40
30
20
10
0
1
2
3
4
5

FIG. 8

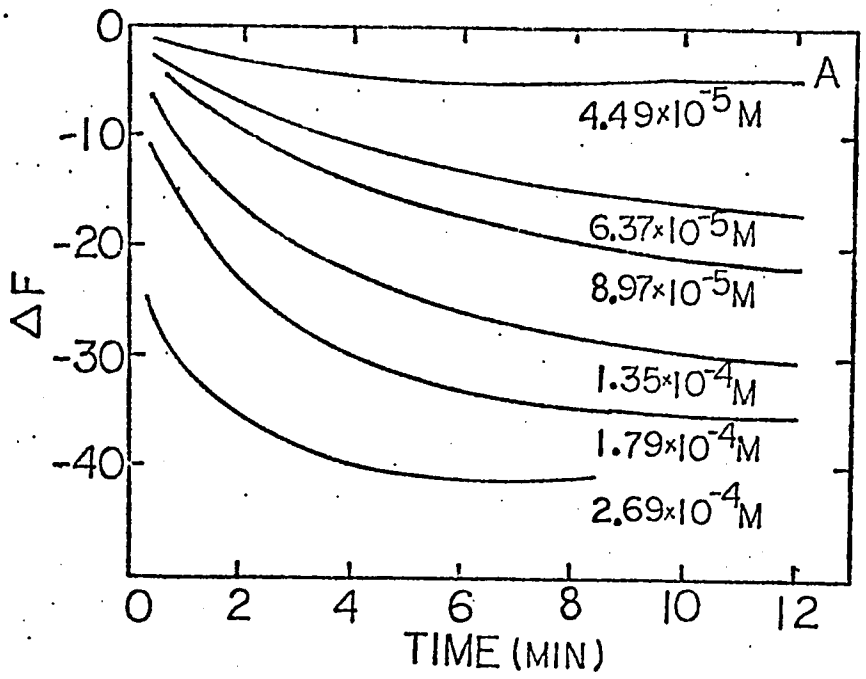
0
-10
-20
-30
-40
ΔF
A
4.49×10⁻⁵M
6.37×10⁻⁵M
8.97×10⁻⁵M
1.35×10⁻⁴M
1.79×10⁻⁴M
2.69×10⁻⁴M
0
2
4
6
8
10
12
TIME (MIN)

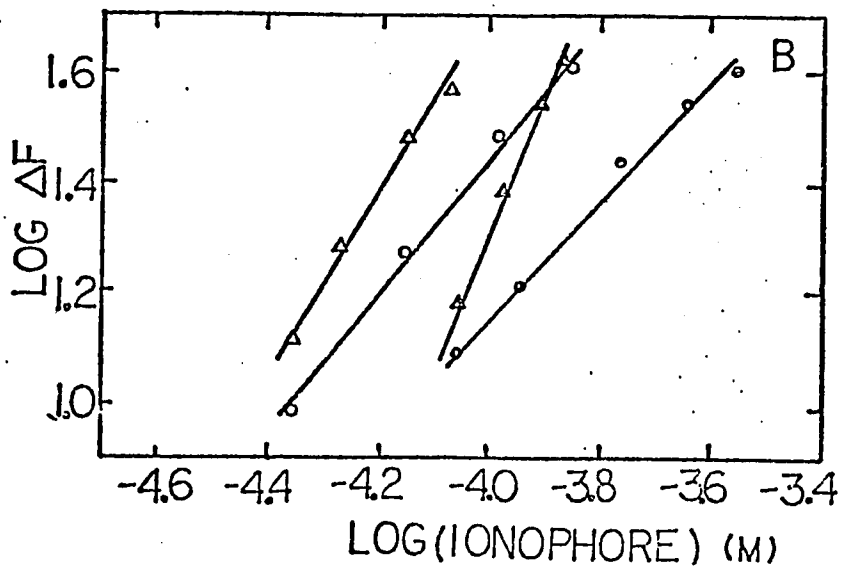
B
1.6
1.4
1.2
1.0
LOG ΔF
-4.6
-4.4
-4.2
-4.0
-3.8
-3.6
-3.4
LOG (IONOPHORE) (M)

Part IV

Ionophorous Properties of Carboxylic Acid and Neutral Ionophores Toward Ca^{2+}, K^{+}, and Na^{+} in Phosphatidylcholine Vesicles.

ABSTRACT: The selectivity of the widely used divalent-cation ionophore A23187 on Na^+, K^+, and Ca^{2+} was studied by direct measurements of its ability to induce the transport of these cations across egg PC vesicles. The results were compared with the rates of cation transport induced by other divalent-cation ionophores, X537A and cis - 1,2 - cyclohexanedioxy-diacetic acid N, N, N', N' - tetra-n-propyl amide (c-C-PR), and by monovalent-cation ionophores, nigericin, valinomycin, and dicyclohexyl-18-crown-6. The carboxylic acid ionophores induce a more rapid cation transport than the neutral ionophores. At high cation concentration (1.5M), the transport of K^+ and Na^+ by A23187 is much faster than that of Ca^{2+}. At lower cation concentration (0.15-1.5 mM Ca^{2+} and 135 mM Na^+ or K^+), the transport of Ca^{2+} is affected by the presence of Na^+ or K^+, indicating that at close to physiological concentration of these cations, the selectivity of A23187 for Ca^{2+}, Na^+, and K^+ is not complete. The rates of cation transport mediated by A23187 and c-C-PR are stimulated by the availability of an exchange mechanism among Ca^{2+}, Na^+, and K^+. The c-C-PR-induced Ca^{2+} transport is electrogenic, as evidenced from the effect of a diffusion potential generated by addition of external valinomycin and K^+ to the vesicles. The rate of transport of Ca^{2+} catalyzed by A23187 is also enhanced by the diffusion potential generated in this way. However, in the absence of valinomycin and K^+, the initial rate of Ca^{2+} transport by A23187 has a second-order dependence on the A23187 concentration, indicating that a possibly neutral $(A23187)_2$-Ca^{2+} complex is the main species transported. The mechanism of A23187-induced Ca^{2+} transport is discussed.

In recent years the selectivities of natural and synthetic macrocyclic ligands for alkali and alkaline-earth metal cations and the stabilities of the complexes have been investigated. Applications have been developed for selective ligands in the study of the role of metal ions (Na^+, K^+, Ca^{2+}, Mg^{2+}) that partake in fundamental biological processes. The ability of A23187, a naturally occurring, carboxylic acid ionophore containing two ether oxygen atoms in a spiroketal linkage and two aromatic groups, to increase the permeability of many biological membranes for divalent cations has been clearly established (Reed and Lardy, 1972; Caswell and Pressman, 1972; Scarpa et al., 1972; Scarpa and Inesi, 1972; Wong et al., 1973). This ionophore has been used extensively to study the effects of the altered distribution of divalent cations on a variety of cellular functions, especially on properties associated with membrane-bound Ca^{2+} pumps (see references in Deber and Pfeiffer, 1976). The properties of this divalent cation ionophore differ from those of other naturally occurring, polyether, carboxylic acid ionophores currently used to modify cation distribution across membranes. Unlike X537A, which catalyzes transport of both monovalent and divalent cations (Scarpa and Inesi, 1972; Celis et al., 1974; Kafka and Holz, 1976), and unlike nigericin, which catalyzes monovalent cation transport (Pressman, 1968), A23187 extracts divalent cations in a two-phase system in a selective manner relative to monovalent cations (Pfeiffer et al., 1974). The conductance of black lipid membranes is not increased by A23187-mediated Ca^{2+} transport (except at high A23187 concentration), suggesting that a charge-neutral, 2:1 A23187-Ca^{2+}

complex is mainly responsible for the increased Ca^{2+} permeability produced by this ionophore (Case et al., 1974; Wulf and Pohl, 1977). The involvement of an electroneutral 2:1 A23187-M^{2+} complex (with both carboxylate groups deprotonated in the complex) in M^{2+} transport was also inferred from the inability of lipophilic anions to enhance metal cation extraction by A23187 (Reed and Lardy, 1972), from the ionophore concentration dependence of cation extraction in a two-phase system (Pfeiffer and Lardy, 1976), and from the dependence of Ca^{2+} efflux on A23187 concentration at a specified range of ionophore concentrations (Hyono et al., 1975). An electroneutral exchange of two protons for a divalent cation across biological membranes has been suggested (Reed and Lardy, 1972; Pfeiffer and Lardy, 1976), but no evidence was found for the catalysis of transport by A23187 of one or two protons per Ca^{2+} across black lipid membranes (Wulf and Pohl, 1977).

The usefulness of A23187 as an agent to study the role of Ca^{2+} in cellular function rests on the assumption that it transports divalent cations across membranes with appreciably greater rates and extents than monovalent cations. The loss of K^{+} from isolated mitochondria (Pfeiffer and Lardy, 1976), parotid slices (Selinger et al., 1974), and erythrocytes (Reed, 1976) induced by A23187 may represent a secondary effect of the ionophore that follows Mg^{2+} or Ca^{2+} depletion, which alters the membrane permeability properties (Duszyński and Wojtczak, 1977; Reed, 1976). On the other hand, A23187 may possess ionophorous activity toward K^{+} and Na^{+} (Pfeiffer and Lardy, 1976).

Significant catalysis of monovalent cation transport by A23187 would greatly complicate the interpretation of the effects of this ionophore on physiological processes involving divalent cations. Therefore, it is essential that its transport properties toward monovalent cations be examined directly.

The synthesis and behavior of acyclic 1, 2-ethylenedioxydiacetamide systems in liquid-membrane electrodes have been reported (e.g., Ammann et al., 1973; Ammann et al., 1975). We have recently described the preparation, metal-ion binding properties, extraction selectivities, and ionophorous properties toward Ca^{2+} of alicyclic and aromatic derivatives of this system (Borowitz et al., 1977; Wun et al., 1977; Wun and Bittman, 1977). In the present study we compare the ionophorous activities of the natural, carboxylic acid ionophores A23187, X537A, and nigericin, with those of the neutral ionophores, valinomycin, dicyclohexyl-18-crown-6, and cis-1,2-cyclohexanedioxydiacetic acid N, N, N', N'-tetra-n-propyl amide (c-C-PR). We report the ionophore-induced efflux of Na^+, K^+, and Ca^{2+} efflux from egg PC[1] vesicles, and the influence of the presence of Na^+ and K^+ in the external medium and of a monovalent cation diffusion potential on Ca^{2+} transport mediated by A23187 and c-C-PR.

Experimental Section

Materials

A23187, nigericin, and valinomycin were gifts from Eli Lilly and Co. X537A was donated by Dr. J. Berger of Hoffmann-LaRoche. Dicyclohexyl-18-crown-6 was a gift from Dr. H. Frensdorff of DuPont Central Research. The ligand c-C-PR was synthesized by Dr. I. J. Borowitz and co-workers

as described previously (Ammann et al., 1975). The diazapolyoxamacrobicyclic ligand, [2.2.1 cryptand], was a gift from Dr. J. M. Lehn. Egg PC (Sigma Chemical Co.) was purified and characterized as cited previously (Wun and Bittman, 1977). Sepharose CL-4B was obtained from Pharmacia. Calcium-45 was purchased from New England Nuclear Corp. Arsenazo III was purchased from Gallard-Schlesinger Chemical Corp. The purification of arsenazo III was carried out by the following procedure. A concentrated aqueous solution of arsenazo III was passed through a column of AG 50W-X8 H^+-form ion exchanger (Bio-Rad Laboratories). Concentrated HCl was then added to make the final concentration of HCl 6 M. Arsenazo III was recrystallized at 4°C and recovered by filtration. Excess H_2O and HCl in the sample were removed by dissolution in acetone and flash evaporation of the solvent. This procedure abolished the peak at 650 nm characteristic of the absorption by the Ca^{2+}-arsenazo III complex.

The methylation of A23187 was carried out by a modification of a method used for the esterification of fatty acids using diazomethane (Lipsky and Landowne, 1963). Diazomethane was generated from diazald (Aldrich Chemical Co.). After methylation, six bands were separated by thin-layer chromatography on silica gel G using cyclohexane: tetrahydrofuran: methanol (20:6: 0.4) as solvent. The major band was the methyl ester (molecular weight of 537) as determined on a CEC 21-110 mass spectrometer run at 70 eV. An impurity (molecular weight 551) of 2% was also present.

Methods

Preparation of ^{45}Ca-Containing Vesicles and Assay of $^{45}Ca^{2+}$ Efflux Induced by Ionophores. Vesicles containing $^{45}Ca^{2+}$ were prepared and ionophore-mediated $^{45}Ca^{2+}$ efflux was measured as described previously (Wun and Bittman, 1977). The vesicles used to obtain the data in Figure 2 were prepared in the same way as described below for Na^+-and K^+-containing vesicles. To compare the sizes of vesicles prepared by sonication in media containing low and high $CaCl_2$ concentrations vesicles were fractionated on a Sepharose CL-4B column (1 X 50 cm). Vesicles prepared in 10 mM imidazole-0.15 mM $CaCl_2$, pH 7.0, were eluted with 10 mM imidazole buffer pH 7.0 containing 2.25 mM choline chloride; those prepared in buffer containing 1.5 M $CaCl_2$ were eluted with buffer containing 2.25 M choline chloride. Each vesicle preparation was resolved into two fractions. The volume required to elute each fraction were very similar, indicating that the vesicles containing low and high Ca^{2+} concentrations had similar sizes.

Preparation of Vesicles Containing Trapped Na^+ or K^+. To a thin film of egg PC (20mg) in a 0.5 x 3.5 cm culture tube, 1 ml of 10 mM imidazole buffer, pH 7.0, containing 1.5M NaCl (or KCl) was added. The suspension was shaken on a Vortex mixer for 2 min, and then sonicated under nitrogen in a bath type sonifier (Multisonic, MSVP-150) for 1 hr at power level 95. The tube was positioned in the bath to obtain maximum sonication intensity. The vesicles were then subjected to an additional brief period of sonication to bring the absorbance at 400 nm to 1.4. To remove NaCl (or KCl) from the external medium, the vesicles were dialyzed against 50 volumes of 10 mM imidazole buffer, pH 7.0, containing 1.5M choline chloride at 4-6°C for 5 times, each

time for 1 hr. The trapped aqueous volume was 0.543 ± 0.031 l/mol phospholipid as calculated from the amount of captured K^+ and Na^+.

Phospholipid concentrations were measured by H_2SO_4 digestion and inorganic phosphate analysis as described before (Wun and Bittman, 1977), except for samples that contained choline chloride. Since choline chloride interfered with the phosphate analysis, it was decomposed by heating in a Bunsen flame for about 2 min before the H_2SO_4 digestion and phosphate analysis were performed.

Assays of Na^+ and K^+ Efflux. Ten microliters of stock solutions of ionophores in dimethylformamide (DMF) were added to 1 ml of Na^+ (or K^+)-containing vesicles. The vesicles were placed in dialysis sacs whose Na^+ and K^+ contents had been reduced by heating at 75°C for 2 hr in the presence of a H^+-form cation exchanger (AG 50W-X8), followed by soaking in distilled water overnight. The dialysis sacs were tied with a small air bubble trapped. The vesicles were then dialyzed in 3.5 x 1.7 cm polyethylene vials against 5 ml of 10 mM imidazole buffer, pH 7.0, containing 1.5 M choline chloride. The vials were rotated at 2 rpm. In Figure 4, where 0.15 M KCl was used, the experimental conditions are described in the figure caption. At various time intervals 0.5-ml aliquots were withdrawn from the dialysis medium. Sodium and potassium were measured using a Model 303 Perkin-Elmer atomic absorption spectrometer equipped with an automatic null recorder. Samples were diluted with medium and/or 1-propanol to give Na^+ concentrations in the range of $0\text{-}1\times10^{-4}$ M and K^+ concentrations of

0-1.8 X 10^{-4}M. Measurements were made at 295 nm for Na^+ and 383 nm for K^+. Standards were prepared in the same medium and in similar concentration ranges.

When the kinetics of ionophore-induced ion efflux was measured in triplicates from the same vesicle preparation, the percentage of efflux varied by less than 3%.

Measurement of Ca^{2+} Efflux Using Arsenazo III as Ca^{2+} Indicator. Egg PC vesicles were prepared in the same way as described for K^+-and Na^+-containing vesicles except that the medium contained 10 mM imidazole, pH 7.0, and 0.10 M $CaCl_2$. To remove external Ca^{2+} the vesicles were passed through a column (1.7 x 30 cm) of 3 g of Sephadex G-50 which had been equilibrated with a medium containing 10 mM imidazole, pH 7.0, and 0.15 M choline chloride. The vesicles were eluted with the latter medium. Stock solutions of A23187 (10 to 50 μM) were prepared in ethanol. Three-μl aliquots of the stock solutions were added to 0.8ml of 10 mM imidazole, pH 7.0, 0.15 M choline chloride, and 0.352 μM arsenazo III. Ca^{2+} efflux from the vesicles was initiated by addition of 40 μl of vesicles and was monitored by the change in absorbance at 650 nm.

The ion flux measurements were carried out at 23-25°C unless noted otherwise. The amount of Ca^{2+} captured in the vesicles was determined from the absorbance of arsenazo III - Ca^{2+} in 50% aqueous 1-propanol.

Results

Na^+, K^+, and Ca^{2+} Efflux from Egg PC Vesicles Induced by Ionophores. The abilities of various types of ionophores to induce Na^+, K^+, and Ca^+

transport across egg PC bilayers were compared by dialyzing the Na^+-, K^+-, or Ca^{2+} - containing vesicles against a medium containing an impermeable electrolyte, choline chloride. The rates of Na^+, K^+, and Ca^{2+} efflux from the vesicles are shown in Figures 1 and 2. The initial rates of efflux of Na^+, K^+, and Ca^{2+} induced by ionophores during the first hour of dialysis are summarized in Table I. The carboxylic acid ionophores, nigericin, X537A, and A23187, which are negatively charged at pH 7.0, have much higher potencies for transport of both K^+ and Na^+ across egg PC vesicles than the neutral ionophores, valinomycin, 18-crown-6, and c-C-PR. The ionophores show a selectivity for K^+ over Na^+ (except c-C-PR, which transports Na^+ at faster rates and greater extent than K^+). The Ca^{2+} transport activities of A23187 and X537A are very low compared with their abilities to catalyze Na^+ and K^+ transport across egg PC vesicles. This suggests that the double charge on Ca^{2+} is less enveloped or neutralized in the Ca^{2+}-ionophore complexes than the univalent charge is in the Na^+- or K^+-ionophore complexes. The [2.2.1] cryptand has no activity at a concentration as high as 141 μM, despite the fact that it forms a very tight complex with Ca^{2+} in aqueous methanol (Lehn and Sauvage, 1975).

The low initial velocity of Ca^{2+} transport by A23187 when the intravesicular $CaCl_2$ concentration is 1.5 M and the external medium is 2.25 M choline chloride is surprising because under different conditions (vesicles containing 0.15 mM Ca^{2+} and 135 mM NaCl inside, and 135 mM NaCl in the external medium) A23187 is very active in transporting Ca^{2+} across vesicles compared with the other Ca^{2+}

ionophores (Wun and Bittman, 1977). The initial rate of A23187-induced Ca^{2+} efflux from vesicles prepared with the high internal Ca^{2+} is about 2 times that of X537A and 14 times that of c-C-PR; with vesicles containing 0.15 mM Ca^{2+} and 135 mM NaCl, the relative rates differ by factors of 114 and 1225, respectively (Wun and Bittman, 1977). This dependence of the relative potencies of A23187, X537A, and c-C-PR on internal Ca^{2+}concentration suggests that A23187 is capable of forming lipophilic A23187-Ca^{2+} complex(es) on the membrane at low Ca^{2+} concentration, wheras X537A and c-C-PR can be saturated with Ca^{2+} on the membrane only when the Ca^{2+} concentration in the medium is high. When the Ca^{2+} concentration is 1.5 M, the difference in the extent of saturation of the ionophores is small and the concentrations of ionophores required to produce 50% Ca^{2+} efflux in 4 hr become closer (e.g., $\sim$100 μM for c-C-PR, $\sim$10 μM for X537A, and $\sim$6 μM for A23187). The concentrations of ionophores required for 50% efflux from vesicles with 0.15 mM captured Ca^{2+} in 4 hr were $\sim$100 μM for c-C-PR, $\sim$10 μM for X537A, and $\sim$0.1 μM for A23187.

To further examine the possibility that the carboxylate group of A23187 plays an important role in ionophorous activity, we compared the Ca^{2+} transport activity of the methyl ester of A23187 (CH_3-A23187) with that of A23187. (It has been reported that CH_3-A23187 forms complexes with divalent cations (Pfeiffer and Lardy, 1976).) When the internal Ca^{2+} concentration is 1.5 M, the relative potency of A23187 to CH_3-A23187 is about 2.7 : 1 (Figure 2 and Table I). When the internal Ca^{2+} concentration is 1.5 mM (Figure 3), the relative potency

of A23187 to CH_3-A23187 is 213:1. Hence, at low Ca^{2+} concentration the presence of the carboxylate group in A23187 gives rise to faster transport of Ca^{2+}.

Figure 2 also shows that a lipophilic anion such as tetraphenylborate greatly enhances c-C-PR-induced Ca^{2+} transport, possibly because an ionophore - Ca^{2+} - lipophilic anion complex is formed in the membrane. Similar enhancements were found when lipophilic anions were added to vesicles containing 0.15 mM Ca^{2+} (Wun and Bittman, 1977).

Since the relative potencies of the ionophores depends on the cation concentration in the medium, the rates of A23187 - and valinomycin - induced K^+ efflux were further compared at closer to physiological concentration of K^+ (0.15 M). Under these conditions the initial rate of valinomycin - induced K^+ transport is about 2.4 times that induced by A23187 (Figure 4); in contrast when the K^+ concentration is 1.5 M, the initial rate of K^+ efflux induced by valinomycin is 0.22 times that induced by A23187 (Table I). This reversal of the relative potencies of A23187 and valinomycin at different K^+ concentrations suggests that the affinity of valinomycin for K^+ is greater than that of A23187 for K^+, but that the rate of transport of the valinomycin - K^+ complex is lower than that of the A23187 - Ca^{2+} complex(es).

The Effect of Monovalent Cation and Diffusion Potential on c-C-PR- and A23187-Mediated Ca^{2+} Transport. Using ion - selective membrane electrodes, Ammann et al. (1975) found that c-C-PR has a selectivity for Na^+ over K^+. The association constant for the binding of c-C-PR

with Na^+ in methanol is higher than that with K^+ (Wun et al., 1977). In egg PC vesicles, c-C-PR has a higher ionophorous activity toward Na^+ than K^+ (Figure 1 and Table I). To examine the possiblity that c-C-PR becomes a more potent carrier of Ca^{2+} across egg PC bilayers when it can return in a complex with a monovalent cation, the experiment illustrated in Figure 5 was conducted. With vesicles containing both NaCl and $CaCl_2$ captured inside (dashed lines), the rate of c-C-PR-mediated Ca^{2+} efflux into NaCl - containing medium is faster than that into KCl-containing medium. Similarly, with vesicles containing trapped KCl and $CaCl_2$ (solid lines), a faster rate of Ca^{2+} efflux is observed when the external medium contains NaCl. However, addition of valinomycin reverses the relative rates of Ca^{2+} efflux into these two media (and also reduces the rates, possibly because valinomycin modifies the packing of the lipids in the bilayer or associates with c-C-PR in the vesicles). This reversal of Ca^{2+} efflux rates arises because valinomycin, which is an electrogenic K^+ ionophore (Moore and Pressman, 1964), induces a membrane potential. On addition of valinomycin to vesicles containing only K^+ inside and only Na^+ in the external medium, a diffusion potential is generated which is positive outside and negative inside (since valinomycin transports K^+ selectively to Na^+; e. g., Table I). The formation of a diffusion potential that is positive outside inhibits the c-C-PR-mediated Ca^{2+} efflux (Figure 5). On the other hand, addition of valinomycin to vesicles containing only Na^+ inside and only K^+ in the external medium results in the formation of the opposite diffusion potential, i.e., positive inside. Since c-C-PR has a greater

selectivity for binding and transport of Na^+ than K^+, the addition of external NaCl makes available an exchange mechanism (involving the transport of Ca^{2+}out and that of Na^+ into the vesicles) that enhances the rate of Ca^{2+}efflux by relieving the membrane potential which would inhibit further efflux. The conclusion that the Ca^{2+} - Na^+ exchange mediated by c-C-PR is electrogenic is supported by the observation that a K^+ diffusion potential generated by the addition of valinomycin affects c-C-PR-mediated Ca^{2+} transport.

Since A23187 forms complexes with monovalent cations and promotes significant monovalent cation transport (Pfeiffer and Lardy, 1976; Figure 1), we sought to establish whether transport of monovalent cations affects A23187-induced Ca^{2+} transport. This would complicate the use of this agent as a probe of Ca^{2+} under physiological conditions. Figure 6 shows that when vesicles were prepared with $CaCl_2$ and NaCl captured inside (Panel A), Ca^{2+} efflux induced by A23187 into a KCl-containing medium is faster than that into a NaCl-containing medium. In view of the higher specificty of A23187 for K^+ than Na^+ (Table I), an A23187-mediated exchange of Ca^{2+} out of the vesicles and K^+ into the vesicles may occur. Valinomycin by itself does not promote Ca^{2+} efflux in egg PC vesicles; however, it enhances A23187-mediated Ca^{2+} transport even under the condition where both the inside and outside of the vesicles contained the same concentration of NaCl. The reason for this apparent synergistic effect is not clear. A further enhancement is observed when KCl is present in the external medium; these conditions generate a diffusion potential that is positive inside and negative outside. With vesicles containing trapped $CaCl_2$ and KCl (Panel B), A23187-

mediated Ca^{2+} transport in the presence of valinomycin is faster in medium containing KCl than in medium containing NaCl. When NaCl is present in the external medium, valinomycin generates a diffusion potential that is positive outside and negative inside. This inhibits A23187-mediated Ca^{2+} efflux relative to conditions where no gradient with respect to monovalent cation exists. Thus these data suggest that A23187-mediated Ca^{2+} transport across vesicles is affected by the presence of a membrane potential and is stimulated by Ca^{2+}/K^{+} exchange.

The Dependence of A23187-Mediated Ca^{2+}Efflux on A23187 Concentration.

Arsenazo III was used to monitor the initial rate of A23187-induced efflux of Ca^{2+} from egg PC vesicles. The initial rate of Ca^{2+} efflux from egg PC vesicles has a second-order dependence on the ionophore concentration (Figure 7). This demonstrates that in the A23187 concentration range between 0.036 and 0.18μM, $Ca^{2+}$is transported across egg PC bilayers principally as a $(A23187)_2$-Ca^{2+}complex. This result appears to conflict with the effect of the diffusion potential generated by valinomycin and K^{+} on the A23187-mediated Ca^{2+} transport (Figure 6). A possible explanation of this difference is that A23187 forms a variety of complexes with Ca^{2+} with different stoichiometries (charged and uncharged) (Pfeiffer and Lardy, 1976). The 2:1 A23187-Ca^{2+} species is mainly responsible for the efflux of Ca^{2+} in the absence of a membrane potential. However, when a membrane potential is imposed, the transport of charged complexes becomes more prominent. Another possible explanation involves the existence of a proton leak which arises because of the higher permeability of protons than of Ca^{2+} in bilayers.[2] Even though A23187

may mediate an electrically silent exchange of Ca^{2+} for $2H^+$, a proton leak would make the vesicles positive outside, inhibiting Ca^{2+} efflux. Addition of valinomycin and K^+ to the external medium would therefore be expected to stimulate Ca^{2+} efflux.

Discussion

Our data demonstrate that A23187 directly induces K^+ and Na^+ transport across egg PC bilayers. The selectivity of A23187 in catalyzing monovalent cation transport across egg PC vesicles ($K^+ > Na^+$) is opposite to the selectivity order for complexation in organic solvent ($Li^+ > Na^+ > K^+$) and for extraction into a two-phase system ($Na^+ > K^+$) (Pfeiffer et al., 1974). Hence complexation in organic solvent and two-phase extraction data do not simulate the interplay of ionophore, cation, and membrane in this case. The demonstration that A23187 can transport K^+ and Na^+ faster than Ca^{2+} across egg PC bilayers at high cation concentration (1.5M) does not preclude the possibility that A23187 may transport Ca^{2+} more specifically when Ca^{2+}, K^+, and Na^+ concentrations are low. At high cation concentration, A23187 may be saturated by Ca^{2+}, K^+, and Na^+, and the major factor in determining the rate and extent of cation transport is the rate of transport of complexes across the bilayer. At low cation concentration, A23187 may be more extensively saturated by Ca^{2+} than by K^+ and Na^+. Under conditions close to physiological concentrations (e.g., 0.135 M KCl or NaCl, 0.15 mM $CaCl_2$), K^+ and Na^+ affect the A23187-induced Ca^{2+} transport (Figure 6), and A23187 induces K^+ efflux from vesicles into choline chloride medium when the vesicles contain 0.15 M KCl. Since

the selectivity of cation transport catalyzed by A23187 is incomplete, caution should be taken in the interpretation of physiological data obtained by the use of this ionophore.

Our observation that Ca^{2+} permeation across egg PC vesicles involves primarily the uncharged 2:1 A23187 - Ca^{2+} complex (Figure 7) agrees with the transport studies in a two-phase extraction system (Pfeiffer and Lardy, 1976) and in black lipid membranes (Case et al., 1974). In the absence of a membrane potential imposed by the addition of valinomycin and K^+, an electrically neutral exchange ($Ca^{2+}/ 2H^+$, $Ca^{2+}/2K^+$, or $Ca^{2+}/2Na^+$) may be catalyzed by A23187, assuming that the ionophore is deprotonated in its complexes [$(A23187^-)_2$ - Ca^{2+}, $(A23187^-)$ - K^+, and $(A23187^-)$ - Na^+]. The stimulation of A23187 - mediated Ca^{2+} efflux in the presence of the membrane potential generated by valinomycin and K^+ (Figure 6) may arise because (a) the ionophore is not fully deprotonated in some of its complexes with cations, (b) Ca^{2+} - A23187 complexation may have varying stoichiometries in this concentration range, or (c) a proton gradient may be generated after $Ca^{2+}/2H^+$ exchange.

Figure Captions

Figure 1: Ionophore-mediated transport of Na^+ and K^+ across egg PC vesicles. (A) Ionophore-induced Na^+ efflux. (B) Ionophore - induced K^+ efflux. The preparation of vesicles and measurement of cation efflux were as described in the Experimental Section. The concentration of phospholipid phosphorus in the dialysis sac was 3.4 mM. The amount of Na^+ captured was 0.67 mol of Na^+/ mol of phospholipid. The amount

of K^+ captured was 0.71 mol of K^+/mol of phospholipid. The ionophore concentrations were: nigericin, 0.24 μM; X537A, 0.24 μM; A23187, 0.48 μM; valinomycin, 1.54 μM; c-C-PR, 141 μM; 18-crown-6, 70.5 μM for Na^+-containing vesicles and 11.8 μM for K^+-containing vesicles.

Figure 2: Ionophore-mediated transport of Ca^{2+} across egg PC vesicles. The preparation of vesicles was the same as described for Na^+- and K^+ - containing vesicles except that 1.5 M $CaCl_2$ (with $^{45}Ca^{2+}$) and 10 mM imidazole were used. To remove Ca^{2+} from the external medium, the vesicles were passed through a column (1.7 x 30 cm) of 3 g of Sephadex G-50 equilibrated with 10 mM imidazole buffer, pH 7.0, containing 2.25 M choline chloride. The vesicles were then dialyzed against a medium containing 2.25 M choline chloride and 10 mM imidazole, pH 7.0. The phospholipid concentration was 2.7 mM. The amount of Ca^{2+} captured was 1.29 mol of Ca^{2+}/mol of phospholipid. The concentrations of the ionophores and Ph_4B^- were 10 μM except in curve (▲) (●) DMF; (□) c-C-PR; (+) CH_3-A23187; (■) c-C-PR + Ph_4B^-; (Δ) X537A; (▲) c-C-PR, 141 μM; (o) A23187.

Figure 3: A23187- and CH_3-A23187- mediated Ca^{2+} transport across egg PC vesicles. The vesicles were prepared in a medium containing 1.5 mM $CaCl_2$ (with $^{45}Ca^{2+}$) and 10 mM imidazole, pH 7.0. To remove Ca^{2+} from the external medium, the vesicles were passed through a column (1.7 x 30 cm) of 4 g of Sephadex G-50 equilibrated with a medium containing 10 mM imidazole, pH 7.0,and 2.25 mM choline chloride. The measurement of Ca^{2+} efflux was carried out by dialyzing the Ca^{2+} - containing vesicles against a medium containing 10 mM imidazole, pH 7.0, and 2.25 mM choline chloride. The

concentration of phospholipid was 4.23 mM. The concentration of ionophores were: A 23187, 0.1 μM; CH_3-A23187, 10 μM.

Figure 4: Ionophore - induced K^+ efflux from egg PC vesicles with 0.15 M KCl trapped. The vesicles were prepared in a medium containing 0.15 M KCl and 10 mM imidazole, pH 7.0, by sonication in a Branson S110 sonifier for 450 s at power level 3. To remove K^+ from the external medium, the vesicles were passed through a column (1.7 x 30 cm) of 4 g of Sephadex G-50 equilibrated with a medium containing 10 mM imidazole, pH 7.0, and 0.15 M choline chloride. The measurement of K^+ efflux was carried out by dialyzing 1 ml of K^+ - containing vesicles against 2 ml of a medium containing 10 mM imidazole, pH 7.0, and 0.15 M choline chloride. Samples (0.3 ml) were taken for K^+ measurement. The concentration of phospholipid was 7.4 mM. The amount of K^+ captured was 0.071 mol of K^+/ mol of phospholipid. The concentration of ionophores were: nigericin, 0.12 μM; valinomycin, 5 μM; A23187, 5 μM; CH_3-A23187, 5μM.

Figure 5: Effect of monovalent cations and diffusion potential on the c-C-PR-mediated transport of Ca^{2+} across egg PC vesicles. The vesicles were prepared in a medium containing 10 mM imidazole, pH 7.0, 0.15 mM $CaCl_2$, and 135 mM KCl (solid lines) or 135 mM NaCl (dashed lines). The vesicles were passed through a column of Sephadex G-50 equilibrated with 10 mM imidazole, pH 7.0. Aliquots of a concentrated KCl or NaCl solution were added to the eluted vesicles to make the KCl or NaCl concentration 135 mM. Vesicles were dialyzed against 4 ml of 10 mM imidazole, pH 7.0, and 135 mM KCl (referred to below as KCl medium) or NaCl (NaCl medium).

Solid curves: Vesicles with KCl and $CaCl_2$ captured. The concentration of phospholipid was 2.8 mM. The amount of Ca^{2+} captured was 0.385 mmol of Ca^{2+}/mol of phospholipid. The temperature was 29°. Dialysis against (Δ) NaCl medium; (o) KCl medium. At the points indicated by the arrow, c-C-PR (141μM) was added. Addition of: (●) c-C-PR (141 μM) + valinomycin (0.62 μM), dialyzed against KCl medium; (▲) c-C-PR (141 μM) + valinomycin (0.62 uM), dialyzed against NaCl medium.

Dashed curves: Vesicles with NaCl and $CaCl_2$ captured. The concentration of phospholipid was 3.2 mM. The amount of Ca^{2+} captured was 0.38 mmol of Ca^{2+}/ mol of phospholipid. The temperature was 23°. Dialysis against: (□) NaCl medium; (◇) KCl medium. Addition of: (Δ) c-C-PR (141 μM), dialyzed against NaCl medium; (0) c-C-PR (141 μM), dialyzed against KCl medium.

Figure 6: Effect of monovalent cations and diffusion potential on A23187-mediated transport of Ca^{2+} across egg PC bilayers.

(A) Vesicles were prepared in a medium containing 10 mM imidazole pH 7.0, 135 mM NaCl, and 1.5 mM $^{45}Ca\ Cl_2$, Dialysis against KCl or NaCl medium was carried out as described in Figure 5. (●) Addition of A23187 and dialysis against NaCl medium; (o) addition of A23187 and dialysis against KCl medium; (▲) addition of A23187 and valinomycin, and dialysis against NaCl medium; (Δ) addition of A23187 and valinomycin, and dialysis against KCl medium. The concentration of phospholipid was 2.6 mM. The amount of $^{45}Ca^{2+}$ captured was 3.32 mmol of Ca^{2+}/mol of phospholipid. The temperature was 27°. The concentration of A23187 was 0.096 μM. The concentration of valinomycin was 0.62 μM.

(B) Vesicles were prepared in a medium containing 10 mM imidazole, pH 7.0, 135 mM KCl, and 0.15 mM $^{45}CaCl_2$. Dialysis against KCl or NaCl medium was carried out as described in Figure 5. (■)Addition of A23187 and valinomycin, and dialysis against NaCl medium; (□) addition of A23187 and valinomycin, and dialysis against KCl medium. The concentration of phospholipid was 3.2 mM. The amount of $^{45}Ca^{2+}$ captured was 0.38mmol of Ca^{2+}/mol of phospholipid. The concentration of A23187 was 0.096 μM. The concentration of valinomycin was 0.62 μM.

Figure 7: Effect of A23187 concentration on the initial rate of Ca^{2+} efflux from egg PC vesicles using arsenazo III as Ca^{2+} indicator. The experimental conditions are as described in the experimental section. The phospholipid concentration was 0.19 mM. The amount of Ca^{2+} captured was 0.079 mol of Ca^{2+}/mol of phospholipid. (A) Absorbance changes induced by different concentrations of A23187: a, 0.0356 μM; b, 0.0445 μM; c, 0.0593 μM; d, 0.0712 μM; e, 0.0890 μM; f, 0.119 μM; g, 0.178 μM. (B) Log-log plot of the initial rate of absorbance change vs. A23187 concentration. The slope of the line is 2.08.

Footnotes

[1] Abbreviations used are: PC, phosphatidylcholine; DMF, dimethylformamide; arsenazo III, 2,7-bis (o-arsonophenylazo)-1,8 - dihydroxynaphthalene-3,6-disulfonic acid; Ph_4B^-, tetraphenylborate.

[2] We are grateful to Dr. P. C. Hinkle for proposing this hypothesis and to Dr. E. Racker for communicating it to us.

Acknowledgment:

We wish to thank Dr. Irving J. Borowitz for supplying c-C-PR and Dr. Wolfgang Benz for the mass spectral analysis of CH_3-A23187.

References

Ammann, D., Bissig, R., Güggi, M., Pretsch, E., Simon, W., Borowitz, I.J., and Weiss, L. (1975), Helv. Chim. Acta 58, 1535-1548.

Ammann, D., Pretsch, E., and Simon, W. (1973), Helv. Chim. Acta 56, 1780-1787.

Borowitz, I.J., Lin, W-O., Wun, T-C., Bittman, R., Weiss, L., Diakiw, V., and Borowitz, G.B. (1977), Tetrahedron 33, 1697-1705.

Case, G.D., Vanderkooi, J.M., and Scarpa, A. (1974), Arch. Biochem. Biophys. 162, 174-185.

Caswell, A.H., and Pressman, B.C. (1972), Biochem. Biophys. Res. Commun. 49, 292-298.

Celis, H., Estrada-O., S.,and Montal, M. (1974), J. Membr. Biol. 18, 187-199.

Deber, C.M., and Pfeiffer, D.R. (1976) Biochemistry 15, 132-141.

Duszyński, J. and Wojtczak, L. (1977), Biochem. Biophys. Res. Commun. 74, 417-424.

Hyono, A., Hendriks, Th., Daemen, F.J.M., and Bonting, S.L. (1975), Biochim. Biophys. Acta 389, 34-46.

Kafka,M.S.,and Holz, R.W. (1976), Biochim. Biophys. Acta 426, 31-37.

Lehn, J.M., and Sauvage, J.P. (1975), J. Am. Chem. Soc. 97, 6700-6707.

Lipsky, S.R.,and Landowne, R.A. (1963), Methods Enzymol. 6, 513-537.

Moore, C., and Pressman, B.C. (1964), Biochem. Biophys. Res. Commun. 15, 562-567.

Pfeiffer, D.R., and Lardy, H.A. (1976), Biochemistry 15, 935-943.

Pfeiffer, D.R., Reed, P.W., and Lardy, H.A. (1974), Biochemistry, 13, 4007-4014.

Pressman, B.C., (1968), Proc. Natl. Acad. Sci. U.S. 27, 1283-1288.

Reed, P.W. (1976), J. Biol. Chem. 251, 3489-3494.

Reed, P.W., and Lardy, H.A. (1972), J. Biol. Chem. 247, 6970-6977.

Scarpa, A., Baldassare, J., and Inesi,G.(1972), J. Gen. Physiol. 60, 735-749.

Scarpa, A., and Inesi, G. (1972), FEBS Lett. 22, 273-276.

Selinger, Z., Eimerl, S., and Schramm, M. (1974), Proc. Natl. Acad. Sci. U.S. 71, 128-131.

Wong, D.T., Wilkenson, J.R., Hamill, R.L., and Horng, J.-S. (1973), Arch. Biochem. Biophys. 156, 578-585.

Wulf, J., and Pohl, W.G. (1977), Biochim. Biophys. Acta 465, 471-485.

Wun, T-C., and Bittman, R. (1977), Biochemistry 16, 2080-2086.

Wun, T-C., Bittman, R., and Borowitz, I.J. (1977), Biochemistry 16, 2074-2079.

Table I. Rate of Ionophore - Mediated Na^+, K^+, and Ca^{2+} Efflux from Egg PC Vesicles into Choline Chloride Medium in the First Hour of Dialysis.[a]

Cation[b]	Rate of Cation Efflux (mol cation / mol ionophore • hr)						
	Nigericin	X537A	A23187	CH_3A23187	Valinomycin	c-C-PR	18-Crown-6
Na^+	$6.78\pm0.13\cdot10^3$	$3.17\pm0.03\cdot10^3$	$2.69\pm0.5\cdot10^2$	-	~0	1.44 ± 0.17	3.31 ± 0.11
K^+	$9.04\pm0.37\cdot10^3$	$7.46\pm0.15\cdot10^3$	$1.23\pm0.28\cdot10^3$	-	$2.69\pm0.22\cdot10^2$	0.58 ± 0.20	51 ± 8
Ca^{2+}	-	27 ± 5.0	57 ± 1	21	-	4.1 ± 0.7	-

[a] The external medium was 10 mM imidazole, pH 7.0, 1.5 M choline chloride for Na^+-and K^+-containing vesicles; 10 mM imidazole buffer, pH 7.0, containing 2.25 M choline chloride was used for Ca^{2+} - containing vesicles. The ionophore concentrations used were: A23187, 0.48 μM; X537A, 0.24 μM for Na^+-and K^+-containing vesicles, and 8.47 μM for Ca^{2+} containing vesicles; nigericin, 0.24 μM; valinomycin, 1.54 μM; c-C-PR, 141 μM; 18-crown-6, 70.5 μM for Na^+ - containing vesicles and 11.8 μM for K^+ - containing vesicles.
Error limits represent the mean of two measurements of ionophore-mediated cation transport with two different vesicle preparations.
The rates of ionophore-mediated cation efflux after 1 hr of dialysis were calculated by subtracting the cation concentration in the dialysate of DMF-treated vesicles after 1 hr of dialysis from that in ionophore-treated vesicles, giving values of mol of cation flux hr^{-1}.

[b] The concentration of trapped cation was 1.5 M.

FIG. 1

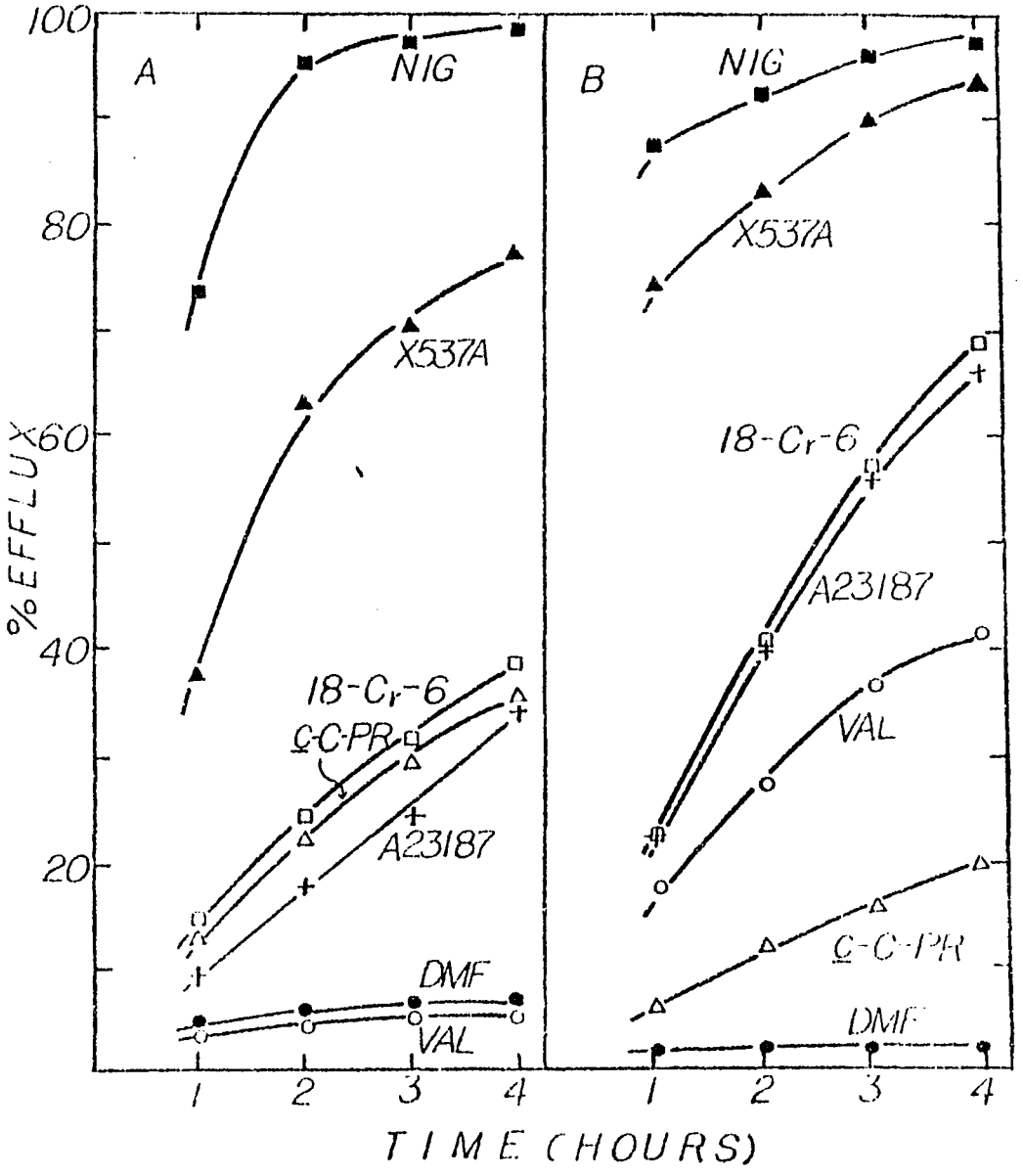
100
80
60
40
20
% EFFLUX
A
NIG
X537A
18-Cr-6
C-C-PR
A23187
DMF
VAL
B
NIG
X537A
18-Cr-6
A23187
VAL
C-C-PR
DMF
1
2
3
4
TIME (HOURS)

FIG. 2

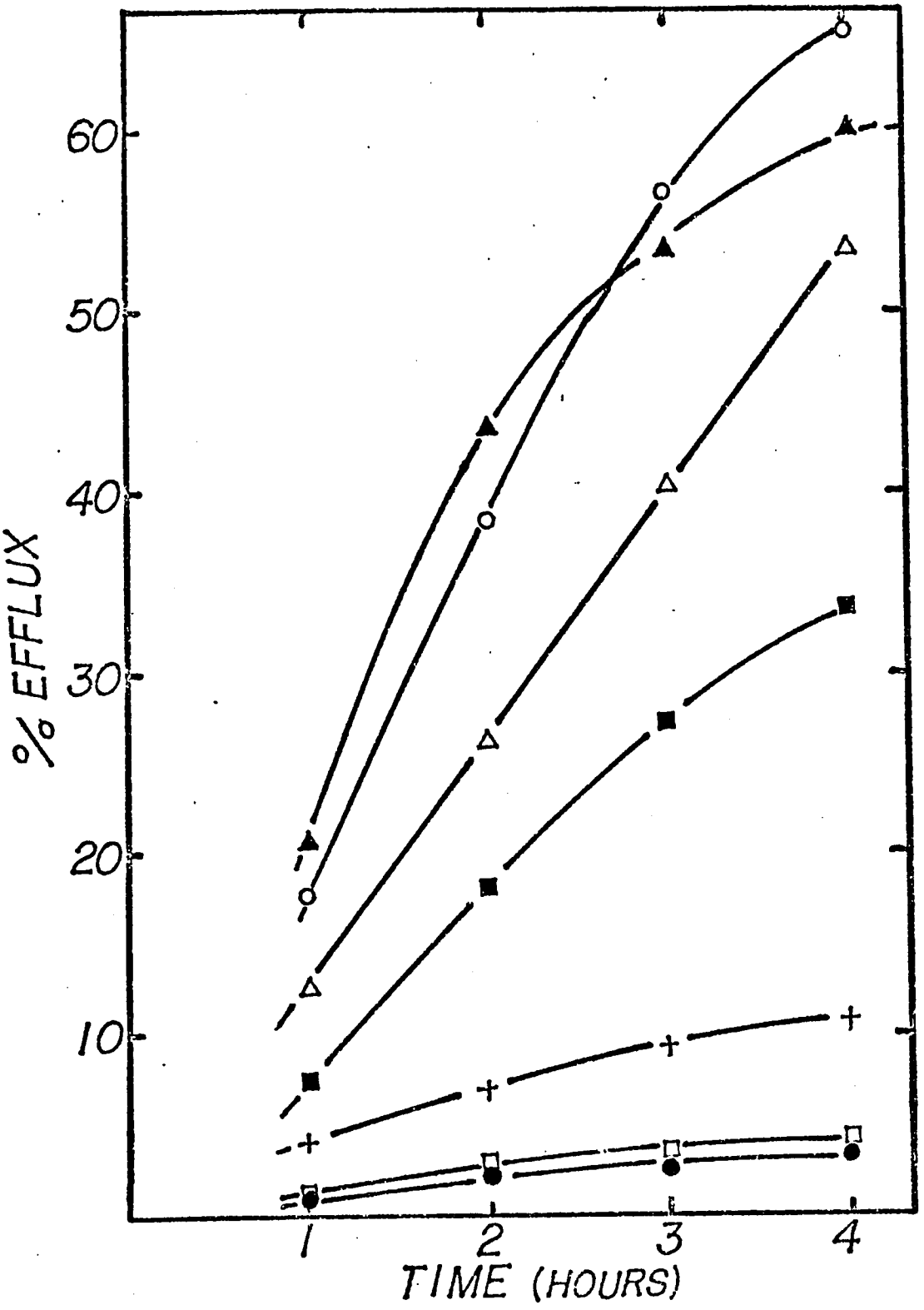

FIG. 3

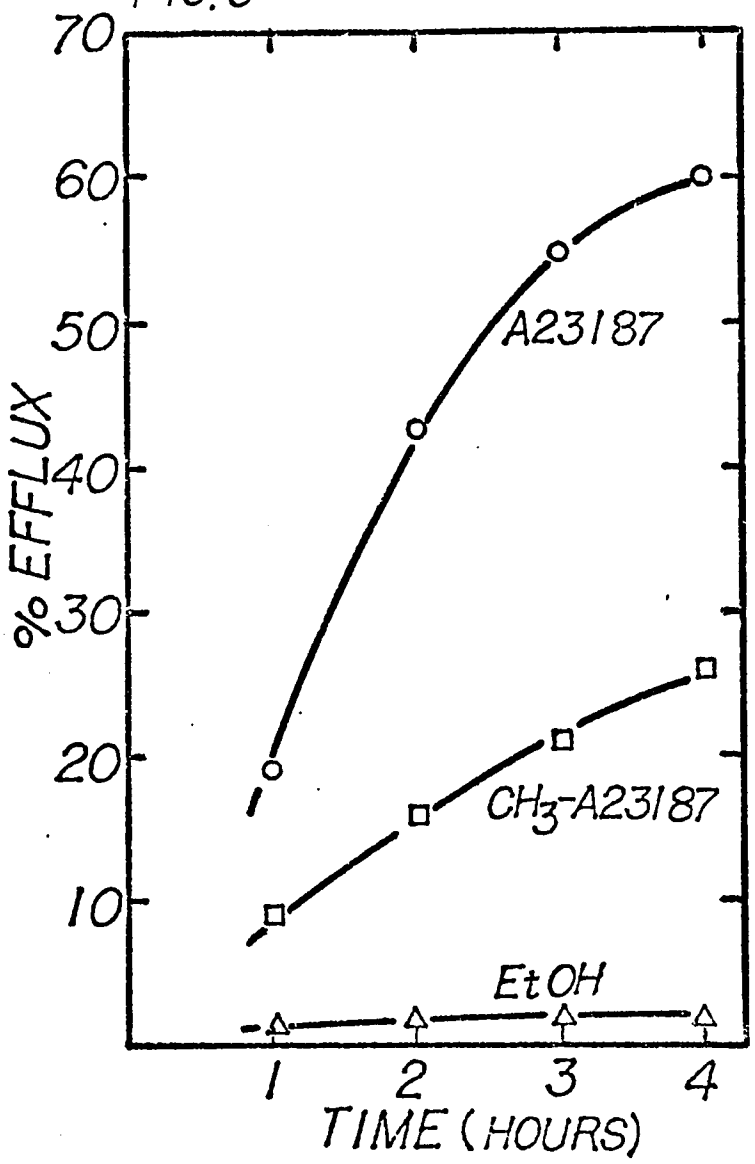
70
60
50
40
30
20
10
% EFFLUX
A23187
CH3-A23187
EtOH
1
2
3
4
TIME (HOURS)

FIG. 4

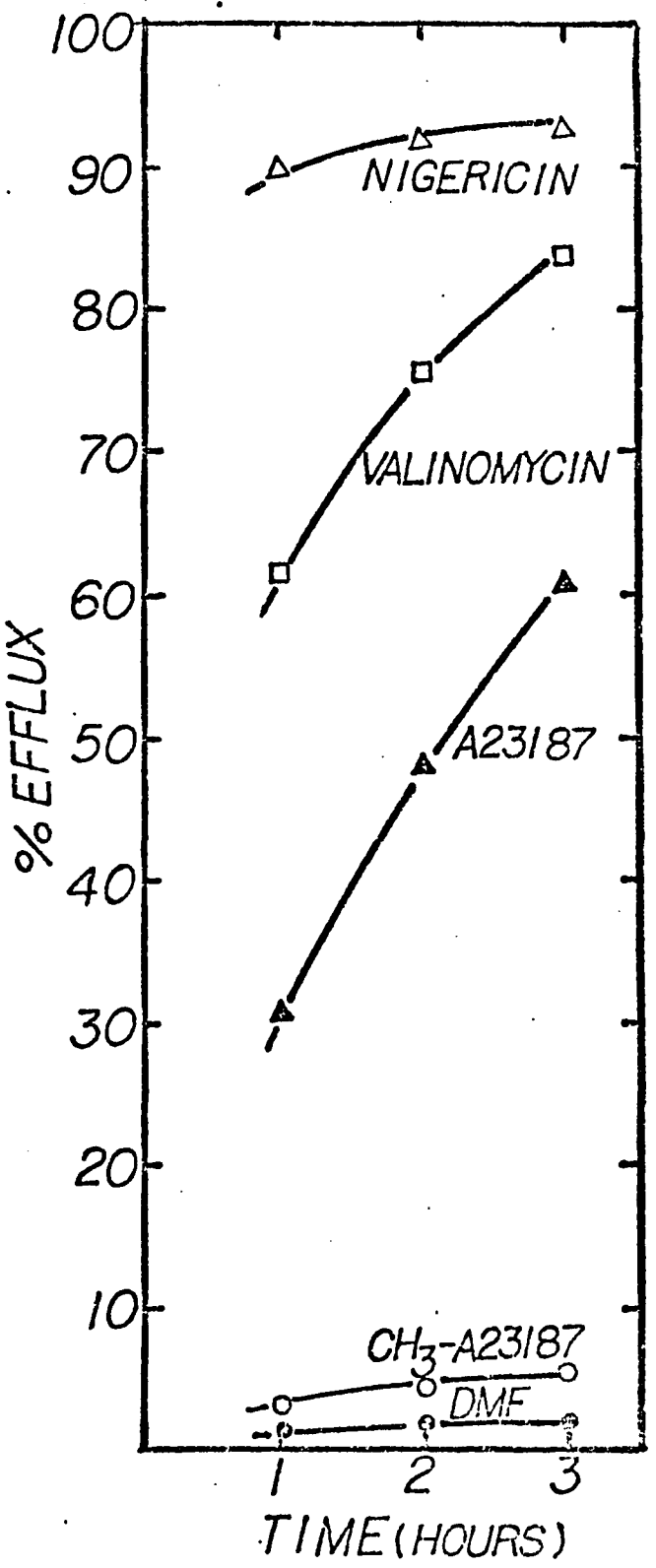
100
90
80
70
60
50
40
30
20
10
% EFFLUX
NIGERICIN
VALINOMYCIN
A23187
CH3-A23187
DMF
1
2
3
TIME (HOURS)

FIG. 5

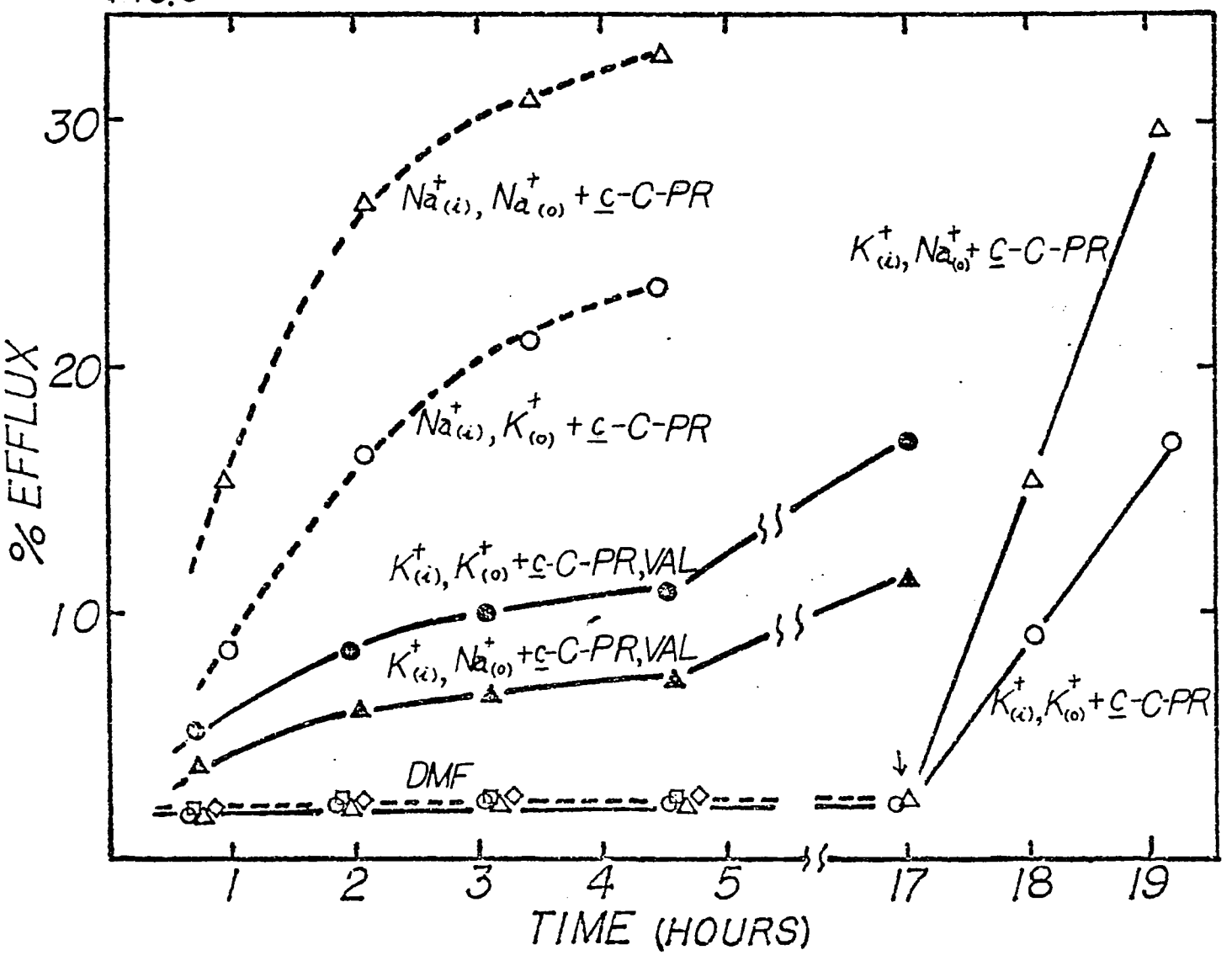
30
20
10
% EFFLUX
$Na^+_{(i)}, Na^+_{(o)}$ + c-C-PR
$Na^+_{(i)}, K^+_{(o)}$ + c-C-PR
$K^+_{(i)}, K^+_{(o)}$ + c-C-PR, VAL
$K^+_{(i)}, Na^+_{(o)}$ + c-C-PR, VAL
DMF
$K^+_{(i)}, Na^+_{(o)}$ + c-C-PR
$K^+_{(i)}, K^+_{(o)}$ + c-C-PR
1
2
3
4
5
17
18
19
TIME (HOURS)

FIG.6

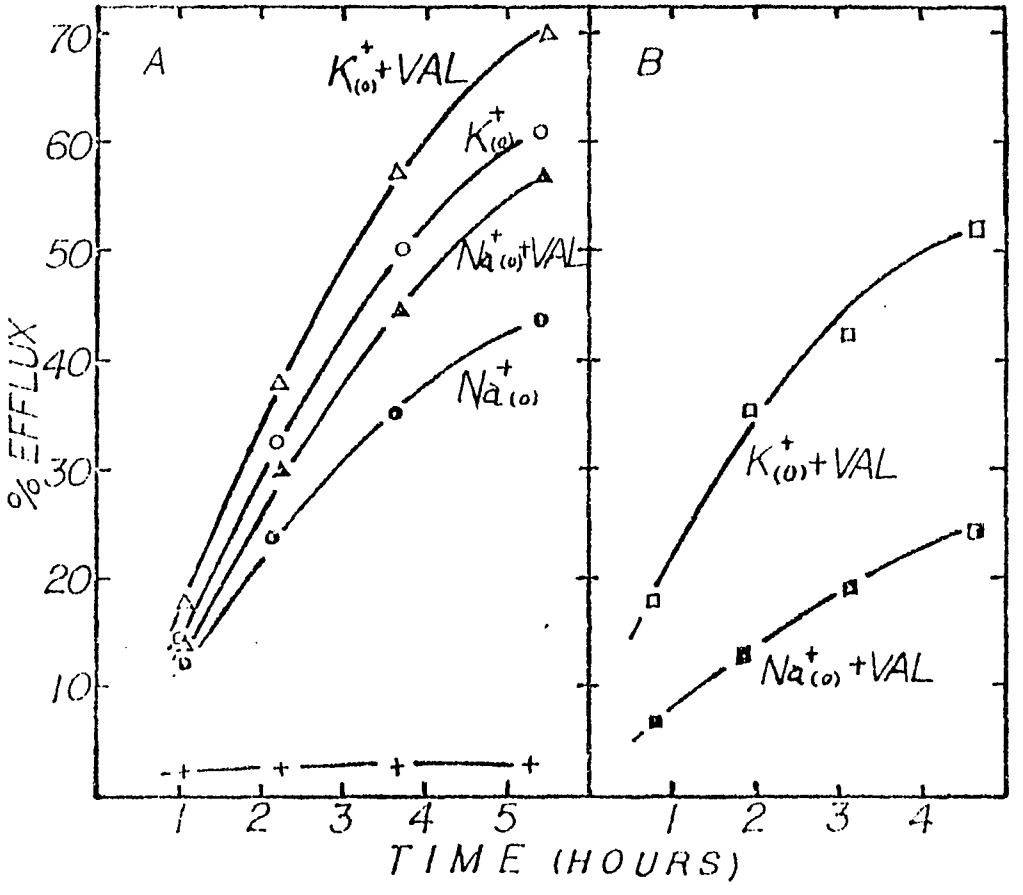
70
60
50
40
30
20
10
% EFFLUX
A
B
$K^+_{(o)}$+VAL
$K^+_{(o)}$
$Na^+_{(o)}$+VAL
$Na^+_{(o)}$
$K^+_{(o)}$+VAL
$Na^+_{(o)}$+VAL
1
2
3
4
5
1
2
3
4
TIME (HOURS)

FIG.7

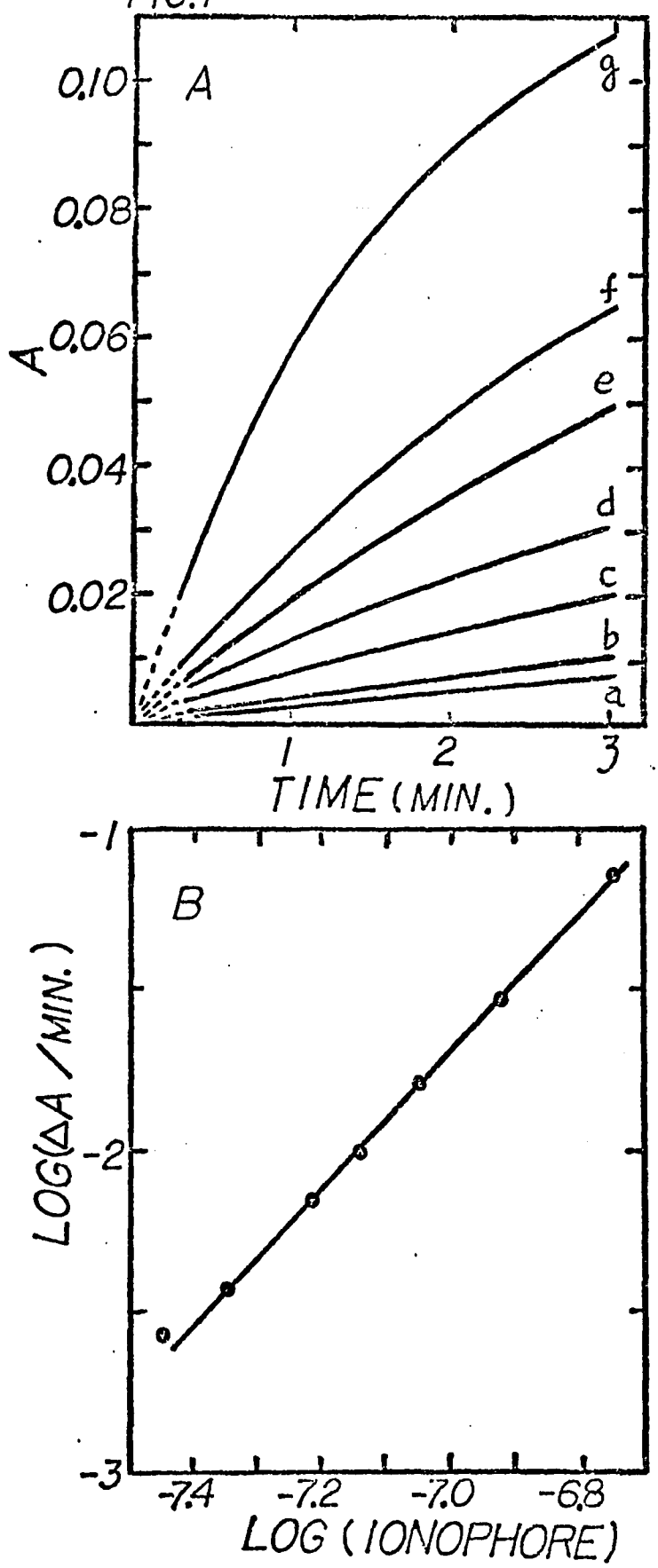
A
0.10
0.08
0.06
0.04
0.02
A
g
f
e
d
c
b
a
1
2
3
TIME (MIN.)
B
-1
-2
-3
LOG(ΔA / MIN.)
-7.4
-7.2
-7.0
-6.8
LOG (IONOPHORE)

Part V

Chlorotetracycline and 8-Anilinonaphthalenesulfonate as Fluorescence Probes of the Complexation of Ionophores with Ca^{2+} in Sarcoplasmic Reticulum Microsomes and Dimyristoylphosphatidylcholine Vesicles.

Abstract

The fluorescent probe chlorotetracycline was used to evaluate the complexation of sarcoplasmic reticulum (SR)- bound Ca^{2+} by A23187, X537A, and neutral diamide ionophores (N,N,N',N'-tetra-n-propyl amides of 1, 2- phenylenedioxydiacetic acid (P-PR), 2, 3- naphthalenedioxydiacetic acid (N-PR), and cis- and trans-1, 2-cyclohexanedioxydiacetic acid (c-C-PR) and t-C-PR), and the N-methyl-N-carbethoxypentyl amide of cis-1, 2-cyclohexanedioxydiacetic acid (c-C-5)). The relative potencies of these ionophores to decrease chlorotetracycline fluorescence agree well with their abilities to induce net transport of Ca^{2+} across vesicles made from SR lipids (A23187 > X537A > c-C-PR > P-PR). The complexation and/or release of Ca^{2+} by the ionophores show a varying order of reaction for A23187, X537A, and the diamide ionophores tested. At high concentration of ionophores, reaction orders approach 2 for A23187, X537A, c-C-PR, and c-C-5. The amount of A23187 required to decrease the fluorescence of chlorotetracycline in SR microsomes is lower than the amount of Ca^{2+} taken up, indicating that the fluorescence decrease reflects turnover of transport. The amount of X537A and diamide ionophores required to decrease chlorotetracycline is the same or larger than the amount of Ca^{2+} taken up into SR microsomes and the fluorescence decrease occurs in the time range of minutes. This indicates that the complexation of SR-bound Ca^{2+} by X537A and diamide ionophores is much slower than that by A23187. N-PR, c-C-PR, and c-C-5 enhance the fluorescence of 8-anilinonaphthalenesulfonate (ANS^-) in dimyristoylphosphatidylcholine vesicles in the presence of Ca^{2+}. Formation of a stoichiometric ionophore $-Ca^{2+}-ANS^-$ complex was found.

Two naturally occurring carboxylic acid ionophores, A23187 and X537A, have been widely used to modulate the Ca^{2+} concentrations in various systems (for reviews, see Pressman, 1976; Gómez and Gómez, 1977). Recently, a series of neutral diamide ligands for alkaline-earth cations was developed (Ammann et al., 1973). The behavior of an acylic 1,2-ethylenedioxydiacetamide system was examined in liquid-membrane electrodes (Ammann et al., 1975). In previous communications we have described the preparation, metal-ion binding properties, extraction selectivities, and ionophorous properties toward Ca^{2+} of alicyclic and aromatic derivatives (Borowitz et al., 1977; Wun et al., 1977; Wun and Bittman, 1977). The present report describes the complexation of these synthetic and the naturally occurring ionophores with sarcoplasmic reticulum (SR)- bound Ca^{2+} using chlorotetracycline as a fluorescent probe. Chlorotetracycline is preferentially partitioned into membranes which selectively retain Ca^{2+} rather than Mg^{2+}, and its fluorescence signal reflects Ca^{2+} bound to the membrane (Caswell and Pressman, 1972; Carvalho and Carvalho, 1977). The fluorescence intensity of chlorotetracycline decreases upon complexation and/or release of SR- bound Ca^{2+} by ionophores, thus permitting measurement of the relative potencies of ionophores and the kinetics of their interaction with membrane- bound Ca^{2+}.

Addition of 8-anilinonaphthalenesulfonate (ANS^-) to Ca^{2+}-containing egg phosphatidylcholine (PC)[1] vesicles enhanced the rate of Ca^{2+} efflux mediated by cis -1,2-cyclohexanedioxydiacetic acid N,N,N',N'-tetra-n-propyl amide (c-C-PR) (Wun and Bittman, 1977). We describe here the

complexation involving Ca^{2+}, neutral diamide ionophores, and ANS^- on the surface of dimyristoyl PC (DMPC) vesicles below the lipid phase-transition temperature. The complexation of three neutral diamide ionophores with Ca^{2+} on the vesicles is increased in the presence of ANS^- through the formation of a possibly charge-neutral ionophore $-Ca^{2+}-ANS^-$ complex.

Experimental Section

Materials

The ligands were synthesized by Dr. I.J. Borowitz and co-workers as described previously (Ammann et al., 1975). The structures of these ligands are shown in Figure 1. They are the N,N-dipropylamides of 1,2-phenylenedioxydiacetic acid (P-PR), 2,3-naphthalenedioxydiacetic acid (N-PR), and cis- and trans- 1,2-cyclohexanedioxydiacetic acid (c-C-PR and t-C-PR). The structure of the N-methyl-N-carbethoxypentylamide of cis-1,2-cyclohexanedioxydiacetic acid is also shown. Dicyclohexyl-18-crown-6 was a gift from Dr. H. Frensdorff of DuPont Central Research. X537A was donated by Dr. J. Berger of Hoffmann-La Roche. A23187 was a gift from Eli Lilly and Co. Chlorotetracycline was purchased from Nutritional Biochemical Corp. ATP and ANS^- were obtained from the Sigma Chemical Co. DMPC was purchased from Calbiochemical Corp. and found to be chromatographically pure on thin-layer analysis using silica gel G plates.

Preparation of SR Microsomes. SR microsomes were prepared from rabbit skeletal muscle by a modified procedure of Martonosi (1968) and were suspended in a medium containing 10 mM imidazole buffer, pH 7.0, and 10% sucrose at a protein concentration of 15-25 mg/ml. The SR preparation was frozen in liquid nitrogen and stored at -70°C. The sample was thawed at room temperature before each experiment. Protein concentration was measured by the method of Lowry et al. (1951) using bovine serum albumin as a standard. The concentration of K^+ was measured with a flame photometer (Model 343, Instrumentation Laboratory, Inc.).

Effect of Ionophores on SR Microsomes Loaded with Ca^{2+}. Complexation and/or release of Ca^{2+} bound to SR microsomes was monitored using chlorotetracycline as a fluorescence indicator as described by Caswell and Pressman (1972). SR microsomes were suspended in the appropriate medium containing 10-13 uM chlorotetracycline. ATP was added to initiate Ca^{2+} uptake. After the fluorescence intensity reached a maximum, 5 µl of a concentrated solution of ionophore in ethanol or DMF was added to the suspension, which was mixed by brief shaking. The final concentration of ethanol or DMF was 0.25% (V/V). The fluorescence intensity was measured in a Hitachi-Perkin Elmer Model MPF-2A spectrofluorometer using excitation and emission wavelengths of 390 and 530 nm, respectively.

Measurement of Initial Reaction by Stopped-flow Spectrophotometry. The measurement of initial reaction was carried out in a stopped-flow apparatus (Durrum Instrument Corp., Palo Alto, Calif.). The change in fluorescence was measured on a Tektronix storage oscilloscope equipped

with a Polaroid camera. The excitation wavelength was 390 nm. A filter which cut off wavelengths below 430 nm was used on the detector side. The experimental conditions are described in the figure caption.

Measurement of Ca^{2+} Contents of SR Microsomes by Millipore Filtration. Millipore filtration was used to measure the uptake and release of $^{45}Ca^{2+}$ by the SR microsomes as described by Martonosi et al. (1964). SR microsomes were suspended in a medium containing 5 mM imidazole buffer, pH 7.0, 0.35 M sucrose, 50 mM $MnCl_2$, 112-350 μM KCl, 20 μM $CaCl_2$, and 10-13 μM chlorotetracycline. The SR protein concentration was 0.098 mg/ml. To initiate Ca^{2+} uptake ATP was added to give a concentration of 0.125 mM. Ionophores were added from stock solutions in ethanol or DMF to give the desired concentrations. The final concentration of ethanol or DMF was 0.25%. Aliquots were removed from the suspension at appropriate time intervals and filtered through 0.45-μm Millipore filters. Aliquots of 50 μl were withdrawn from the original suspensions and from the filtrates for radioactivity counting. Radioactivity was measured in Bray's solution (Bray, 1960) using a Beckman LS 50 liquid scintillation counter.

Detection of Ionophore - Cation - ANS^- Complexes on Phospholipid Vesicles. Vesicles were prepared by ultrasonic irradiation as described previously (Wun and Bittman, 1977). ANS^- (40.1 μM) was added to a suspension of DMPC (0.36 mM) vesicles in 1 mM imidazole buffer, pH 7.0, at 15°C. The enhancement in fluorescence intensity was initiated by the addition of Ca^{2+} and/or ionophores. In equilibrium

studies, the above mixtures were incubated at 15°C for 3 hrs. Fluorescence measurements were made with excitation and emission wavelenths of 380 and 470 nm, respectively.

Results

Effect of the Ionophores on the Chlorotetracycline Fluoresence in SR Microsomes. Chlorotetracycline monitors the ATP-induced uptake of Ca^{2+} in SR microsomes and the effects of ionophores on Ca^{2+}-loaded SR microsomes (Caswell and Pressman, 1972). Figure 2 shows that the fluorescence of chlorotetracycline increases when Ca^{2+} accumulation is initiated by ATP. After the maximum fluorescence increase was reached (corresponding to a steady-state level of 60 nmol of Ca^{2+} per mg of SR membrane protein), addition of c-C-PR caused a decrease in fluorescence. The rate of fluorescence decrease and the steady-state fluorescence intensity reached were dependent on the amount of c-C-PR added. All of the other divalent cation ionophores described in this paper produced similar decreases in fluorescence but at different concentration ranges. We found that while the fluorescence increase induced by ATP roughly paralleled the uptake of $^{45}Ca^{2+}$ into SR microsomes under this condition, the decrease in fluorescence intensity of chlorotetracycline induced by addition of ionophore was not parallel to the total amount of Ca^{2+} retained in SR microsomes (T.C. Wun and R. Bittman, unpublished results). Thus the decrease in chlorotetracycline fluorescence accompanying interaction of ionophore with SR-bound Ca^{2+} is a measure of cation-ionophore complexation and/or release rather than

a quantitative measure of the change in the total intravesicular Ca^{2+}.

Figure 3 shows the relative abilities of ionophores to decrease the fluorescence of chlorotetracycline in SR microsomes preloaded with Ca^{2+}. The fraction of fluorescence decrease was measured 4 min after the addition of the ionophores. The relative capacity of ionophores to decrease chlorotetracycline fluorescence in SR loaded with Ca^{2+} follows the order A23187>X537A>N-PR>c-C-PR>c-C-5≥P-PR≈18-crown-6 (Table 1). This sequence is very similar to their ability to induce Ca^{2+} efflux from vesicles prepared from extracted SR lipids (Wun and Bittman, 1977). Hence, the decrease in chlorotetracycline fluorescence following the addition of ionophores corresponds to displacement of accumulated Ca^{2+} from the vicinity of the fluorescent probe by the divalent-cation ionophores rather than a non-specific quenching process. Further evidence of a specific Ca^{2+}-ionophore interaction is that dibenzo-18-crown-6, which is primarily a ligand for monovalent cations (Christensen et al., 1974), did not produce a decrease in fluorescence intensity up to 10^{-3} M; moreover, the ionophore concentration required to decrease the fluorescence by one-half depends on the amount of Ca^{2+} in the SR microsomes (Figure 3).

Kinetics of the Initial Reactions of Ionophores with SR-Bound Ca^{2+}. In order to obtain kinetic information about the interaction of the ionophores with SR-bound Ca^{2+}, the initial rates of decrease in fluorescence intensity were determined by extrapolating the measured initial slope to the time of ionophore addition. A log-log plot of

the initial rate of fluorescence decrease vs. ionophore concentration provides information about the reaction order with respect to ionophores.. Figure 4 shows that for A23187, X537A, N-PR, and c-C-PR, the initial rates of reaction do not follow a simple first-order or second-order dependence over the concentration of ionophores used. At high concentration of these ionophores, the reaction orders with respect to these ionophores increase.

Stopped-flow kinetic investigations of the initial reactions between the ionophores and SR microsomes containing accumulated Ca^{2+} were undertaken. The interaction of A23187 with SR-bound Ca^{2+} exhibits a lag period (Figure 5A), which become shorter as the A23187 concentration is increased from 0.01 to 2 uM. A phase of decreasing fluorescence intensity follows the lag period. This process corresponds to the ionophore-induced alteration of membrane permeability toward Ca^{2+}. Figure 5B shows that at high ionophore concentration (relative to the concentration of bound Ca^{2+}) a single phase of fluorescence decrease occurs in the interaction of c-C-PR with SR microsomes containing accumulated Ca^{2+}. Similar traces were obtained for X537A, c-C-5, P-PR, and 18-crown-6. The order of the initial reaction of ionophores with Ca^{2+} bound to SR microsomes was analyzed by stopped-flow kinetic measurements (Figure 5C) The reaction orders with respect to ionophore concentration, as calculated from the curves, are somewhat larger than those in Figure 4, where lower ionophore concentrations were used. At the higher concentration of ionophores (Figure 5C), the reaction orders with respect to ionophore concentration approach 2 for A23187, X537A, c-C-PR, and c-C-5.

Formation of Ionophore - Ca^{2+} - ANS^- Complex on DMPC Vesicles.

Since the formation of the cation-ionophore complex on the membrane surface is presumed to be one of the several steps in ionophore-mediated transport (Haynes, 1972; Ciani et al., 1973; Benz and Läuger, 1976), we sought to study the complexation reaction by measuring the enhancement of the fluorescence intensity of ANS^- upon association with the positively charged cation-ionophore complex. Figure 6A shows the time course of the fluorescence enhancement of ANS^- in DMPC vesicles induced by Ca^{2+} and the ionophore c-C-5. Addition of ANS^- to DMPC vesicles at 15°C (which is below the lipid phase-transition temperature) gives a fluorescence intensity about one-half that found when ANS^- is added to DMPC vesicles at 27°C (which is above the lipid phase-transition temperature) and its fluorescence is measured at 15°C. Addition of c-C-5 in DMF (or addition of DMF alone) caused a slight decrease in fluorescence intensity. In c-C-5-treated vesicles, a gradual fluorescence enhancement was observed after the initial decrease (Figure 6A). This slow enhancement in ANS^- fluorescence upon adition of ionophore represents the formation of ionophore-Ca^{2+}-ANS^- complexes at or near the surface of DMPC vesicles. On preincubation of vesicles with c-C-5 and Ca^{2+}, the time course of ANS^- fluorescence enhancement was slightly more rapid (presumably because of preformation of some ionophore-Ca^{2+} complex on the bilayer surface) than that without preincubation (Figure 6B). The facts that preincubation of vesicles with c-C-5 and Ca^{2+} or with ANS^- and Ca^{2+} give similar rates of fluorescence enhancement upon addition of

ANS^- or c-C-5, and that these rates are not very much faster than those observed with no prior incubation suggest that the formation of ionophore $-Ca^{2+}-ANS^-$ complexes on the DMPC bilayer surface is a slow process at 15°C. These results indicate that ANS^- enhances the fraction of ionophore bound to Ca^{2+} by forming a possibly neutral ionophore $-Ca^{2+}-ANS^-$ complex on the membrane. The observation that the initial fluorescence enhancement is not fast (Figure 6B) suggests that the slow fluorescence enhancement we observed cannot be attributed to an ionophore-induced transmembrane diffusion of ANS^- at temperatures below the phospholipid phase-transition temperature. If the formation of the complex on the outer surface of DMPC vesicles were fast and were then followed by a transmembrane diffusion of ANS^-, we would expect either (a) a rapid initial fluorescence enhancement followed by a slower transmembrane diffusion of ANS^- to the inner surface (reflected by a slow fluorescence enhancement), or (b) a single rapid fluorescence enhancement if the transmembrane permeation process is fast. Figure 6C shows the effects of several ionophores on the net fluorescence enhancement of ANS^- in DMPC vesicles. The relative rates of fluorescence enhancement follow the order c-C-PR ≃ N-PR > c-C-5 > P-PR, t-C-PR, 18-crown-6. Negligible fluorescence enhancement was observed for P-PR, t-C-PR, and 18-crown-6 under these conditions. At 30°C, the extent of ANS^- binding to vesicles is increased, probably as a result of the loosening of the bilayer structure and the transbilayer distribution of ANS^- on both the inner and outer bilayer surfaces, and the net fluorescence enhancements upon addition of ionophores are smaller (data not shown). The time course of

fluorescence enhancement varied to some extent when different preparations of DMPC vesicles were used (cf. Figure 6A and 6B).

If a single class of binding sites for ANS^- exists, and the change in fluorescence is proportional to the amount of ANS^- bound, then the ionophore-Ca^{2+}-ANS^- equilibria in DMPC vesicles at 15°C are analyzed using the following equation:

$$\frac{1}{\Delta F} = \frac{1}{K_{app} \cdot \Delta F_{max}} \cdot \frac{1}{[Ca^{2+}]} + \frac{1}{\Delta F_{max}}$$

K_{app} is the apparent association constant for ionophore-Ca^{2+}-ANS^- complexation, ΔF is the net fluorescence enhancement at a given Ca^{2+} concentration, ΔF_{max} is the maximum net fluorescence enhancement, and $[Ca^{2+}]$ is the total Ca^{2+} concentration. Figure 7 shows a double-reciprocal plot of ionophore-induced fluorescence enhancement vs. the total Ca^{2+} concentration in the medium. The identical intercept on the ordinate for c-C-PR, N-PR, and c-C-5 indicates that the maximum fluorescence change is the same for these ionophores, suggesting that the number of binding sites for ANS^- and the environment of ANS^- are similar in the Ca^{2+}-ionophore-ANS^- complexes. Since a constant amount of ionophores was added, formation of a stoichiometric complex of ionophore- Ca^{2+}-ANS^- on the bilayer membrane is suggested. The apparent binding constants, K_{app}, of ionophore-Ca^{2+}-ANS^- association calculated from the quotient of y-intercept/slope, are 1.2×10^4, 1.2×10^4, and 5×10^3 M^{-1} for c-C-PR, N-PR, and c-C-5, respectively, when the ANS^- concentration is 40 μM.

Discussion

Two fluorescence probes have been used to provide information about processes involved in the action of the neutral diamide ionophores in membranes and to permit comparisons to be made with naturally occurring ionophores. Chlorotetracycline monitors membrane-bound Ca^{2+} movement (Caswell and Pressman, 1972). We found that the time course of Ca^{2+} uptake (measured directly by millipore filtration) by SR microsomes from the medium described in the caption to figure 2 was closely parallel to that for chlorotetracycline fluorescence enhancement. Therefore, under these conditions of Ca^{2+} uptake chlorotetracycline can be used to probe Ca^{2+} bound to the SR membrane. It is interesting to note, however, that when medium containing 50 to 100 μM $CaCl_2$ is used, these SR microsomes take up 120 nmol of Ca^{2+}/mg of protein and the fluorescence of chlorotetracycline does not detect Ca^{2+} that is retained free or precipitated in the intravesicular space (Carvalho and Carvalho, 1977). ANS^- has been used as an indicator of valinomycin-K^+-ANS^- complexes in vesicles (Haynes, 1972) and of the variation of electrostatic surface potential as a function of membrane surface charge (Haynes, 1974). For the formation of neutral diamide ionophore - Ca^{2+} - ANS^- complexes in DMPC vesicles, the time course of enhancement of ANS^- fluorescence is slow (minutes to hours) below the phase transition temperature (Figure 6). In contrast, the valinomycin - K^+ - ANS^- complex is formed within seconds or less in DMPC vesicles at temperatures where the lipid is in the gel phase (Haynes and Simkovitz, 1977). Using the intrinsic fluorescence properties of X537A and A23187,

we monitored the rates of formation of the X537A - Ca^{2+} and A23187 - Ca^{2+} complexes in egg PC vesicles (Wun and Bittman, submitted). The time range for complexation of 2.3 mM Ca^{2+} with 3.33 μM X537A is minutes at 24° C, whereas that with 3.33 μM A23187 is seconds or less.

The concentrations at which the various ionophores decrease the fluorescence of chlorotetracycline in SR microsomes (Figures 3-5) reflect their potencies, since the same activity order was found for the initial rates of ionophore-mediated Ca^{2+} efflux from vesicles derived from SR lipids (Wun and Bittman, 1977). However, the activity order in SR microsomes and artificial vesicles does not correlate well with the order of apparent binding strengths for complexation of Ca^{2+} in methanol. The ionophores that form 1:1 complexes with Ca^{2+} have the following values of K_{app} in methanol : X537A, 3.7×10^4 M^{-1} (Degani and Friedman, 1974); N-PR, 4.8×10^4 M^{-1} and P-PR, 7.3×10^4 M^{-1} (Wun et al., 1977). The selectivity order for extraction of Ca^{2+} by these ionophores from water into dichloromethane in the presence of picrate is c-C-PR > c-C-5 > N-PR (Borowitz et al., 1977). The rates of association of Ca^{2+} with X537A and the neutral diamide ionophores are much faster in methanol than in SR microsomes and egg PC vesicles (T.C. Wun and R. Bittman, unpublished results). Therefore, the relative abilities of these ionophores to complex membrane-bound Ca^{2+} is not simulated by association with Ca^{2+} in methanol solutions.

The interaction of ionophores with SR-bound Ca^{2+} displays a variable order with respect to ionophore concentration (Figure 5). Some of these ionophores have been reported to bind to Ca^{2+} in organic solvents with

variable stoichiometries, depending on the ionophore concentration (see references in Wun et al., 1977). At high concentrations of A23187 (~0.02-0.1 μM) and X537A (~10-30 μM), 1:2 Ca^{2+} - ionophore complexes have been postulated in vesicles prepared from retina lipids (Hyono et al., 1975), but at low concentrations (~0.001-0.005 μM A23187 and~0.3-3 μM X537A) Ca^{2+} is transported by X537A as a 1:1 complex and by A23187 as a 2:1 Ca^{2+} - ionophore complex. The permeability to Ca^{2+} of black lipid membranes formed from PC and cholesterol increases as the square of X537A concentration, but a 1-1.7 power dependence was found for A23187 (Kafka and Holz, 1976).

References

Ammann, D., Pretsch, E., and Simon, W. (1973), Helv. Chim. Acta 56, 1780-1787.

Ammann, D., Bissig, R., Güggi, M., Prestsch, E., Simon, W., Borowitz,I.J., and Weiss, L. (1975), Helv. Chim. Acta 58, 1535-1548.

Benz, R., and Läuger, P. (1976), J. Membr. Biol. 27, 171-191.

Borowitz, I.J., Lin, W-O., Wun, T-C., Bittman, R., Weiss, L., Diakiw, V., and Borowitz, G. B. (1977), Tetrahedron, 33, 1697-1705.

Bray, G. A. (1960), Anal. Biochem. 1, 279-285.

Carvalho, C.A.M., and Carvalho, A.P. (1977), Biochim. Biophys. Acta 468,21-33.

Caswell, A. H., and Pressman, B.C(1972), Biochem. Biophys. Res. Commun. 49, 292-298.

Christensen, J.J., Eatough, D.J., and Izatt, R.M. (1974), Chem. Rev. 74, 351-384.

Ciani, S.M., Eisenman, G., Laprade, R., and Szabo, G. (1973), In Membranes, Vol. 2, (Eisenman, G. ed.) p.61-175, New York, Dekker.

Degani, H., and Friedman, H. L. (1974), Biochemistry 13, 5022-5031.

Gómez - Puyou, and Gómez - Lojero (1977), Curr. Top. Bioenerg. 6, 221-257.

Haynes, D. H. (1972), Biochim. Biophys. Acta 255, 406-410.

Haynes, D. H. (1974), J. Membr. Biol. 17, 341-366.

Haynes, D. H., and Simkovitz, P. (1977), J. Membr. Biol. 33, 63-108.

Hyono, A., Hendriks, Th., Daemen, F.J.M., and Bonting, S.L. (1975), Biochim. Biophys. Acta 389, 34-46.

Kafka, M. S. and Holz, R. W. (1976), Biochim. Biophys. Acta 426, 31-37.

Lowry, O. H., Rosebrough, N. J., Farr. A. L., and Randall, R. J. (1951), J. Biol. Chem. 193, 265-275.

Martonosi, A. (1968), J. Biol. Chem. 243, 71-81.

Martonosi, A., and Feretos, R. (1964), J. Biol. Chem. 239, 648-658.

Pfeiffer, D. R., and Lardy, H. A. (1976), Biochemistry 15, 935-943.

Pfeiffer, D. R., Reed, P. W., and Lardy, H. A. (1974), Biochemistry 13, 4007-4013.

Pressman, B. C. (1976), Ann. Rev. Biochem. 45, 501-530.

Wun, T. C., and Bittman, R. (1977), Biochemistry 16, 2080-2086.

Wun, T. C., and Bittman, R., and Borowitz, I. J. (1977), Biochemistry 16, 2074-2079.

Table I : Relative Abilities of Ionophores to Decrease the Fluorescence Intensity of Chlorotetracycline in SR Microsomes Preloaded with Ca^{2+}.

Ionophores	A23187	X537A	N-PR	c-C-PR	c-C-5	P-PR	18-Crown-6
Relative Potencies[a]	100	2.4	0.15	0.046	0.017	0.012	0.011

[a] The potencies of the ionophores relative to A23187 were calculated by dividing the concentration of A23187 required to lower the fluorescence level by one-half by the concentrations of the other ionophores producing a 50% reduction in fluorescence intensity. A23187 was assigned arbitrarily a value of 100.

Figure Captions

Figure 1 : Molecular structures of P-PR, N-PR, c-C-PR, t-C-PR, and c-C-5.

Figure 2 : Increase in fluorescence intensity of chlorotetracycline during ATP-dependent Ca^{2+} accumulation into SR microsomes and the subsequent fluorescence decrease induced by c-C-PR. The reaction mixture (2 ml) contained 5 mM imidazole buffer, pH 7.0, 0.35 M sucrose, 50 μM $MnCl_2$, 20 μM $CaCl_2$, 112 μM KCl, 10 μM chlorotetracycline, and 0.109 mg of SR protein / ml. Ca^{2+} uptake was initiated by the addition of 0.125 mM ATP. The fluorescence intensity was recorded with excitation and emission wavelengths of 390 and 530 nm, respectively. The arrow indicates the time of addition of ionophore or DMF.

Figure 3 : Ca^{2+}-ionophore interaction measured by chlorotetracycline fluorescence decrease in SR microsomes preloaded with Ca^{2+}. The experimental conditions are the same as described in Figure 2. After the maximum level of fluorescence was reached (3.6 min in this preparation), various amounts of ionophores were added and the fluorescence intensity was continuously recorded. The ordinate ($\log \Delta F/\Delta F_T$) is the log of the ratio of fluorescence decrease 4 min after addition of ionophore (ΔF) to the fluorescence intensity 4 min after addition of DMF or ethanol (ΔF_T). The arrow on the ordinate shows the point of 50% fluorescence decrease. The temperature was 24°C. The amounts of Ca^{2+} taken up 3.6 min after addition of ATP were 50 (solid lines) and 60 (dashed lines) nmol/mg of SR protein.

Figure 4 : Log-log plot of the initial rate of fluorescence decrease of chlorotetracycline in SR microsomes vs. ionophore concentration. The slopes of the lines for P-PR, c-C-5, and 18-crown-6 were 0.7, 1.0, and 0.9, respectively. The slopes of the steeper portion of the curves for the other ionophores were greater than 1.5.

Figure 5 : Stopped-flow studies of the initial rate of fluorescence decrease of chlorotetracycline in SR microsomes. The reaction medium was the same as described in Figure 2. One syringe contained buffer with or without ionophore. The other syringe contained SR microsomes (0.21 mg of protein/ml) and 0.125 mM ATP. The Ca^{2+} uptake process by SR microsomes contained in this syringe was allowed to proceed for 4 min, reaching 60 nmol of Ca^{2+} per mg of SR protein. Then the contents of the two syringes were mixed rapidly within 3 ms, and the fluorescence intensity was monitored. An excitation wavelength of 390 nm was used; a 430-nm filter was used for emission. The concentration of chlorotetracycline was 10 μM. No decrease in fluorescence intensity was observed when ionophore was omitted. The temperature was 24°C. The change in fluorescence intensity, ΔF, was measured in mV. (A) Free run trace of the fluorescence decrease induced by 1.2 μM A23187. (B) Trace of the fluorescence decrease induced by 90.8 μM c-C-PR. (C) Log-log plot of the fluorescence decrease of chlorotetracycline in SR microsomes vs. ionophore concentrations. The slopes of lines are : A23187 (0.6-2.0), X537A (2.0), c-C-PR (1.7), c-C-5 (1.9), and 18-crown-6 (1.2).

Figure 6 : Time course of the fluorescence enhancement of ANS^- in DMPC vesicles induced by Ca^{2+} and ionophores. The conditions were described in the Experimental Section. (A) Solid lines: effect of addition of c-C-5 to a vesicle suspension containing ANS^- and Ca^{2+}. ANS^- (40.1 μM) was added to a suspension of vesicles (0.36 mM DMPC) in 1 mM imidazole buffer, pH 7.0, at 15°C. The enhancement in fluorescence intensity was initiated by addition of $CaCl_2$ and then ionophores (curve 1). Curve 2 shows the effect of adding DMF. The Ca^{2+} concentration was 1.19 mM; the ionophore concentration was 35.2 μM and the DMF concentration was 1 % (v/v). Dashed line : Conditions were the same as in curve 1, except that ANS^- was added to the vesicles at 27°C. Fluorescence measurements were made at 15°C. (B) Effect of preincubation of vesicles with Ca^{2+} and either c-C-PR or ANS^-. Dashed line : Vesicles were preincubated with ionophore and Ca^{2+} for 30 min at 15°C and then ANS^- was added (t=0). Solid line : Vesicles were preincubated with ANS^- and Ca^{2+} at 15°C for 30 min and then c-C-5 was added (t=0). Experimental conditions were the same as in (A). The Δ Fluorescence Intensity was obtained by subtracting the fluorescence intensity in the presence of Ca^{2+} and ANS^- from that in the presence of ionophore, Ca^{2+}, and ANS^-. (C) Effect of c-C-PR, N-PR, and c-C-5 on the time course of the net fluorescence enhancement of ANS^- in a DMPC vesicle suspension containing Ca^{2+} and ANS^-. The experimental conditions were the same as in (A). In the absence of Ca^{2+}, addition of N-PR to DMPC vesicles caused a small enhancement in the fluorescence of ANS^-. This contribution was subtracted. Additions of : (a) c-C-PR; (b) N-PR; (c) c-C-5. The concentration of each ionophore was 35.2 μM.

Figure 7 : Double-reciprocal plot of the fluorescence enhancement of ANS^- vs. Ca^{2+} concentration. The data were obtained from experiments similar to those described in Figure 6 except that the reaction mixtures were incubated at 15°C for 3 hr before fluorescence measurements were made. The Ca^{2+} concentration was varied from 59.5 μM to 1.19 mM. The ionophore concentrations were 35.2 μM. (o), c-C-PR; (□), N-PR; (Δ), c-C-5.

FIG. 1

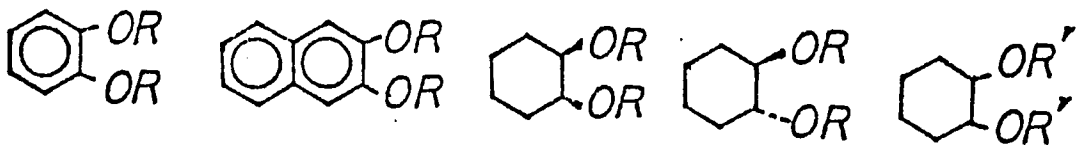

P-PR N-PR c-C-PR t-C-PR c-C-5

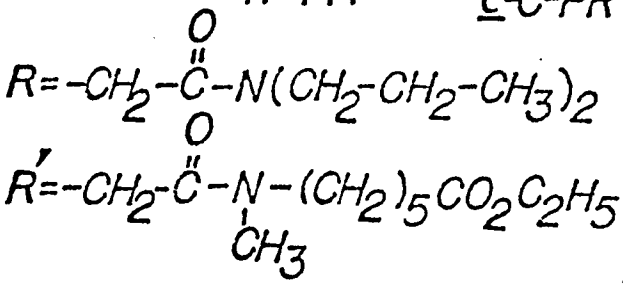

FIG. 2

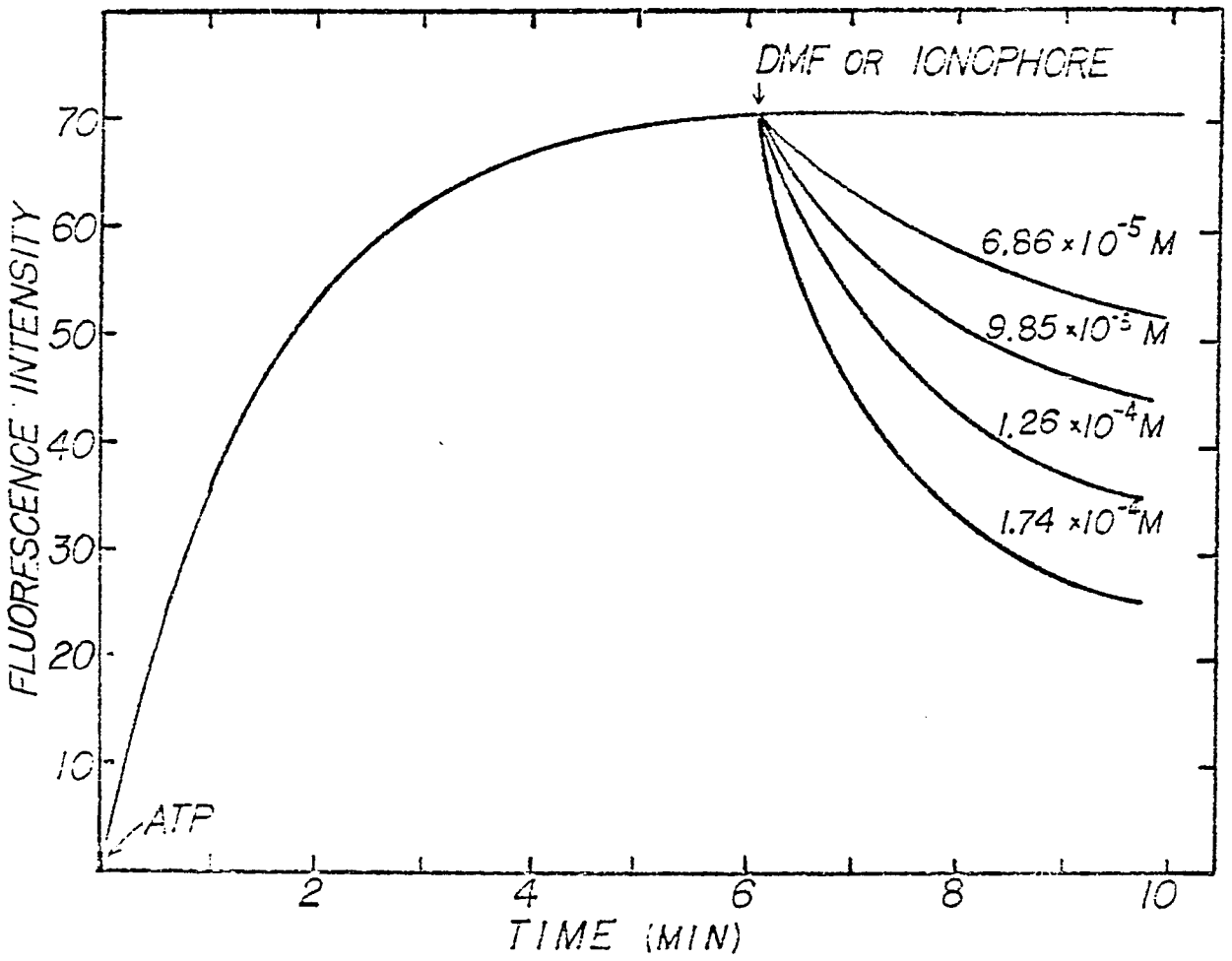
DMF OR IONOPHORE
6.86 x 10⁻⁵ M
9.85 x 10⁻⁵ M
1.26 x 10⁻⁴ M
1.74 x 10⁻⁴ M
ATP
FLUORESCENCE INTENSITY
TIME (MIN)
10
20
30
40
50
60
70
2
4
6
8
10

FIG.3

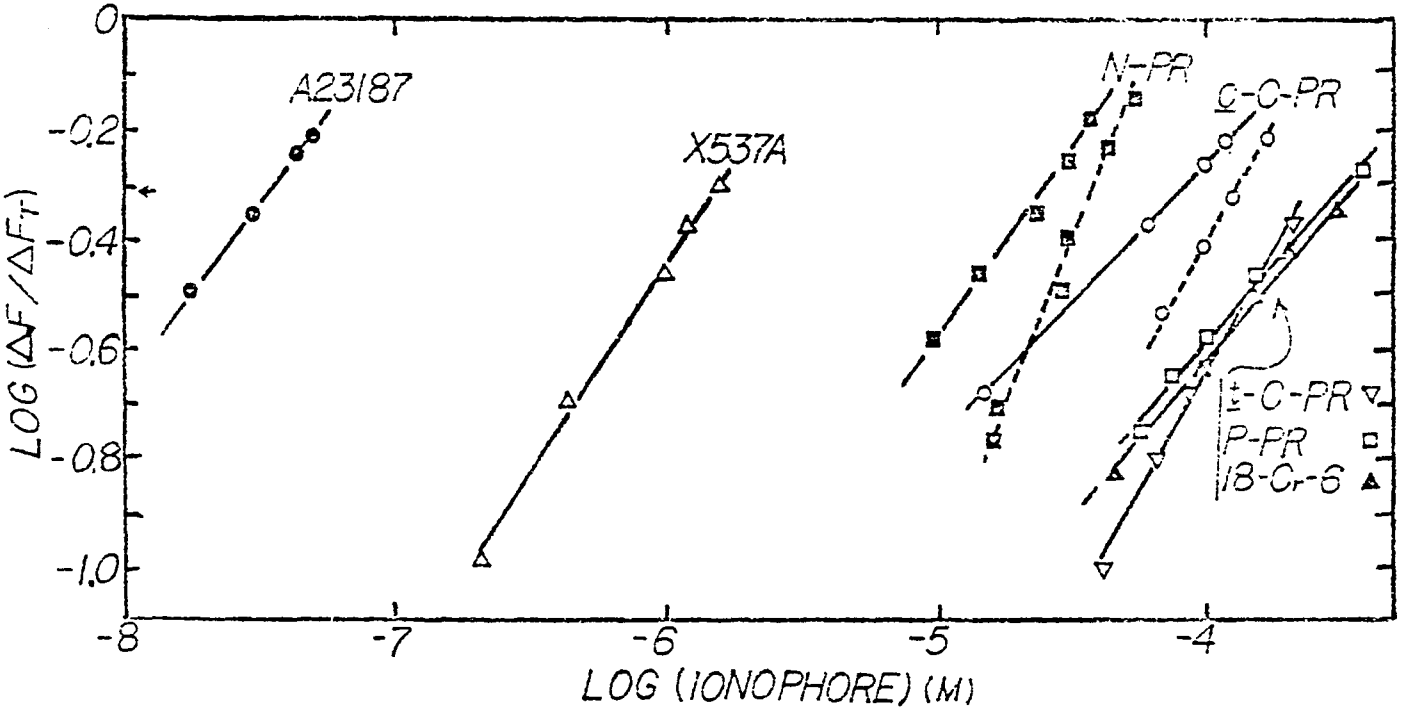
0
-0.2
-0.4
-0.6
-0.8
-1.0
LOG (ΔF/ΔF_T)
A23187
X537A
N-PR
C-C-PR
±-C-PR
P-PR
18-Cr-6
-8
-7
-6
-5
-4
LOG (IONOPHORE) (M)

FIG. 4

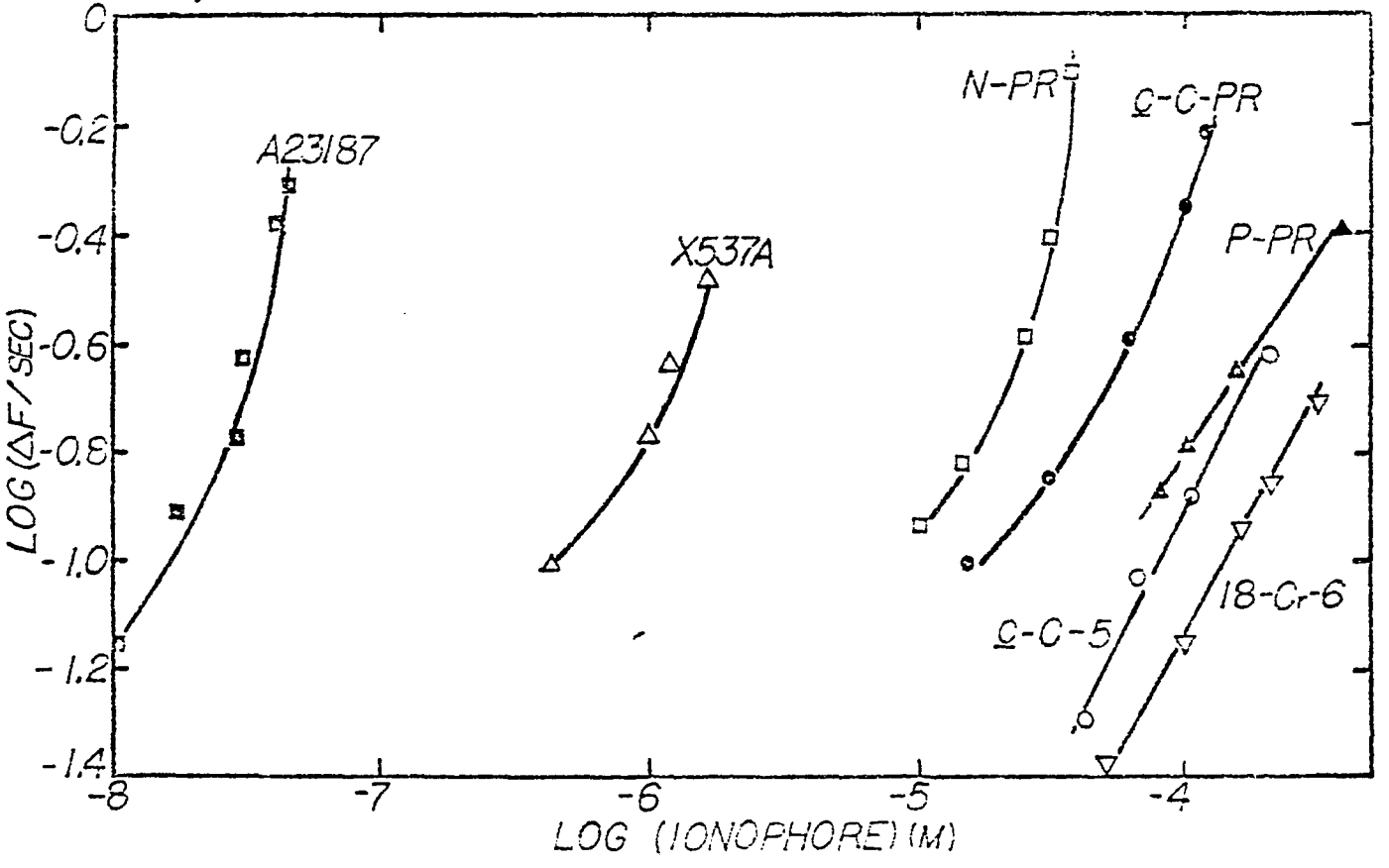
0
-0.2
-0.4
-0.6
-0.8
-1.0
-1.2
-1.4
LOG (ΔF/SEC)
-8
-7
-6
-5
-4
LOG (IONOPHORE) (M)
A23187
X537A
N-PR
C-C-PR
P-PR
C-C-5
18-Cr-6

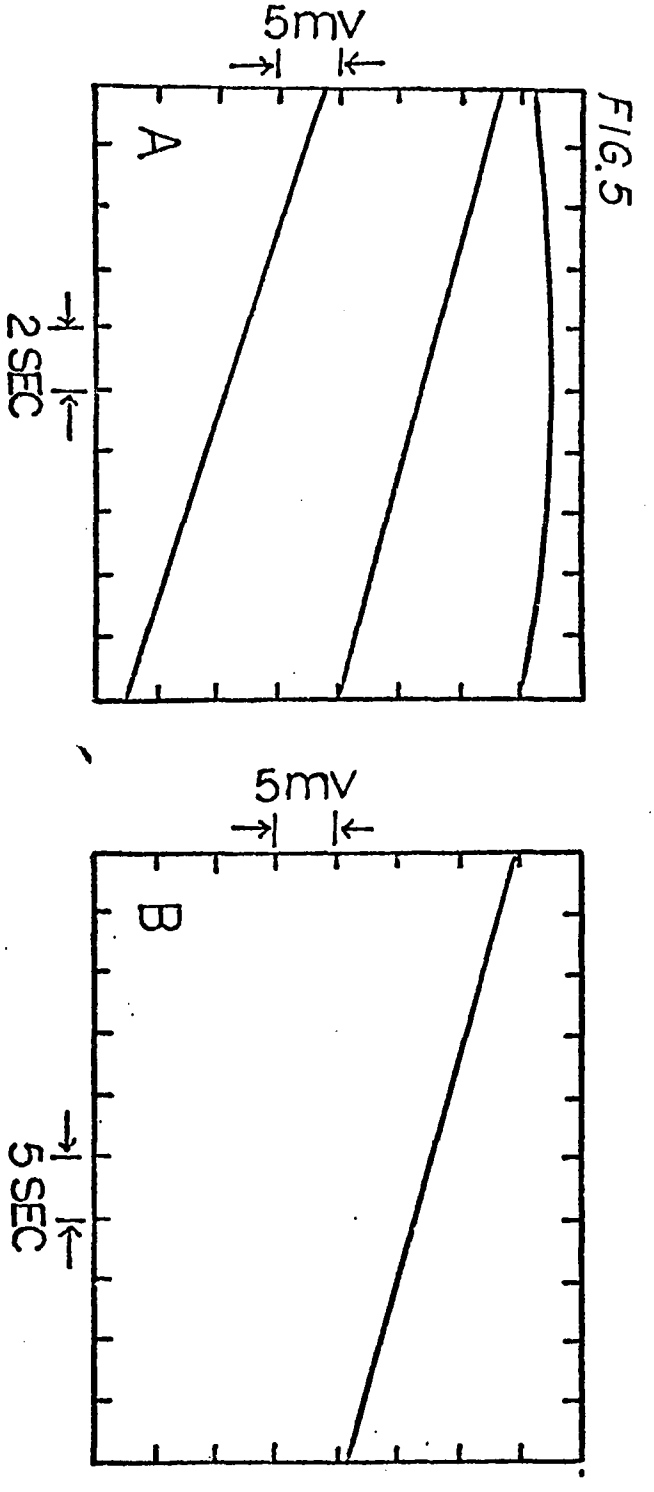

FIG. 5

FIG. 5

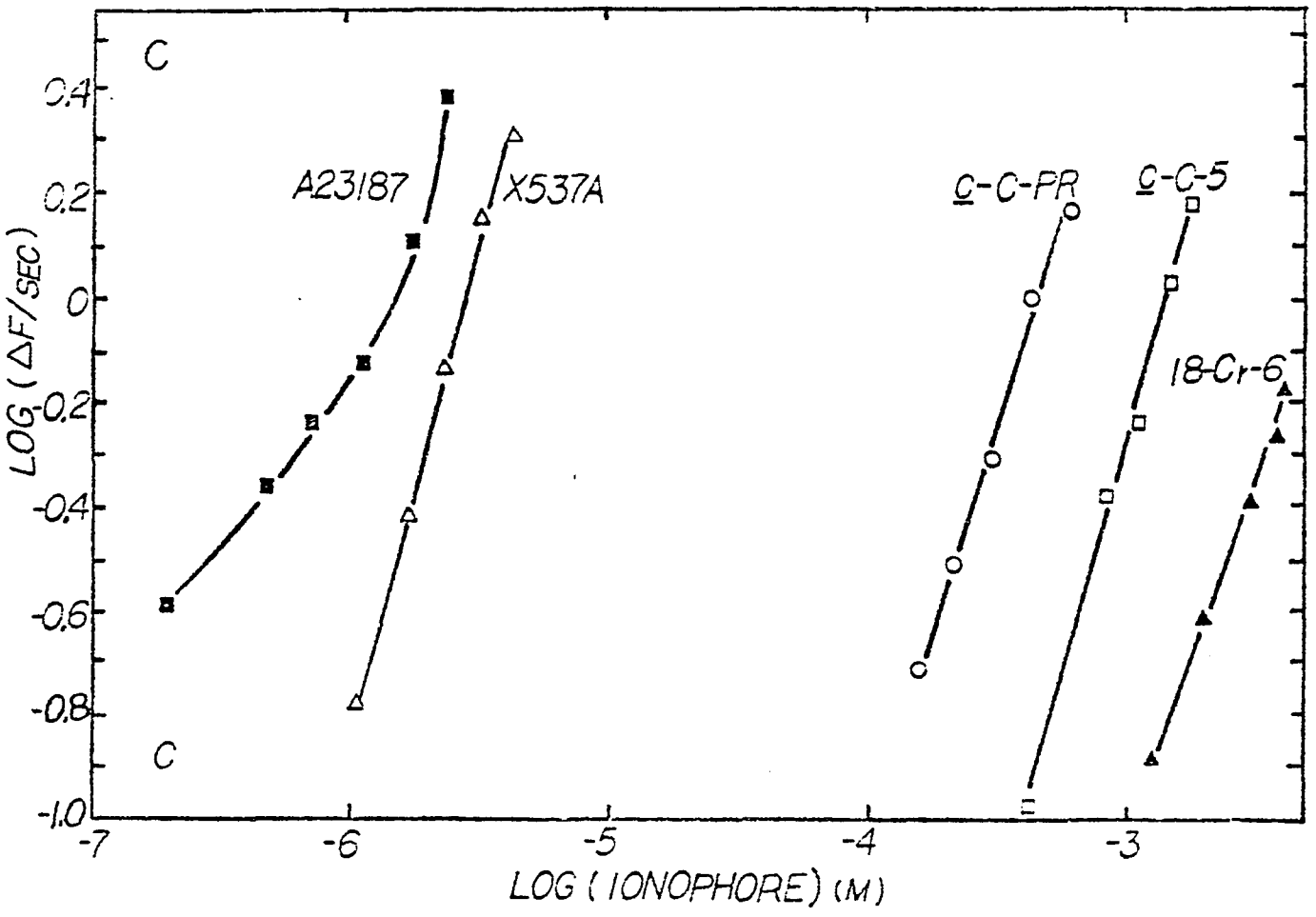
C
0.4
0.2
0
-0.2
-0.4
-0.6
-0.8
-1.0
LOG (ΔF/SEC)
A23187
X537A
C-C-PR
C-C-5
18-Cr-6
C
-7
-6
-5
-4
-3
LOG (IONOPHORE) (M)

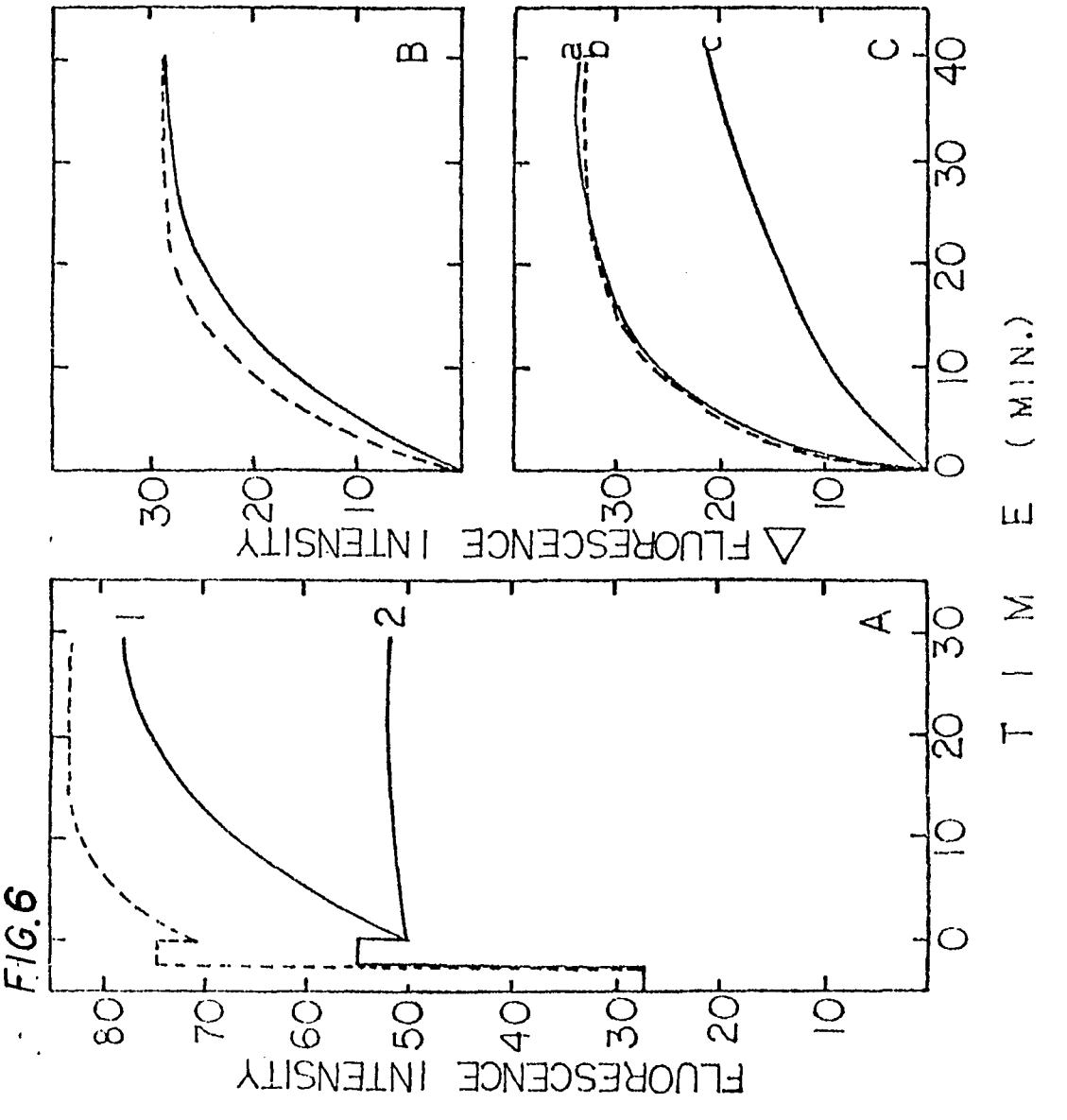
FLUORESCENCE INTENSITY
A
1
2
B
C
a
b
c
Δ FLUORESCENCE INTENSITY
TIME (MIN.)

FIG.6

FIG7

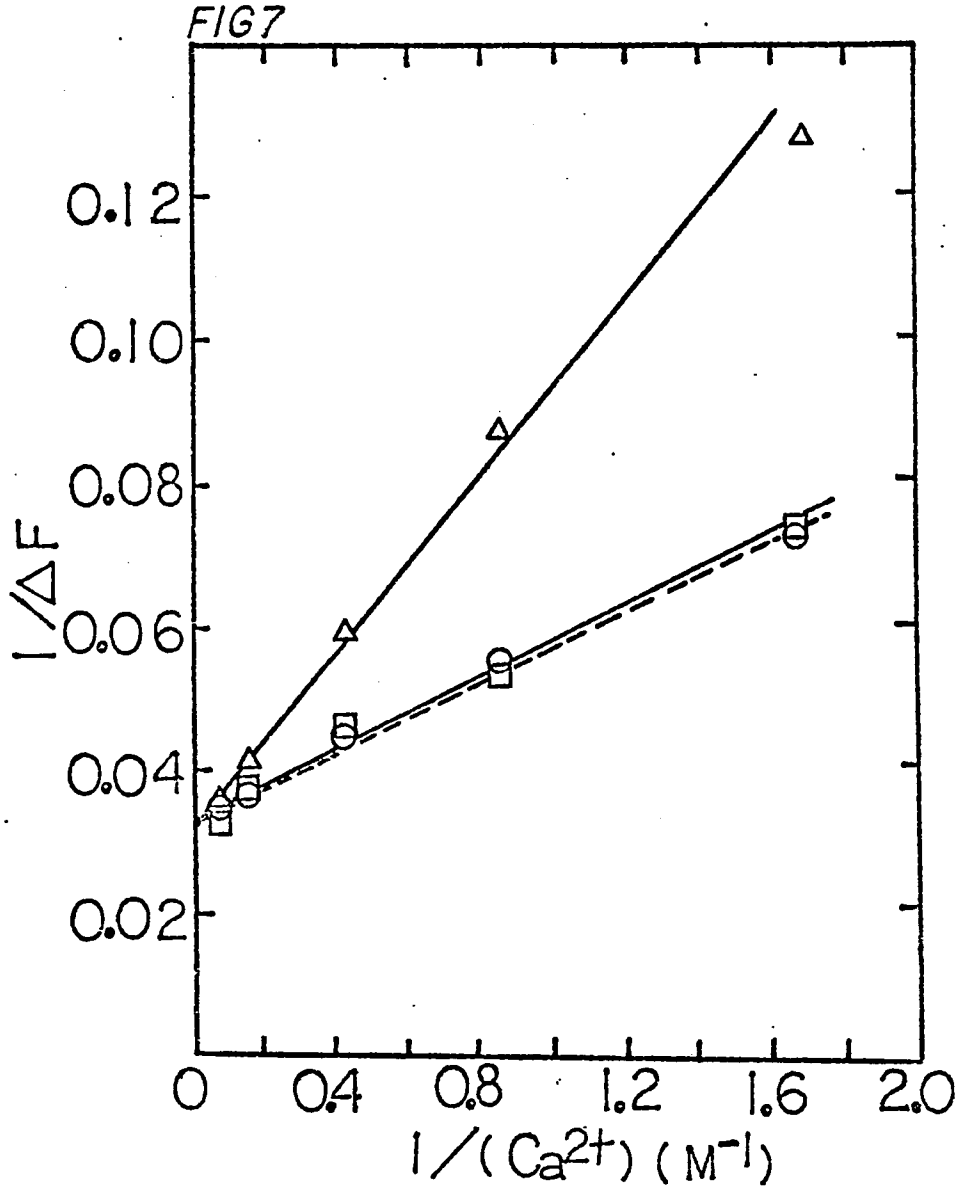

Part VI

Absorption and Fluorescence Studies of A23187 and X537A and Their Complexation with Ca^{2+} in Methanol, Ethanol, Egg Phosphatidylcholine (PC) and Egg PC-Cholesterol Vesicles.

ABSTRACT: The complexation of A23187 and X537A with Ca^{2+} in methanol, ethanol, and phospholipid vesicles was studied by ultraviolet and fluorescence spectroscopy. The stoichiometry of the interaction of X537A with Ca^{2+} in methanol was found to be 1:1, and the association constant was $3.7 \times 10^4\ M^{-1}$ at 25°C. Aggregation of A23187 was noted at concentrations higher than 10^{-6} M, as judged from the deviation from Beer's law and a change in the fluorescence excitation spectrum. A23187 (3.33μM) in egg phosphatidylcholine (PC) or egg PC-cholesterol vesicles also exists as aggregates, as judged from the fluorescence spectra. The binding of A23187 with Ca^{2+} in methanol does not follow a simple stoichiometry throughout the titration. In ethanol, the stoichiometry of binding of A23187 with Ca^{2+} is 2:1. UV and fluorescence spectral titrations show that the aggregated form of A23187 binds Ca^{2+} with high affinity, but the more dispersed A23187 has very low affinity for Ca^{2+}. At 0.36 μM A23187 in methanol in the presence of 0.67 mM Tris - base, the binding of A23187 with Ca^{2+} can be fit into a 1:1 binding equation with an association constant of $3.7 \times 10^2\ M^{-1}$. The binding of Ca^{2+} to X537A in egg PC vesicles and egg-PC cholesterol vesicles was studied by the fluorescence change of X537A. The rate of complexation of X537A with Ca^{2+} in the presence of cholesterol was much faster than that in the absence of cholesterol. The rate of complexation of A23187 with Ca^{2+} on egg PC or egg PC-cholesterol vesicles is much faster than that of X537A on egg PC vesicles.

Ionophorous antibiotics that reduce the membrane permeability barrier to biologically important cations are powerful tools for studying the role of transmembrane cation distributions in regulating complex biological phenomena. Two carboxylic acid ionophores, A23187 and X537A, are now used widely to investigate the involvement of Ca^{2+} in the control of cellular function (for reviews, see Pressman, 1976; Gómez and Gómez, 1977). The binding and transport properties of these two ionophores were extensively studied. Some uncertainties regarding the stoichiometry of the ionophore-cation complexation remain. Circular dichroism and fluorescence studies showed that X537A forms a 1:1 complex with Ca^{2+} in methanol; however, in hexane, both 2:1 and 1:1 X537A - Ca^{2+} complexes are formed (Degani and Friedman, 1974). Fluorescence titration of A23187 with Ca^{2+} in 50% aqueous methanol and 80% aqueous ethanol gave a 1:1 stoichiometry (Caswell and Pressman, 1972). In contrast, 2:1 A23187 - Ca^{2+} complexation in 50% ethanol was reported by Case et al. (1974). UV titration in ethanol gave a stoichiometry of 2:1 A23187 - Ca^{2+} (Pfeiffer et al.,1974). In this report we extend the study of the ultraviolet and fluorescence spectral properties of A23187 and X537A and their complexes in methanol, ethanol, and phospholipid vesicles. Evidence of the aggregation of A23187 in these media and its effect on Ca^{2+} binding are described.

Incorporation of cholesterol into egg phosphatidylcholine (PC) vesicles enhanced the rate of Ca^{2+} efflux mediated by X537A but decreased the rates of Ca^{2+} efflux mediated by A23187 and several synthetic ionophores (Wun and Bittman, 1977). We report here an enhanced rate of the complexation of X537A with Ca^{2+} in cholesterol-containing vesicles compared with that in pure egg PC vesicles.

Experimental Section

Materials

The antibiotics A23187 and X537A were gifts from Eli Lilly and Co. and Hoffmann-LaRoche, respectively. A23187 was dissolved in chloroform and treated with a H^+-form cation exchanger (Bio-Rad Laboratories). The solution was then vacuum dried. No difference in UV and fluorescence spectra were detected before and after this treatment. A molar extinction coeficient of 15900 M^{-1} cm^{-1} at 300 nm was used to calculate the concentration of A23187 in methanol when the concentration was below 1.3 μM. Stock solutions of A23187 in methanol or ethanol were prepared in concentrations of about 3 mM. X537A was used as obtained. Stock solutions were prepared in methanol. Spectro-analyzed methanol and absolute ethanol were used. Anhydrous $CaBr_2$ was obtained from ROC/RIC and kept in a dessicator. Imidazole (Sigma) was recrystallized three times from ethyl acetate. Tris-base, cholesterol, and egg PC were obtained from the Sigma Chemical Co. Cholesterol was recrystallized from methanol. Egg PC was purified by chromatography on a silicic acid column as cited previously (Bittman and Blau, 1972). A single spot was found by thin-layer chromatography on silica gel G plates.

Methods

Absorption spectra were measured using a Cary 14 spectrophotometer. Fluorescence spectra were measured using a Perkin-Elmer MPF 2A spectrophotometer. Spectrophotometric titrations were done with microsyringes. Job and Scatchard plots were obtained using the methods described previously (Wun et al., 1977). Egg PC and egg PC - cholesterol vesicles were prepared by sonication in a medium containing 1 mM imidazole, pH 7.0, as described before (Wun and Bittman, 1977). The association constants of X537A with

Ca^{2+} in the vesicles and the error limits represent the average of two measurements. All of the spectra were recorded at 23-25°C. The spectra of the solutions containing the ionophores were corrected for the baseline spectra of the solvents or the vesicle suspensions.

Results

UV Spectral Properties of X537A in Methanol. The ultraviolet absorption spectrum of X537A as the free acid in methanol is shown in Figure 1. Addition of $CaBr_2$ causes a change in the spectrum with distinct isosbestic points. The spectral change measured during titrations of X537A with $CaBr_2$ is used to study the complexation. Figure 2A shows the Job plot of the complexation of X537A with $CaBr_2$. Figure 2B shows the Scatchard plot of the binding of X537A to $CaBr_2$, which confirms the 1:1 stoichiometry obtained from the Job plot. The apparent association constant is 3.7×10^4 M^{-1}.

UV Spectral Properties of A23187 in Methanol and Ethanol. The UV absorption spectrum of A23187 as the free acid in methanol is shown in Figure 3. Addition of $CaBr_2$ causes a change in the spectrum (Figure 3). The solution state of A23187 in methanol appears to be complicated. The insert to Figure 3 shows that in the 10^{-6} - 10^{-5} M region deviation from Beer's law occurs, suggesting the aggregation of A23187. A Job plot (Figure 4) of the spectral titration of A23187 with $CaBr_2$ shows a very unusual binding isotherm. When the concentration of A23187 is larger than 2×10^{-5} M, $CaBr_2$ at one-fifth of the concentration of A23187 produced a large absorbance change. With concentrations of A23187 below 1×10^{-5} M, there are no absorbance changes when stoichiometric or somewhat larger amounts of $CaBr_2$ are added. For example, when the concentration of A23187 was 3.55 μM, a 380 - fold excess $CaBr_2$ did not give a detectable absorbance change. These data suggest that the aggregation state of A23187 has a profound effect on its ability to bind Ca^{2+}. The binding of A23187 with

Ca^{2+} in ethanol is very different from that in methanol. A Job plot (Figure 5) indicates a 2:1 A23187 - Ca^{2+} complexation. The binding is very strong, making the binding constant difficult to determine.

Fluorescence Properties of A23187 in Methanol and Ethanol.

Figure 6 shows the excitation and emission spectra of A23187 at various concentrations and the effect of $CaBr_2$. At the lowest concentration tested (Figure 6C), there is a peak at 330 nm and another at 372 nm. As the concentrations are increased, the shorter wavelength peak (peak I) of the excitation spectrum is shifted toward shorter wavelengths and the longer wavelength peak (peak II) is red shifted (Figure 6 A,B, and C). The relative intensity of peak I to peak II becomes smaller as the A23187 concentration becomes higher (Table I). Addition of $CaBr_2$ in general caused peak II to decrease in intensity and to shift toward shorter wavelength, whereas peak I increased in intensity at low Ca^{2+} concentration and decreased in intensity at high Ca^{2+} concentration (except Figure 6C). Several conclusions can be made about these spectra. (1) The peak I:...peak II ratio appears to be related to the aggregation state of A23187. (The change in peak I intensity is mainly responsible for the ratio change; see Figure 7.) (2) The binding of $CaBr_2$ to A23187 at high A23187 concentration does not appear to disperse the aggregation state of A23187, since the spectra in Figure 6A and B do not have an excitation peak at 330 nm, which appears when A23187 is in a more disaggregated state (Figure 6C). (C) At high A23187 concentration (e.g., Figure 6A), titrations show that low Ca^{2+} concentrations produce an increase

in peak I intensity. As the Ca^{2+} concentration is increased, the intensity of peak I decreses. This behavior may result from a change in stoichiometry of binding, slight dispersion of aggregates, and / or deprotonation during the titration. (4) When the A23187 concentration is high (e.g., Figure 6A), a small amount of Ca^{2+} produces a large spectral change. When the concentration of A23187 is low (Figure 6C), very high concentrations of $CaBr_2$ are needed to produce a spectral change. This supports the result in Figure 5, in that the aggregated state of A23187 binds Ca^{2+} with high affinity while the more dispersed A23187 has low affinity for Ca^{2+}.

Similar studies of fluorescence properties of A23187 were carried out in ethanol and are summarized in Table II. The same disaggregation process appears to occur in ethanol. However, a comparison of Table I and II indicates that disaggregation occurs less extensively in the less polar solvent, ethanol. Hence, it is very likely that the fluorescence spectral change upon dilution in polar solvent results from the solvation of the hydrophilic portion of the molecule. When the A23187 concentration is high (e.g., $\sim$ 3 mM), self association of A23187 molecules in methanol or ethanol appears to protect A23187 from being solvated at the hydrophilic portion. This conclusion is based on the observations that : (1) a stock solution ($\sim$3 mM) of A23187 in methanol or ethanol does not give spectra characteristic of dispersed solution immediately after dilution, (2) a dispersed A23187 solution in methanol has very low affinity for Ca^{2+} but titration of a A23187 solution in ethanol immediately after dilution of the stock solution gives stoichiometric 2:1 A23187 - Ca^{2+} binding (Figure 5). The spectral change upon dilution is reversible since concentration of a dilute sample reverses the spectrum to that typical of high concentration.

Evidence that the effect of $CaBr_2$ on the fluorescence of A23187 is due to the binding of Ca^{2+} is obtained from the fact that choline bromide in the same concentration range as $CaBr_2$ did not produce similar changes in the spectra of A23187.

Upon dilution of a concentrated solution of A23187 with methanol, disaggregation occurs, with the peak at 310 nm gradually shifting to 330 nm and peak I gradually increasing in intensity (Figure 7A). Peak II, however, undergoes a much smaller change. Figure 7B shows the time course of the fluorescence enhancement of peak I. A time lag before fluorescence enhancement is observed.

The effect of adding Tris-base to the free acid form of A23187 in methanol is shown in Figure 8. The addition of Tris-base to low concentration of A23187 caused a fluorescence increase, possibly because of deprotonation and / or disaggregation of A23187. Addition of $CaBr_2$ to the A23187 solution in the presence and in the absence of Tris-base both cause a fluorescence decrease. In the absence of Tris-base, the double-reciprocal plot of fluorescence decrease vs. Ca^{2+} concentration gives a nonlinear curve (Figure 9) which may reflect disaggregation, a change in stoichiometry, or H^+-Ca^{2+} competition for A23187 during the titration. In the presence of Tris-base, however, the double-reciprocal plot of fluorescence decrease vs. Ca^{2+} concentration is linear (Figure 10A), and the data can be fit into a 1:1 Scatchard equation, as shown in Figure 10B. The apparent association constant of A23187 with Ca^{2+} in the presence of Tris-base is $3.7 \times 10^2\ M^{-1}$, which is surprisingly low compared with the interaction of Ca^{2+} with X537A or the synthetic diamide ionophores in the same solvent (Wun and Bittman,1977).

Since A23187 in the absence of Tris-base does not give a simple binding stoichiometry, a less quantitative comparison of the binding of A23187 with Ca^{2+} in the presence and in the absence of Tris-base is shown in Figure 11. It shows that at low A23187 concentration, A23187 has a higher affinity for Ca^{2+} in the absence of Tris-base than its presence.

Fluorescence Properties and Complexation of A23187 and X537A with Ca^{2+} in Egg PC and Egg PC-Cholesterol Vesicles. The excitation and emission spectra of A23187 in vesicles prepared from egg PC and egg PC-cholesterol closely resemble those in methanol or ethanol in a similar concentration range (Figure 12). In the presence of the cholesterol-containing vesicles, the fluorescence intensity of A23187 is slightly decreased. The blue shift in the presence of cholesterol implies a difference in the environment of A23187 in these vesicles relative to A23187 in egg PC vesicles. A double-reciprocal plot of the Ca^{2+}-induced fluorescence decrease of A23187 in vesicles prepared from egg PC and egg PC-cholesterol shows biphasic isotherms, possibly reflecting a changing stoichiometry of binding and / or disaggregation during the titration (Figure 13). The fluorescence decrease is completed within the time required to mix the reaction mixture (~10 sec). The fluorescence intensity of X537A in vesicles prepared from egg PC and cholesterol is less than half that in egg PC vesicles when both vesicles contain the same concentration of lecithin (Figure 13). In contrast to the effect of Ca^{2+} on the fluorescence intensity of A23187, the addition of $CaCl_2$ to X537A caused an increase in fluorescence intensity in the presence of the vesicles. Figure 15 shows the double-reciprocal plot of the Ca^{2+}-induced fluorescence enhancement of X537A

in egg PC and egg PC-cholesterol vesicles. The insert shows the time course of the fluorescence enhancements. The rate of the Ca^{2+}-induced fluorescence enhancement of X537A is markedly increased in the presence of cholesterol. This rapid rate of fluorescence enhancement was found in vesicles prepared from egg PC and cholesterol (1:1 molar ratio) at total lipid concentrations of 0.5 and 1.0 mM. The apparent association constants of X537A with Ca^{2+} in egg PC and egg PC-cholesterol vesicles as calculated from y-intercept/slope, are $6\pm1 \times 10^3$ M^{-1} and $1.1\pm0.1 \times 10^3$ M^{-1}, respectively.

Discussion

UV spectral titration of X537A as the free acid in methanol with $CaBr_2$ gave a 1:1 stoichiometry and an apparent association constant of $3.7 \times 10^4\ M^{-1}$ (Figures 1 and 2). These results are in good agreement with those of Degani and Friedman (1974), who titrated the X537A anion (controlled by 2×10^{-4} M LiOH or tributylamine). Haynes and Pressman (1974) showed that the carboxyl group of X537A has a pKa of 4.35 ± 0.15 in methanol. Hence, these results suggest that under either condition, the carboxyl group of the ionophore is dissociated and the dominant reaction is $M^{2+} + X537A^{-1} \rightleftharpoons (M : X537A)^{+1}$.

The reported ambiguities in the stoichiometry of Ca^{2+} binding to A23187 is possibly related to the effect of polar solvents on the binding affinity of A23187 for Ca^{2+} and the aggregation state of the A23187 molecules, We have also observed that preincubation of A23187 in an aqueous medium for a few hours induces a smaller rate and extent of Ca^{2+} efflux from egg PC vesicles than without preincubation (unpublished data).

The nature of the interaction between A23187 molecules, and between A23187 and solvents is not clear at the present, nor is the size of the aggregates known. The varying affinity of A23187 for Ca^{2+} in different states may have a significant role in giving rise to the rapid transmembrane transport of Ca^{2+}. The aggregates of A23187 on the membrane may serve to complex Ca^{2+} with high affinity, while dissociation of the Ca^{2+} complex can also occur with ease, in the polar environment at the membrane-water interface where disaggregation of A23187 may occur.

We reported previously that X537A induced a more rapid efflux of Ca^{2+} from 1:1 egg PC-cholesterol vesicles than from pure egg PC vesicles (Wun and Bittman, 1977). This observation is unexpected, because A23187 and the synthetic diamide ionophores showed a depressed activity in the presence of cholesterol. Valinomycin-facilatated exchange of Rb^{+} was also found to have lower activity when cholesterol was incorporated into the bilayer (de Gier et al., 1970). The depressed activity in the presence of cholesterol in the presence of cholesterol is consistent with the view that cholesterol increases the rigidity of the membrane and hence decreases the rate of movement of ionophore-cation complexes. In the present study we found that the increased Ca^{2+} transport by X537A across egg PC-cholesterol vesicles may arise from the enhanced rate of complexation on the membrane surface (Figure 15), since the association constant actually decreases in these vesicles compared with that in pure egg PC vesicles.

References

Bittman, R., and Blau, L. (1972), Biochemistry 11, 4831-4839.

Case, G.D., Vanderkooi, J.M., and Scarpa, A. (1974), Arch. Biochem. Biophys. 162, 174-185.

Caswell, A.H., and Pressman, B.C. (1972), Biochem. Biophys. Res. Commun. 49, 292-298.

de Gier, J., Haest, C.W.M., Mandersloot, J.G., and van Deenen, L. L. M. (1970), Biochim. Biophys. Acta 211, 373-375.

Degani, H., and Friedman, H. L. (1974), Biochemistry 13, 5022-5031.

Gómez-Puyou, and Gómez-Lojero (1977), Curr. Top. Bioenerg. 6, 221-257.

Haynes, D.H., and Pressman, B.C. (1974), J. Membr. Biol. 16, 195-205.

Pfeiffer, D.R., Reed, P.W., and Lardy, H.A. (1974), Biochemistry 13, 4007-4013.

Pressman, B.C. (1976), Ann. Rev. Biochem. 45, 501-530.

Wun, T.C., and Bittman, R. (1977), Biochemistry 16, 2080-2086.

Wun, T.C., Bittman, R., and Borowitz, I.J. (1977), Biochemistry 16, 2074-2079.

Table I. Fluorescence of A23187 in Methanol at Various Concentrations and the Effect of $CaBr_2$.

A23187	Excitation (No Ca^{2+})		Ratio of Peak I:	Excitation (+452 μM $CaBr_2$)	
Concentration	Peak I	Peak II	Peak II	Peak I	Peak II
0.117 μM	330 nm	372 nm	1.34	330 nm	372 nm
0.743	312	373	0.95	312	372
1.19	310	375	0.50	310	372
44.4	305	380	0.15	315	375

Table II. Fluorescence of A23187 in Ethanol at Various Concentrations and the Effect of $CaBr_2$.[a]

A23187	Excitation (No Ca^{2+})		Ratio of Peak I:	Excitation (+6.17 μM $CaBr_2$)	
Concentration	Peak I	Peak II	Peak II	Peak I	Peak II
0.093 μM	330 nm	372 nm	0.91	330 nm	372 nm
0.310	314	372	0.62	330	372
1.24	302	380	0.25	310	372

[a] The experimental conditions are the same as described in the caption to Figure 6 except that A23187 solutions were prepared in ethanol from a stock solution 5 hours before spectra were recorded.

FIGURE CAPTIONS

Figure 1: UV spectra of X537A in methanol and the effect of the addition of $CaBr_2$. (——), spectrum of 105 μM X537A; (—·—), spectrum after the addition of 67 μM $CaBr_2$; (—··—), addition of 670μM $CaBr_2$.

Figure 2: Interaction of $CaBr_2$ with X537A in methanol. (A) Job plot of the interaction of $CaBr_2$ with X537A. The sum of the concentrations of $CaBr_2$ and X537A was kept constant at 210 μM. The change in absorbance was measured at 320 nm. (B) Scatchard plot of the binding of $CaBr_2$ to X537A. The concentration of X537A was 104 μM. The concentration of $CaBr_2$ was varied from 13.3 to 186 μM.

Figure 3: Absorption spectrum of A23187 in methanol and the effect of addition of $CaBr_2$. (——), absorption spectrum of 17.7 μM A23187; (– – –), spectrum after addition of 67 μM $CaBr_2$. Insert: Absorbance changes upon increasing A23187 concentration. The concentration of A23187 was varied by adding 4-μl adiquots of a concentrated A23187 solution (2.52 mM) to methanol. The absorbance was recorded at 310 nm.

Figure 4: Job plot of the interaction of A23187 with $CaBr_2$ in methanol. The sum of the concentrations of $CaBr_2$ and A23187 was kept constant at 25.2 μM. The change in absorbance was measured at 310 nm.

Figure 5: Job plot of the interaction of A23187 with $CaBr_2$ in ethanol. The sum of the concentrations of A23187 and $CaBr_2$ was kept constant at 18.5 μM. The change in absorbance was measured at 310 nm.

Figure 6: Excitation and emission spectra of A23187 and the effect of $CaBr_2$ in methanol. (A) The spectra of 44.4 μM A23187 in the presence of added $CaBr_2$. (——), spectrum of 44.4 μM A23187; (—·—), spectrum after addition of 6.70 μM $CaBr_2$; (—··—), addition of 677 μM $CaBr_2$;

(– – – –), addition of 1347 μM $CaBr_2$. (B) The spectra of 1.19 μM A23187 in the presence of added $CaBr_2$. (——), spectrum of 1.19 uM A23187; (—•—), spectrum after addition of 6.70 μM $CaBr_2$; (—••—), addition of 677 μM $CaBr_2$. (C) The spectra of 0.117 μM A23187 in the presence of added $CaBr_2$. (——), spectrum of 0.117 μM A23187; (———), addition of 6.70 μM $CaBr_2$; (– – –), addition of 677 μM $CaBr_2$.

Excitation and emission monochromator band passes were kept at 3 and 5 nm, respectively, for all of these spectra. Samples of A23187 in methanol were prepared by injecting a few μl of a concentrated stock solution of A23187 in methanol and allowing the solution to stand at room temperature (~25°C) for more than 3 hr before spectra were taken. Excitation and emission wavelengths were 370 and 430 nm, respectively.

Figure 7: Time-dependent change in the fluorescence spectrum of A23187 upon dilution. (A) (——), addition of 1 μl of 0.355 mM A23187 to 3 ml of methanol, and the spectrum was immediately recorded; (—• —), spectrum after 5 min; (—••—), spectrum after 15 min. Excitation and emission wavelengths were 370 and 430 nm, respectively. Each excitation spectrum took about 2 min to run. (B) Time course of the change in fluorescence intensity. Timing was started upon addition of 1 μl of 0.355 mM A23187 to 3 ml methanol. The fluorescence intensity change was followed with excitation and emission wavelengths set at 330 and 430 nm, respectively.

Figure 8: Excitation and emission spectra of A23187 and the effect of Tris-base and $CaBr_2$. (——), 0.237 μM A23187 in methanol; (—•—), addition of 0.333 mM or 0.666 mM Tris-base; (—••—), addition of 1.20 mM $CaBr_2$ in the presence of 0.667 mM Tris-base.

Figure 9: Double-reciprocal plot of the fluorescence change of A23187 vs. $CaBr_2$ concentration in methanol. The concentration of A23187 was 0.237 μM. The fluorescence intensity was measured using excitation and emission wavelengths of 370 and 430 nm, respectively.

Figure 10: Binding of $CaBr_2$ to A23187 in methanol in the presence of Tris-base. (A) Double-reciprocal plot of fluorescence change vs. $CaBr_2$ concentration. The concentration of A23187 was 0.237 μM. The concentration of Tris-base was 0.333 mM. (B) Scatchard plot of the binding of $CaBr_2$ to A23187. The reaction conditions are the same as in (A).

Figure 11: Fluorescence change of the titration of A23187 with $CaBr_2$ in the presence and absence of Tris-base. (●), in the presence of 0.333 mM Tris-base; (○), in the absence of Tris-base. The concentration of A23187 was 0.237 μM. The maximum fluorescence changes were obtained by extrapolation of the double-reciprocal plots in Figure 9 and 10.

Figure 12: Excitation and emission spectra of A23187 with and without Ca^{2+} in egg PC vesicles and egg PC-cholesterol vesicles. Excitation and emission monochromator band passes were both 3 nm. Excitation wavelength, 380 nm, emission wavelength, 430 nm. (——), 3.33 μM A23187 in 0.5 mM egg PC vesicles; (- - - -), addition of 2.3 mM $CaCl_2$; (—•—), 3.33 μM A23187 in 1:1 egg PC-cholesterol vesicles (1 mM total lipid concentration); (—••—), addition of 2.3 mM $CaCl_2$.

The spectra of A23187 were taken 10 min after addition of the ionophore to the vesicles. The spectra of A23187 in the presence of $CaCl_2$ were taken immediately after addition of $CaCl_2$ to the above suspensions.

Figure 13: Double-reciprocal plot of the Ca^{2+}-induced fluorescence decrease of A23187 in egg PC and egg PC-cholesterol vesicles. ΔF refers to the fluorescence decrease upon the addition $CaCl_2$. The medium contained 3.33 μM A23187, 1 mM imidazole, pH 7.0, and 0.5 mM egg PC or 1:1 egg PC-cholesterol vesciles (1 mM total lipid concentration). The excitation and emission wavelengths were 380 nm and 430 nm, respectively. (o), egg PC vesicles; (•), egg PC-cholesterol vesicles.

Figure 14: Excitation and emission spectra of X537A with and without Ca^{2+} in egg PC vesicles and egg PC-cholesterol vesicles. The excitation and emission monochromator band passes were both 3 nm. The excitation wavelength was 310 nm, and the emission wavelength was 410 nm. (——), 3.33 μM X537A in 0.5 mM egg PC vesicles;(- - - -), addition of 3.07 mM $CaCl_2$; (—·—), 3.33 μM X537A in 1:1 egg PC-cholesterol vesicles (1 mM total lipid concentration);(—··—), addition of 3.07 mM $CaCl_2$. The spectra of X537A in the presence of Ca^{2+} were taken 5 min after addition of $CaCl_2$.

Figure 15: Double-reciprocal plot of the Ca^{2+} - induced fluorescence enhancement of X537A in egg PC and egg PC-cholesterol vesicles. ΔF refers to the fluorescence increase upon the addition of $CaCl_2$. The medium contained 3.33 μM X537A, 1 mM imidazole, pH7.0, and 0.5 mM egg PC or 1:1 egg PC-cholesterol vesicles (0.5 mM total lipid concentration). The excitation and emission wavelengths were 310 nm and 410 nm, respectively. The fluorescence enhancement was measured 10 min after each addition of $CaCl_2$. (o), in egg PC (E) vesicles; (Δ) in egg PC-cholesterol (E+C) vesicles. Insert: Time course of Ca^{2+}-induced fluorescence enhancement of X537A in egg PC (——), and egg PC-cholesterol (- - - -) vesicles.

FIG. 1

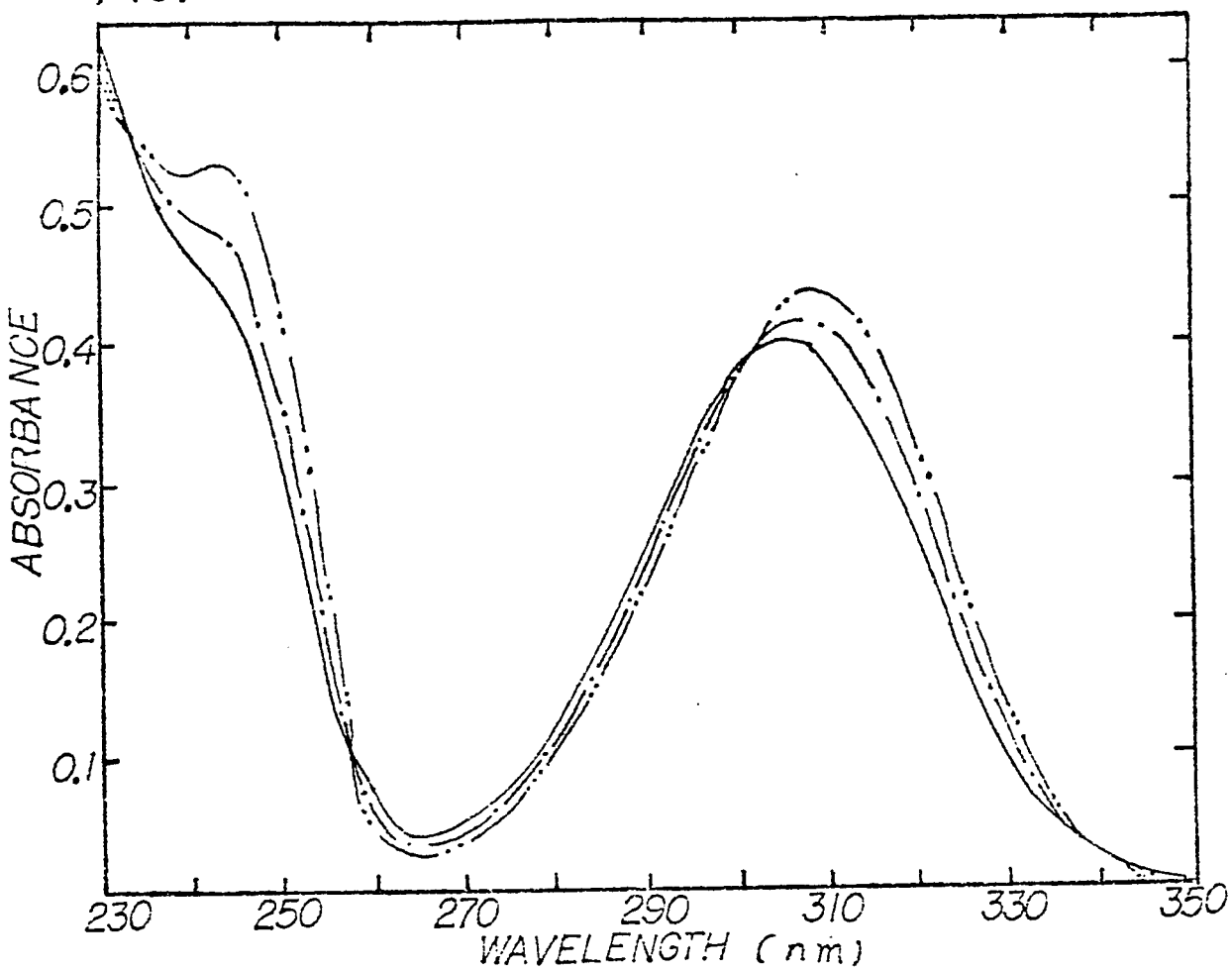
0.6
0.5
0.4
0.3
0.2
0.1
ABSORBANCE
230
250
270
290
310
330
350
WAVELENGTH (nm)

FIG. 2

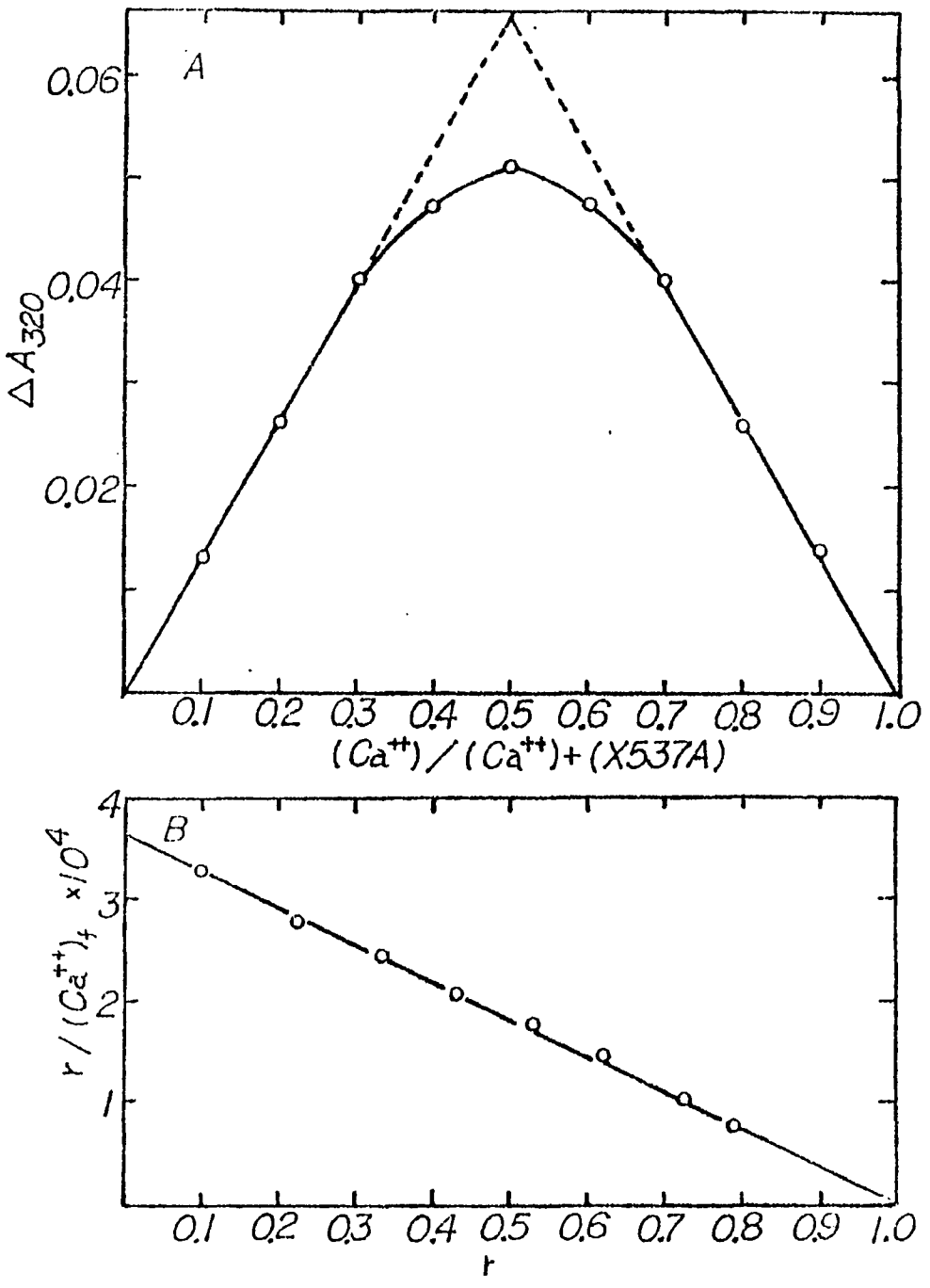
A
0.06
0.04
0.02
ΔA320
0.1 0.2 0.3 0.4 0.5 0.6 0.7 0.8 0.9 1.0
(Ca++) / (Ca++)+(X537A)
B
4
3
2
1
r / (Ca++)4 x10^4
0.1 0.2 0.3 0.4 0.5 0.6 0.7 0.8 0.9 1.0
r

FIG. 3

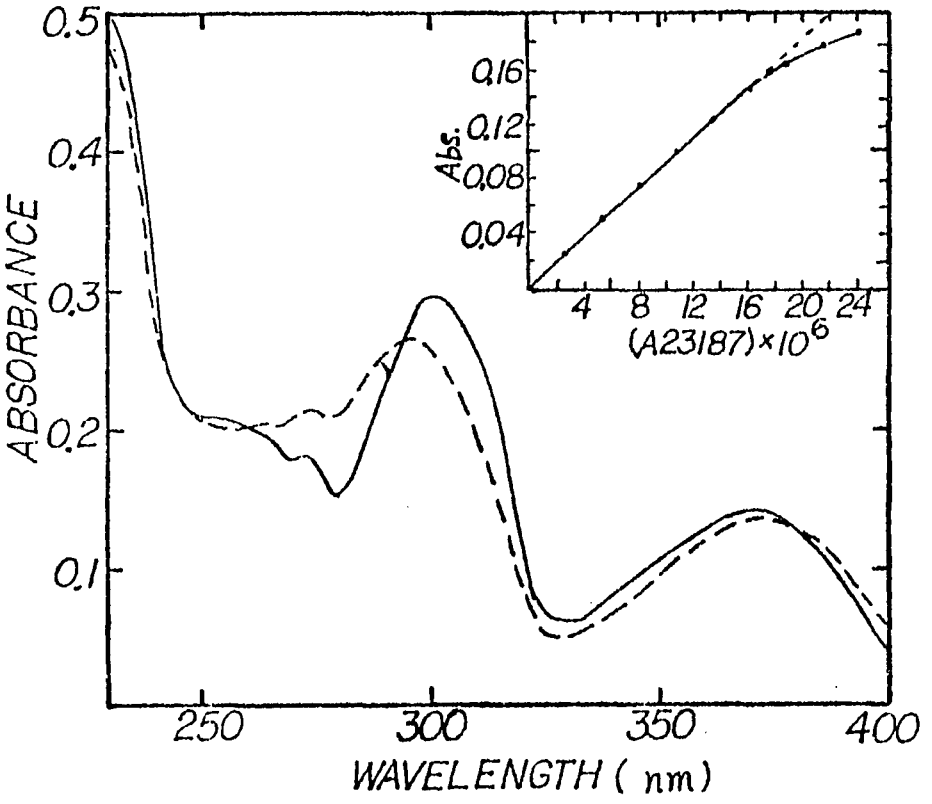
0.5
0.4
0.3
0.2
0.1
ABSORBANCE
250
300
350
400
WAVELENGTH (nm)
0.16
0.12
0.08
0.04
Abs.
4
8
12
16
20
24
(A23187)×10^6

FIG. 4

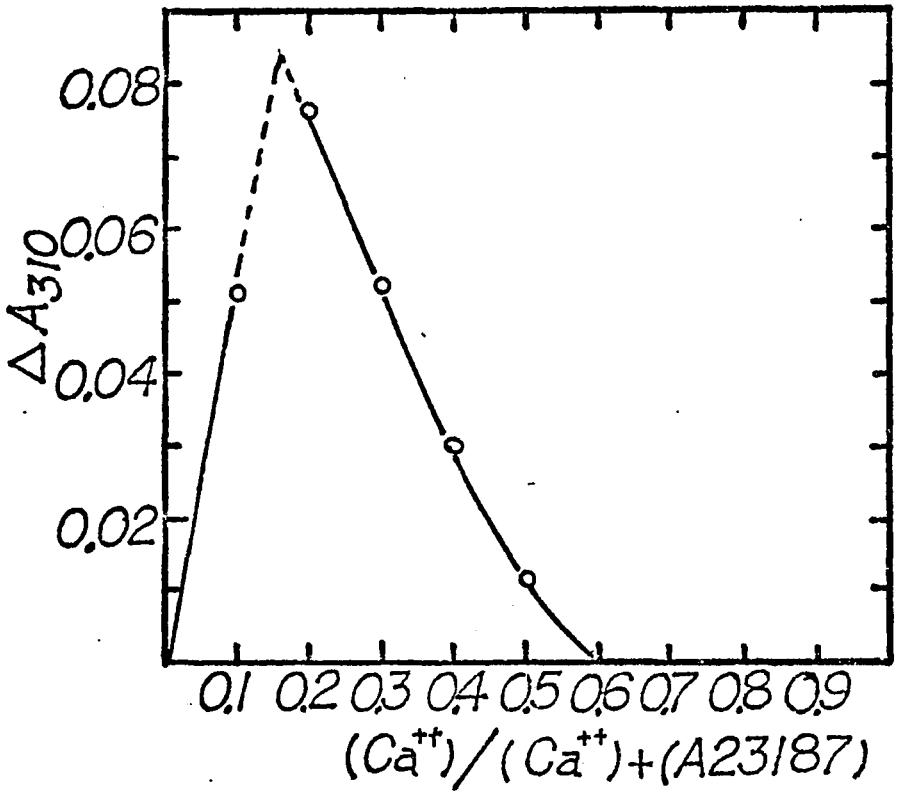

FIG.5

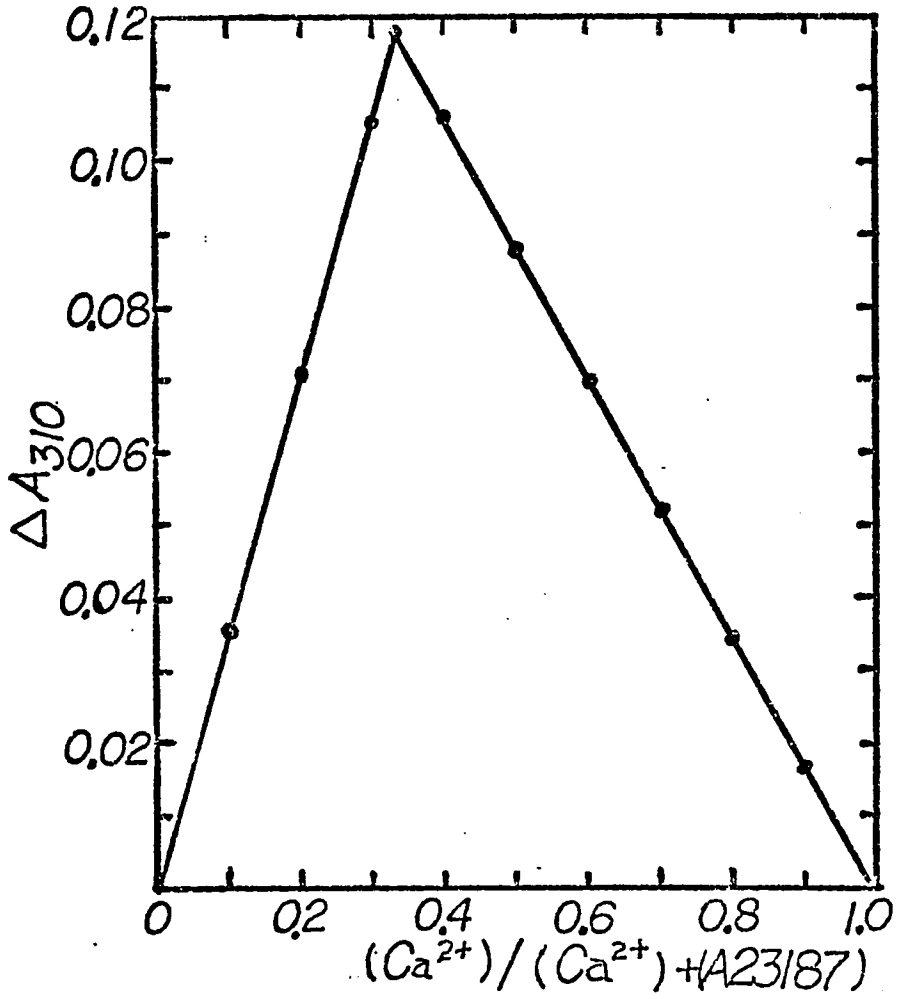

FIG 6

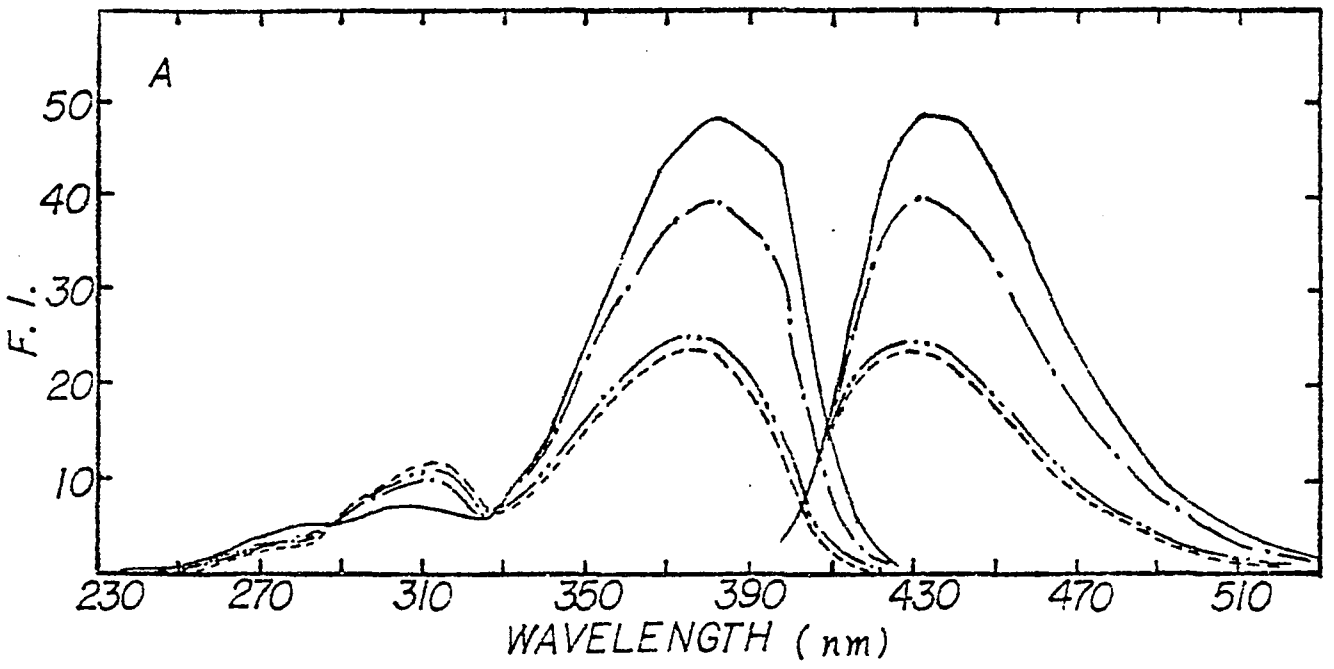

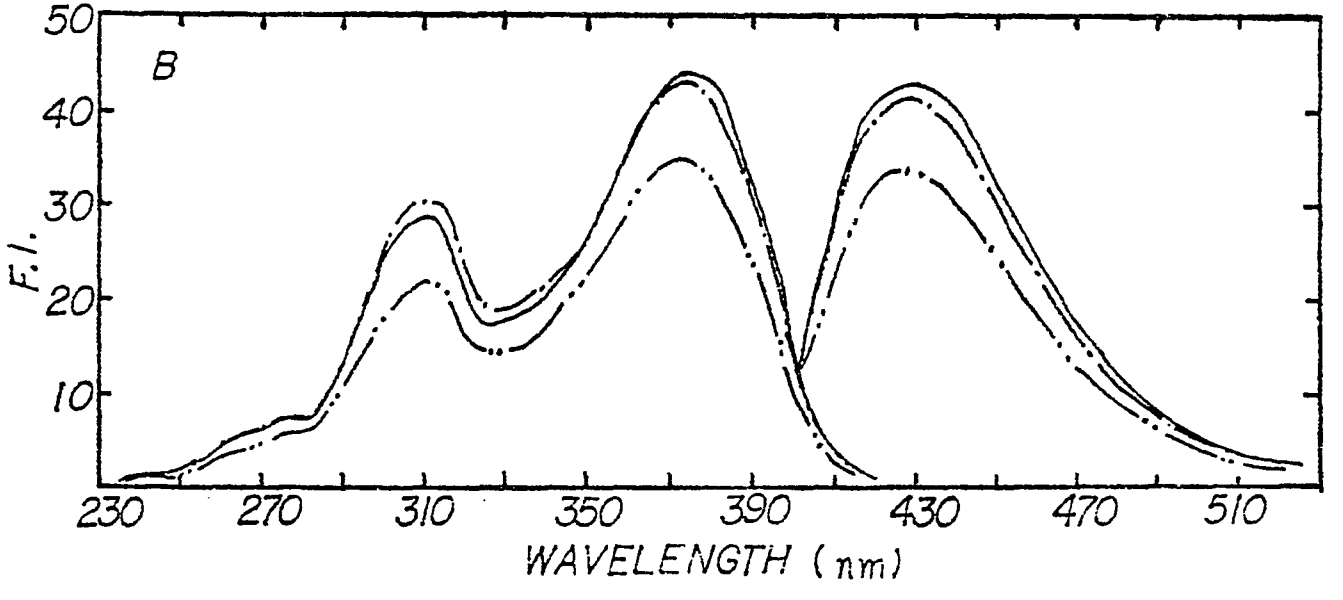
B
50
40
30
20
10
F.I.
230
270
310
350
390
430
470
510
WAVELENGTH (nm)

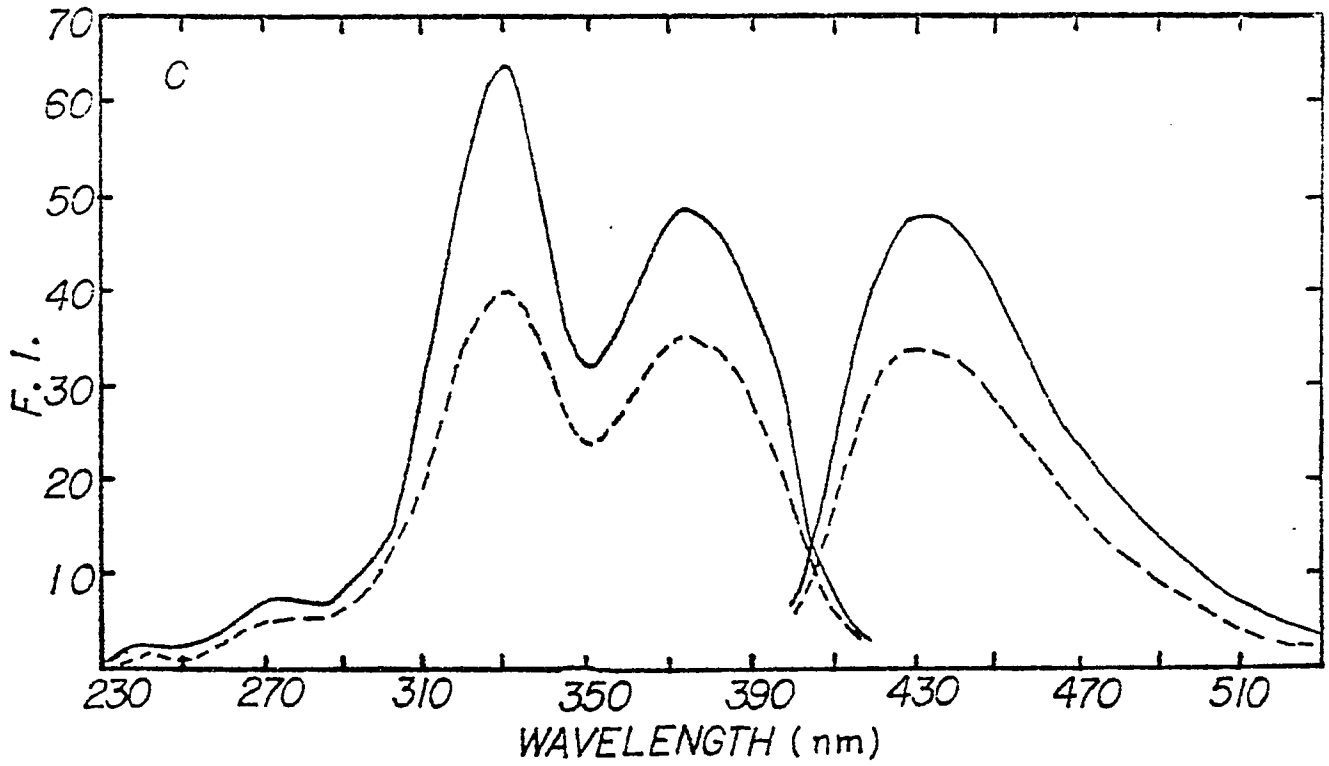
C
70
60
50
40
30
20
10
F. I.
230
270
310
350
390
430
470
510
WAVELENGTH (nm)

FIG. 7

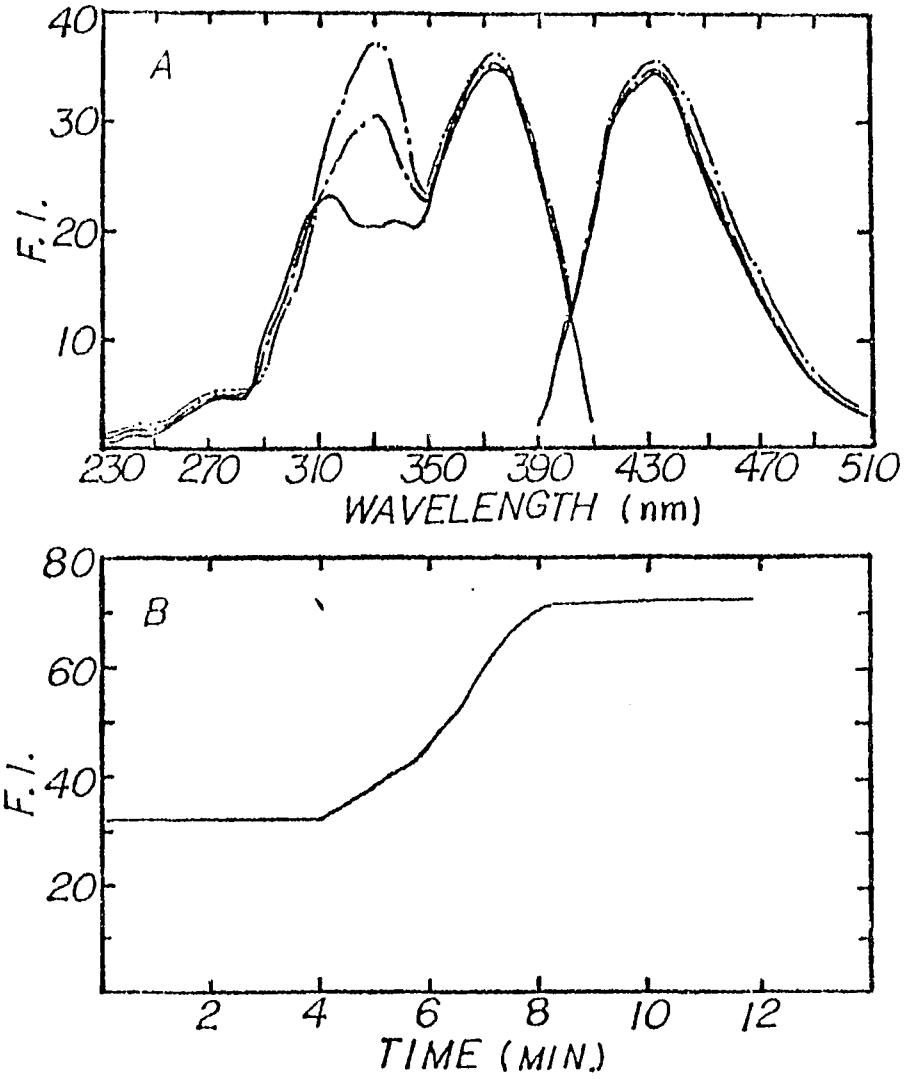
A
F.I.
40
30
20
10
230
270
310
350
390
430
470
510
WAVELENGTH (nm)
B
F.I.
80
60
40
20
2
4
6
8
10
12
TIME (MIN.)

FIG.8

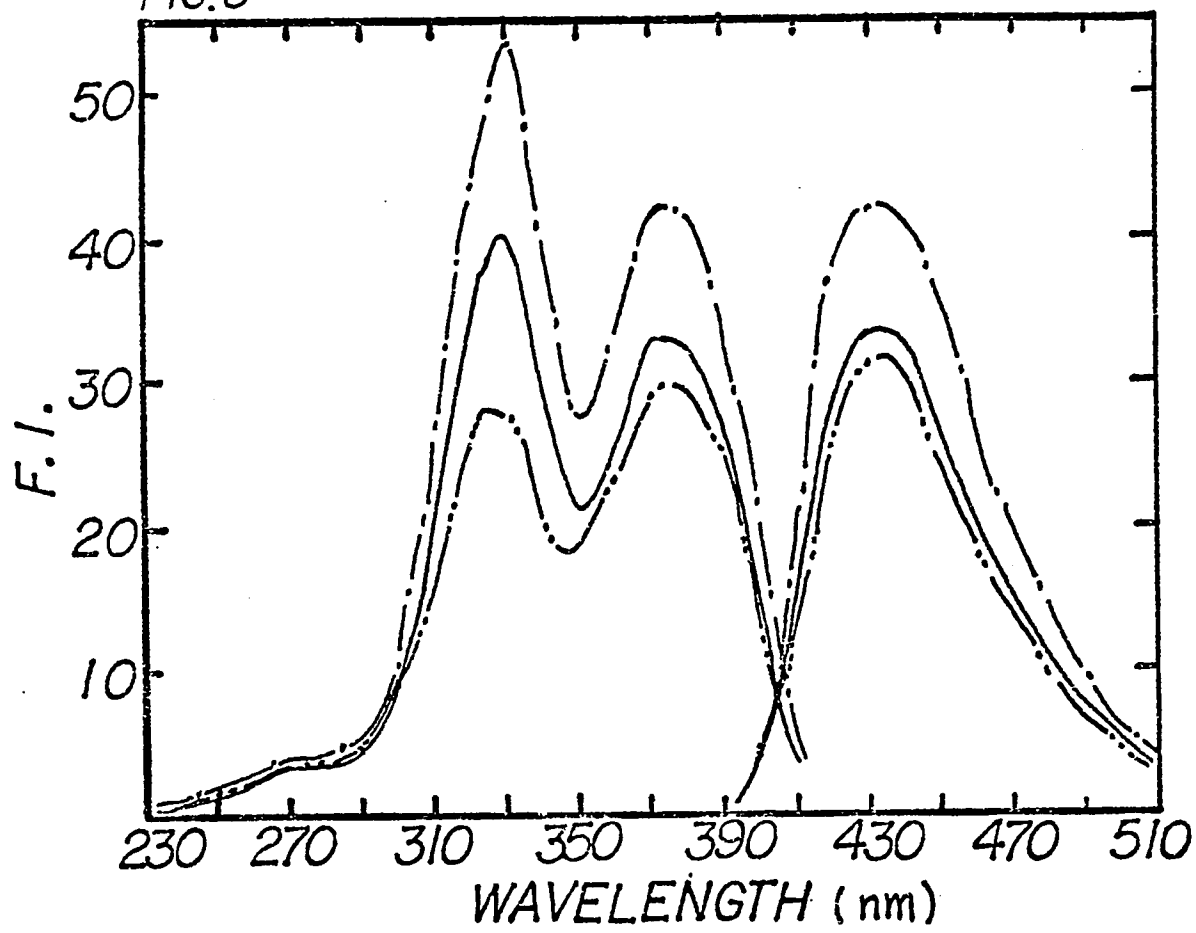

FIG. 9

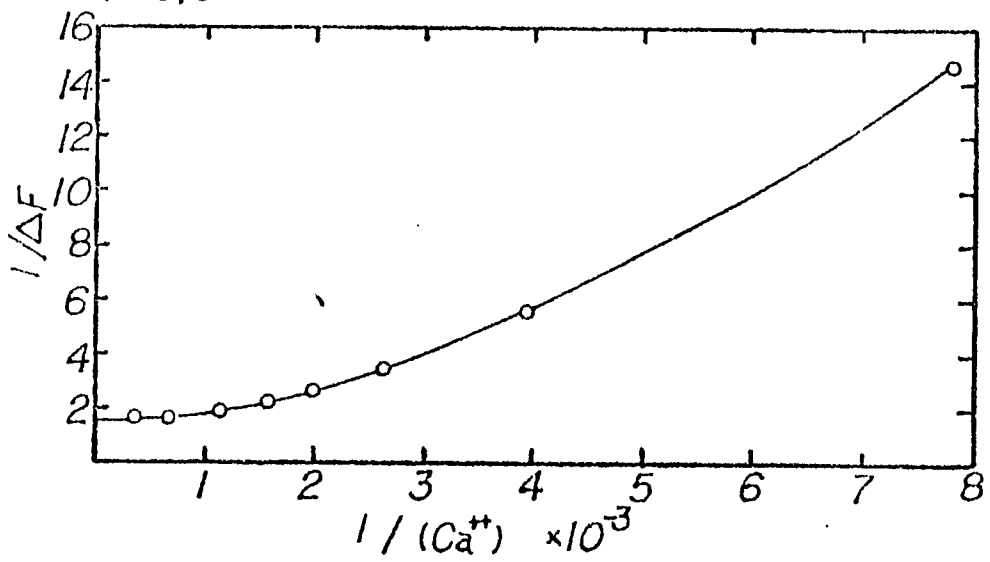

FIG. 10

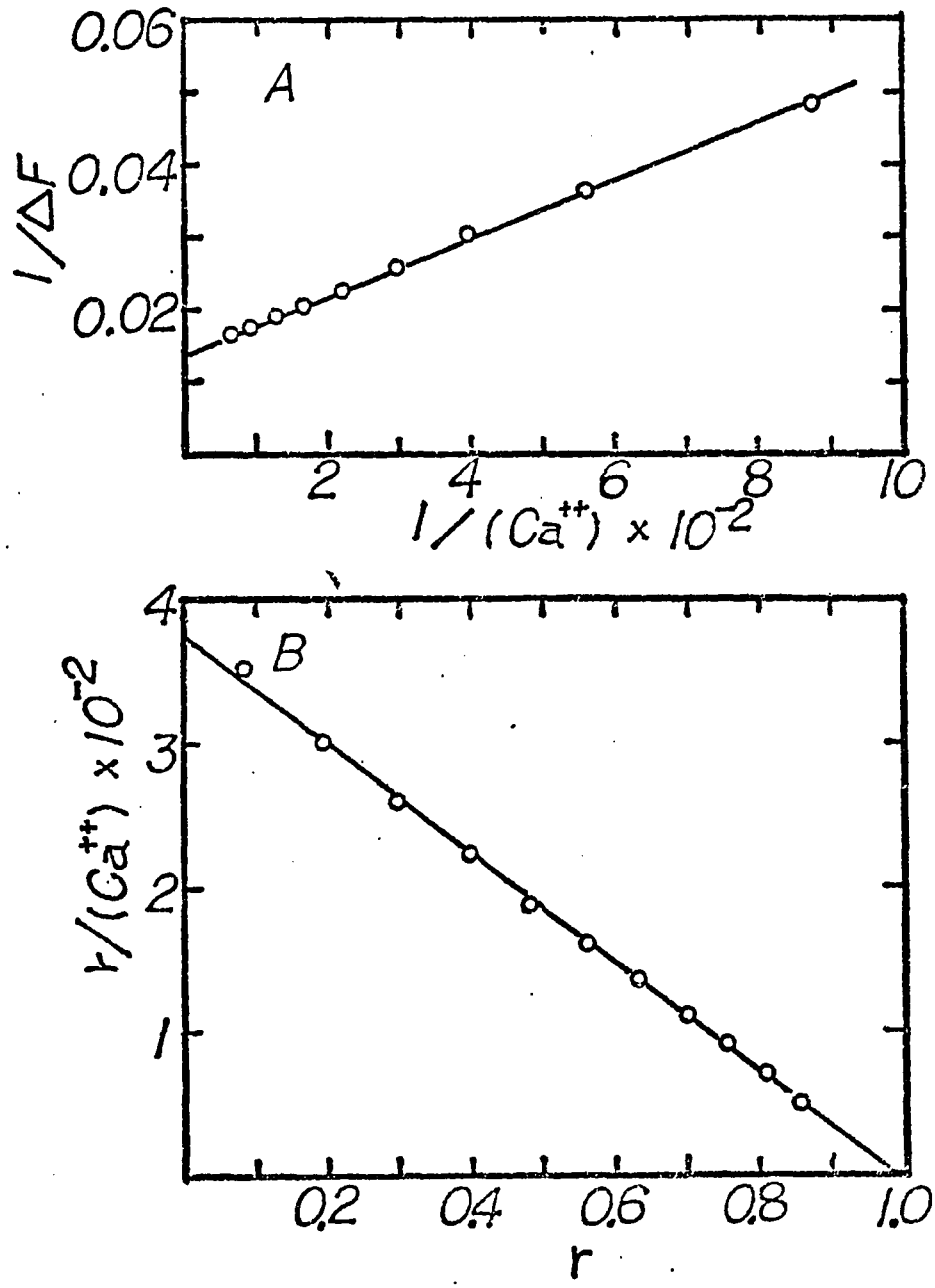

FIG. 11

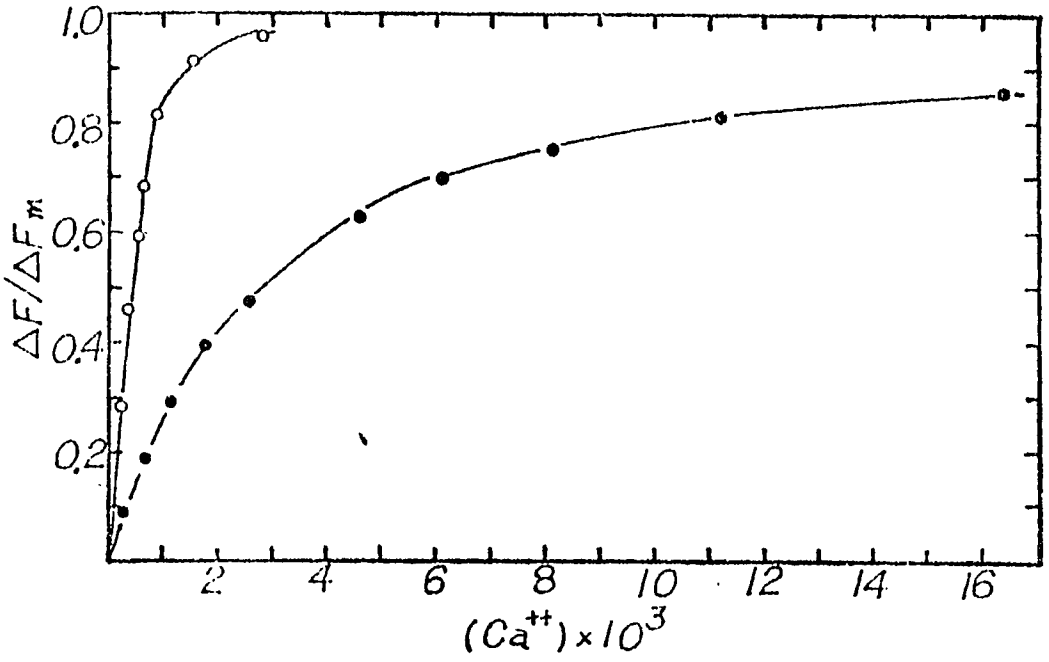

FIG. 12

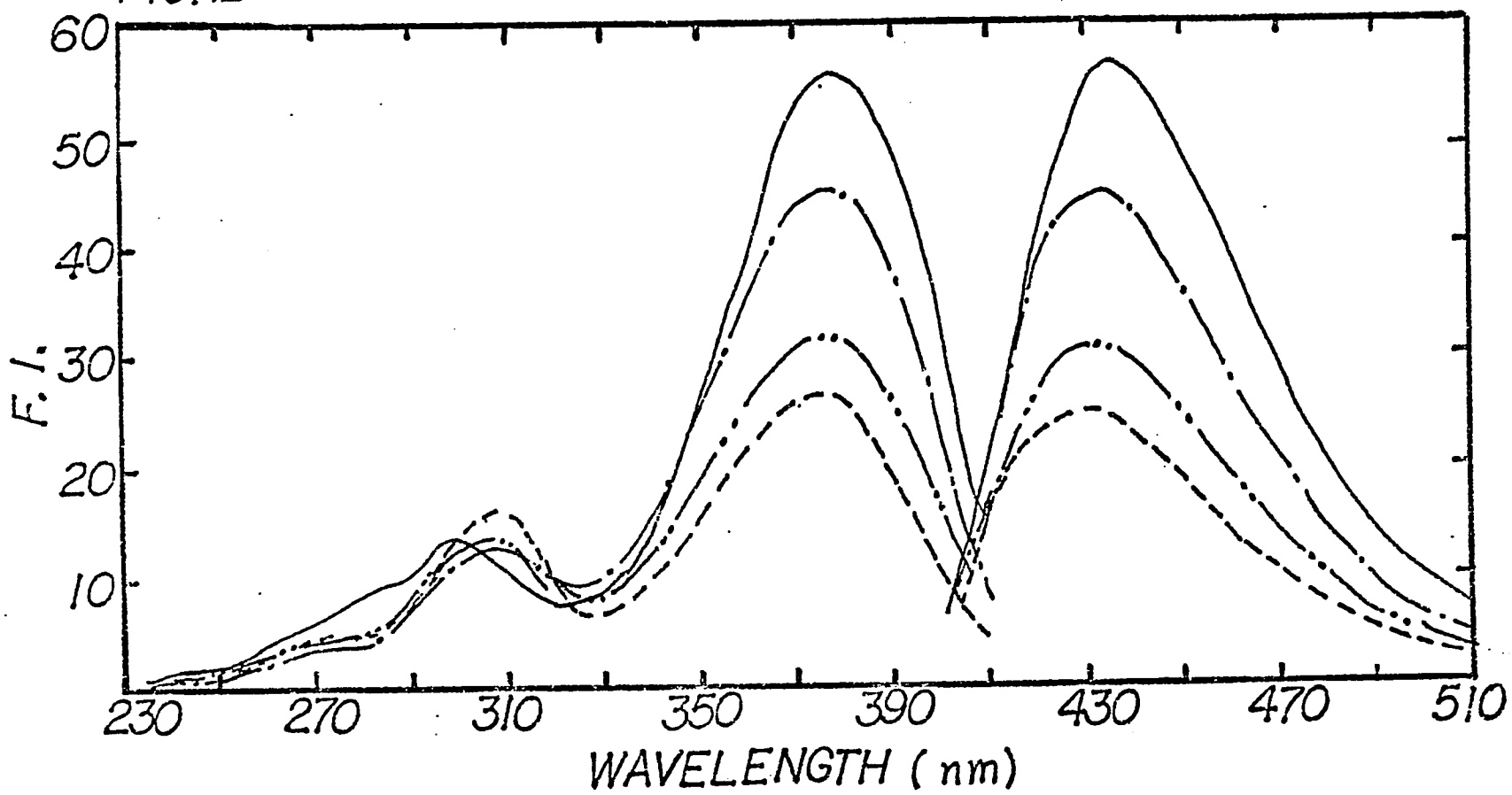
60
50
40
30
20
10
F. I.
230
270
310
350
390
430
470
510
WAVELENGTH (nm)

FIG. 13

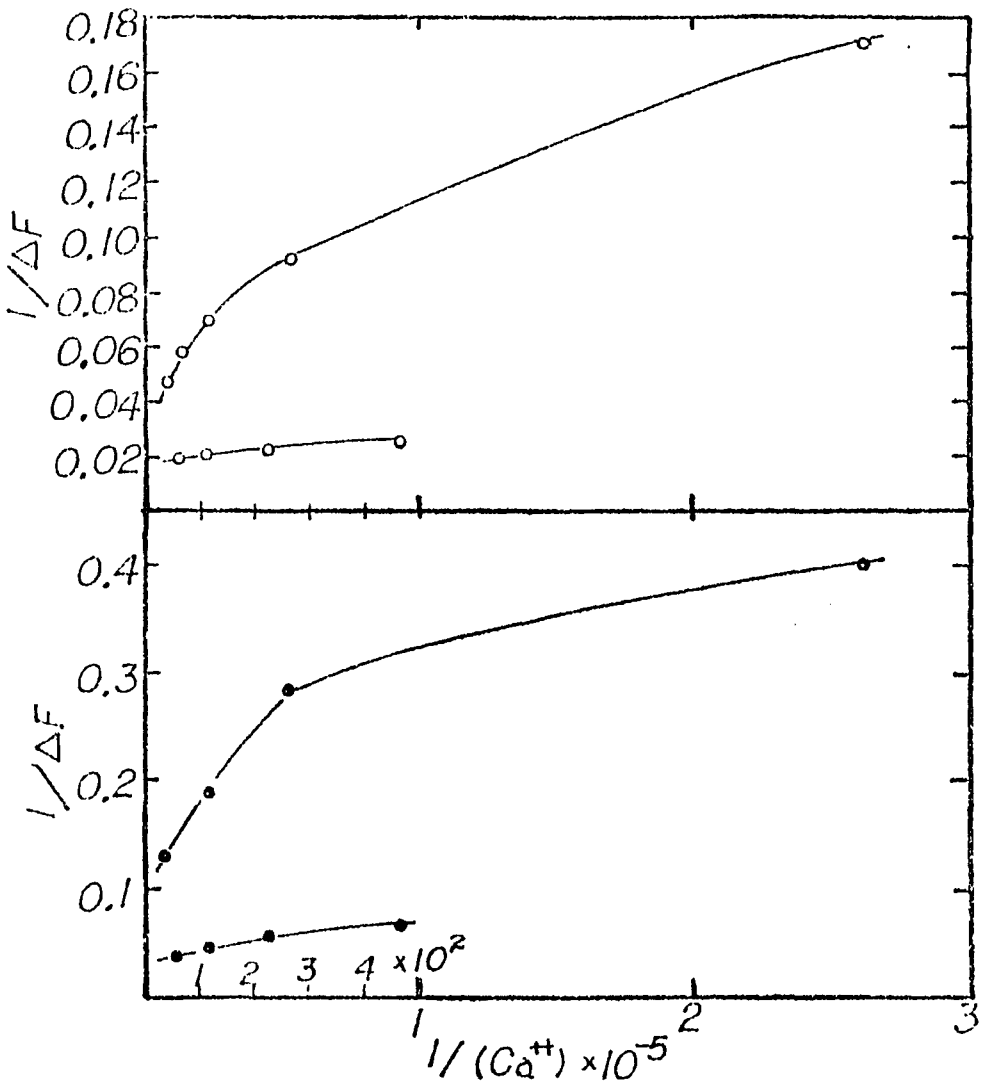
0.18
0.16
0.14
0.12
0.10
0.08
0.06
0.04
0.02
1/ΔF
0.4
0.3
0.2
0.1
1/ΔF
1
2
3
4 x10²
1
2
3
1/(Ca⁺⁺) x10⁻⁵

FIG. 14

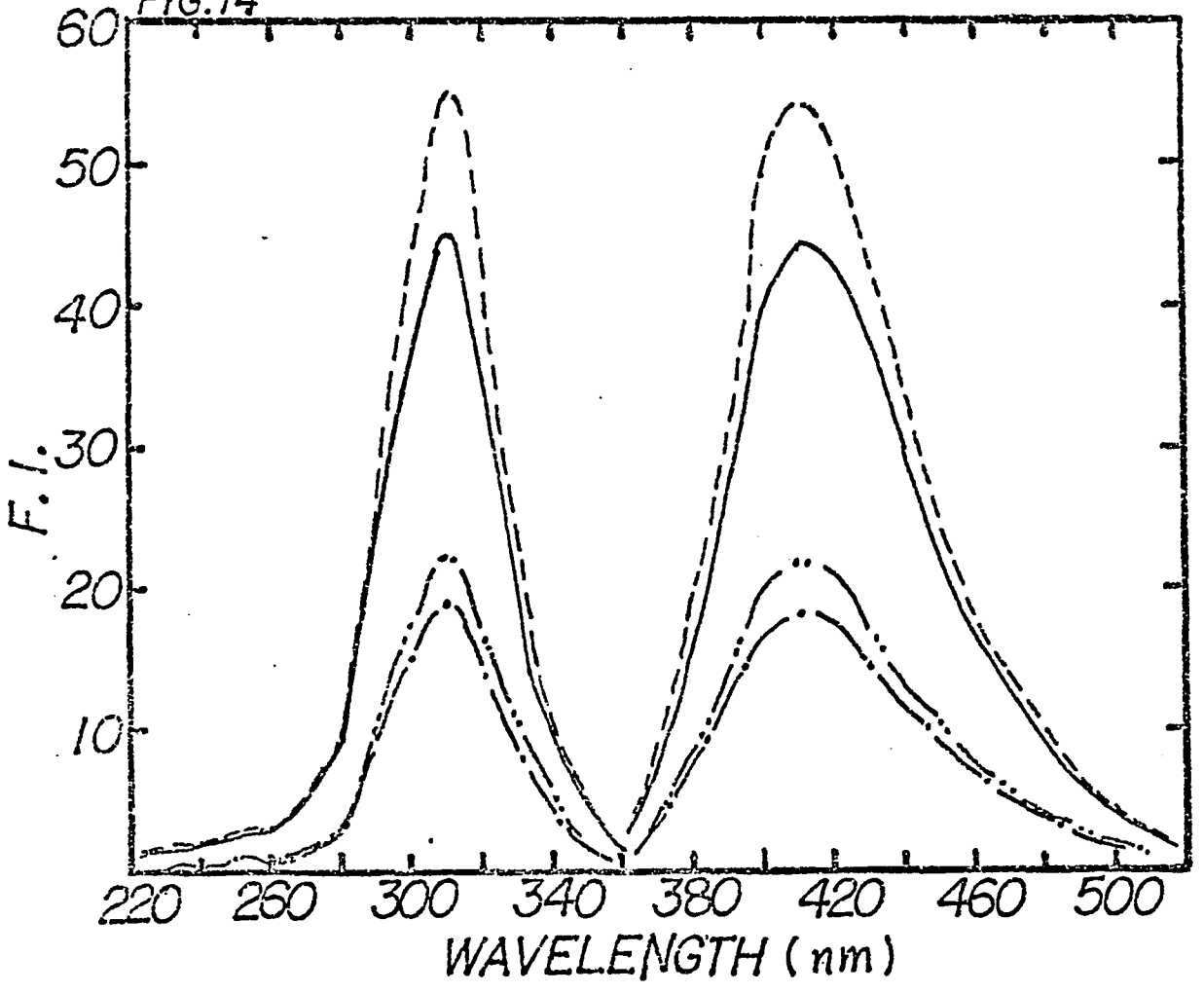
60
50
40
30
20
10
F. I.
220
260
300
340
380
420
460
500
WAVELENGTH (nm)

FIG. 15

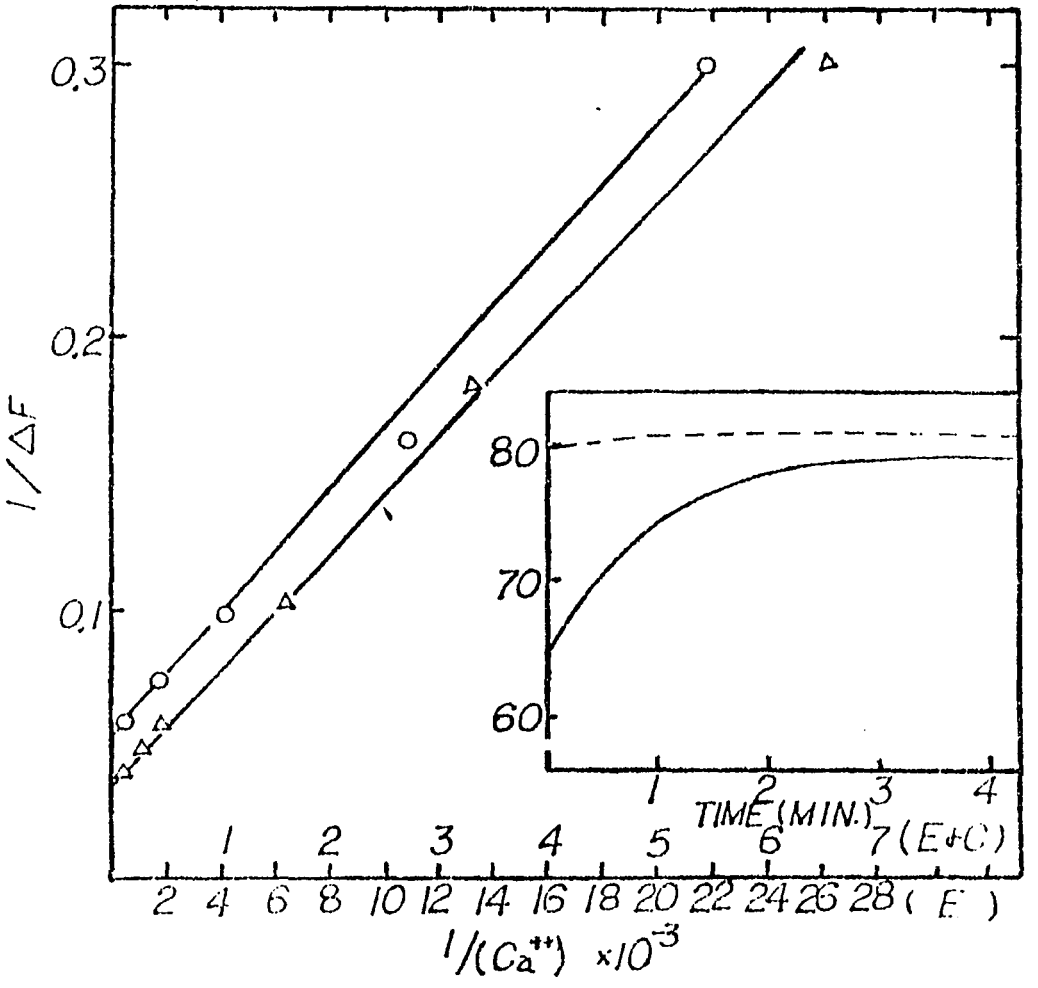
0.3
0.2
0.1
1/ΔF
80
70
60
1
2
3
4
TIME (MIN.)
1
2
3
4
5
6
7 (E+C)
2 4 6 8 10 12 14 16 18 20 22 24 26 28 (E)
1/(Ca++) ×10-3